HYDROLOGICAL MODELING OF URBAN WATERSHED WITH SNOWFALL FOR THE INDIAN CREEK BASIN

A THESIS IN
Environmental and Urban Geosciences

Presented to the Faculty of the University
of Missouri-Kansas City in partial fulfillment of
the requirement for the degree of

MASTER OF SCIENCE

by
GUSTAVO A. OROZCO

B.S., Francisco José de Caldas District University, Bogotá, Colombia, 1997

Kansas City, Missouri
2017

HYDROLOGICAL MODELING OF URBAN WATERSHED WITH SNOWFALL FOR THE INDIAN CREEK BASIN

Gustavo Adolfo Orozco Sarmiento, Candidate for the Master of Science Degree

University of Missouri-Kansas City, 2017

ABSTRACT

The present study explores the transport rate of urban pollutants by using snow melting processes by road salts and electrical conductance in the Indian Creek and Tomahawk Creek in Kansas. We adopted a cross-correlation method to explore which water quality parameter would be more indicative for snowfall and melting processes, and compared their relationships to the runoff estimation from the ArcSWAT model. The cross-correlation analysis shows that the peak of electric conductance in the creeks trails snowfalls was with average lags between 2 and 3 days. The ArcSWAT model shows that the effect of snowmelt on the electric conductance in the creeks was almost immediate with the average transport rate of 2.4 days and the snowmelt had negative impact on the turbidity. Also, the present study showed that in average times of concentration for the farthest point of the sub-basin to the main streams was 48 minutes. The findings will measure the transport rate of the pollutant's entrance into the water system and will allow water managers to implement better pollution control strategies during snow events.

APPROVAL PAGE

The faculty listed below, appointed by the Dean of the College of Arts and Sciences have examined a thesis titled "Hydrological Modeling of Urban Watershed with Snowfall for the Indian Creek Basin," presented by Gustavo A. Orozco, a candidate for the Master of Science degree, and certify that in their opinion it is worthy of acceptance.

Supervisory Committee

Jejung Lee, Ph.D., Committee Chair and Research Advisor
Professor
Department of Geosciences

Wei Ji, Ph.D.
Professor
Department of Geosciences

James B. Murowchick, Ph.D.
Professor
Department of Geosciences

TABLE OF CONTENTS

LIST OF ILLUSTRATIONS

Figure Page

LIST OF TABLES

Table Page

ACKNOWLEDGEMENTS

I would like to give special thanks to my advisor and friend Dr. Jejung Lee for his permanent and dedicated support and for sharing his knowledge and great expertise during the whole research process. Also, I want to thank Dr. Ji and Dr. Murowchick, members of the graduate committee, for their invaluable feedback and time.

I want to thank the Automated Information Mapping System (AIMS) and the High Plains Regional Climate Center (HPRCC) for their generous contribution and multiple State and Federal Institutions for the accessibility to their information.

Also, I want to thank my wonderful wife, for her amazing support and patience, and all her lonely nights during this process; without her this accomplishment would not have been possible. Thank you as well to my beautiful mother for all her prayers and unconditional love.

Finally, I express my profound thanks to my creator and personal friend, Jesus, my Savior and God; he has been my main engine and my strength now and always.

To my family:

My gorgeous and incredible wife

Paola Orozco-Loaiza

My beautiful and always joyful mother

Angela Sarmiento Gómez

CHAPTER 1

INTRODUCTION

1.1 Background

Non-point source (NPS) pollution in urban areas is an important topic due to the accelerated construction pace of new buildings and urban infrastructure and the relevance for the study of water quality problems. The estimation of NPS requires a considerable amount of information and knowledge regarding hydrological techniques. Contrary to point source pollution that is already identified and located, NPS is more complicated due to its diffuse and unknown origin. According to the United States Environmental Protection Agency (2017), "NPS pollution generally results from land runoff, precipitation, atmospheric deposition, drainage, seepage or hydrologic modification. NPS pollution, unlike pollution from industrial and sewage treatment plants, comes from many diffuse sources. NPS pollution is caused by rainfall or snowmelt moving over and through the ground. As the runoff moves, it picks up and carries away natural and human-made pollutants, finally depositing them into lakes, rivers, wetlands, coastal waters and ground waters".

Also, NPS pollution may include oils, chemicals, sediments, bacteria, nutrients, fertilizers, and pesticides among other elements and it is consider a major water quality issue (United States Environmental Protection Agency, 2017). The Clean Water Act established in 1987, Section 319 is a Federal amendment that helps states and local agencies to centralize NPS efforts and resources of multiple types to support the development of NPS projects and programs (United States Environmental Protection Agency, 2017).

NPS pollution models show that rainfall and runoff are common variables for water quality evaluation in the modeling techniques. Techniques such as constant concentration, spreadsheets, statistical, rating curve or regression, and buildup/washoff are used to predict NPS pollution (Donigian Jr. and Huber 1991). The constant concentration technique assumes a runoff with same pollutant concentrations. Spreadsheets technique is simply the automation of hydrological analysis that uses precipitation depth and rainfall coefficients, usually varying with land use, as basis for predictions. Statistical technique assumes an event mean concentration (EMC) with log normal distributions and derived runoff volumes and it is used mostly for quantitative studies of urban runoff. Rating curve or regression technique is simply a regression analysis that establishes the relationship between concentrations and volumes. Buildup and washoff technique is a concept built upon the bases of accumulation of sediments and pollutants that produce runoff during precipitation events. All these previous techniques are well applied as screening tools that can be implemented in the models (Donigian Jr. and Huber, 1991).

The effect of snowmelt salts on urban hydrologic systems has been widely study in the past. The majority of the current ice melters have salt as the main component. It is not a surprise; salt lowers the freezing point of the water which makes the snow to become liquid much faster than the natural process. Hem (1992) and Christensen, Jian and Ziegler (1999) suggested that in the ideal situation well-defined relations between dissolved solids and specific conductance may increase the concentration of constituents such as chloride, which is a chemical almost always present in the waters exposed to snow melt water. Hence, the presence of high concentrations of chlorides increases the conductivity of the waters (Peinado-Guevara et al., 2012). According to Wenner, Ruhlman, and Eggert (2003), more

than 2 years test between conductance and health of streams concluded that specific conductivity shows the quality of streams; this technique was used to detect impaired streams within the nearby locations. Among physical and chemical parameters, specific conductivity is a variable that gives an indication of streams water quality. The specific conductivity may lead to conclusions that affect whether we can classified the water as poor or good; high specific conductivity indicates pollution (Wenner, Ruhlman and Eggert 2003).

Although several studies have been created around the surface runoff and the time of entrance of pollutants into the water system, little have been known about the effects of snowfall and the implications of snow melting in the hydrological system in urban areas. The transport of contaminants in urban areas is the most important factor to evaluate, however it is essential to take into account how much and how fast runoff would be flowing into a basin.

1.2 Research Objectives

The main objective is to develop a computational model of urban hydrologic system for the urban water quality using snowfall events in the Indian Creek and Tomahawk Creek. It is fundamental to research the time of entrance of the chlorides or other constituents due to the salt compounds applied to the urban surface during snowfall.

The initial hypothesis is that watershed characteristics at a basin level are spatially correlated to water quality, and snow melting is correlated to physical factors that accelerate the introduction of pollutants into the basin. The positive spatial correlation could help to identify human activities that significantly contribute to water contamination, identify areas at risk, and promote management practices to reduce non-point and point source pollution. Snow data may be a good source of meaningful information that the present research will rely on.

1.3 Study Area: Indian Creek Basin

The Indian Creek Basin is located in the northeast section of the state of Kansas and the northwest section of the state of Missouri, including one portion of the east of Johnson County in Kansas and another portion of the southeast of Jackson County in Missouri. The majority of the basin, with 92% of the area, is located in Johnson County and the other portion of the basin, with 8% of the area, is located in Jackson County. The area contains the Indian River Basin, of which main streams are Indian Creek, Tomahawk Creek, Dyke Branch, and James Branch. The present research focuses on the Indian Creek and Tomahawk Creek. The study area is of approximately 47,128 acres (73.64 square miles).

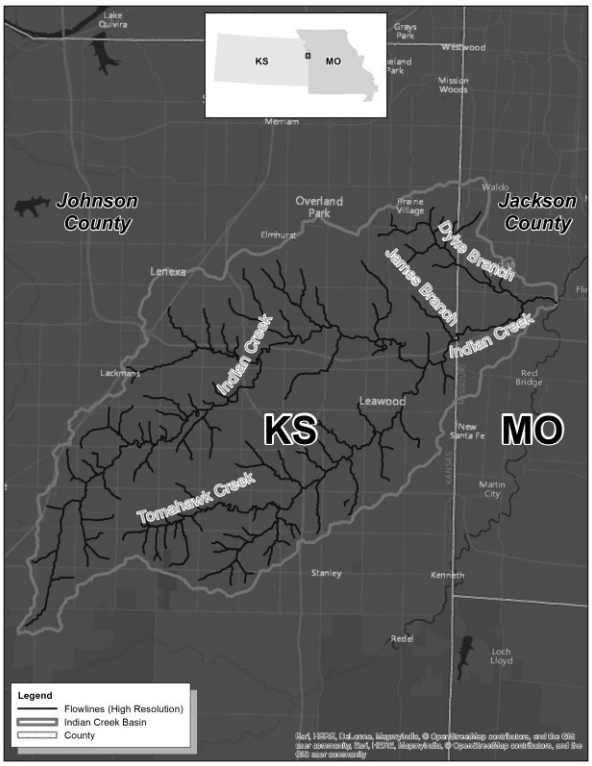

Figure 1. Location of the study area – Indian Creek Basin. The study area is divided by two States KS and MO. Base maps from (ESRI Data Maps 2016) and (USGS NHD Dataset 2016).

The area of study has a midwest climate, with very hot and humid summers and very cold winters. According to the National Oceanic & Atmospheric Administration (NOAA), of which station is located in the Kansas City Downtown Airport, the average annual mean temperature was 57.2 (°F) from 1997 to 2016. Also for these past 20 years, the average maximum temperature was 102.4 °F in the period from the end of July to the beginning of August as the warmest days, and the average minimum temperature was -0.4 °F in the period from the end of December to the end of January as the coldest days. The average number of days with maximum temperatures below or equals 32 °F was 21.5 days. The average precipitation was 37.9 inches, and the average extreme maximum precipitation per day was 3.33 inches. For the period of 1997 to 2010 the average snowfall was 11.2 inches with the maximum values of 22.0 inches in 1997 and 18.0 inches in 2007. Finally, the average maximum snowfall per day was 3.1 inches with the maximum values of 5.5 inches in 1997 and 4.5 inches in 2009 (See appendix A). The location of the study area has relatively flat terrain with the elevations ranging between 761.07 and 1,109.67 feet above sea level.

According to the National Land Cover Dataset (NLCD) (2011) developed by the United States Geological Survey (USGS), the majority of the land is in a low, medium or high intensity urban development areas or urban open space such as golf courses, comprising about 92.6% of the basin. The rest of the area is comprised by hay/pasture, forest, and herbaceous with 5.5% of the total basin area, cultivated crops occupying 1.5% of the area, wetlands occupying 0.23%, and open water at last with barely 0.13% of the total basin area.

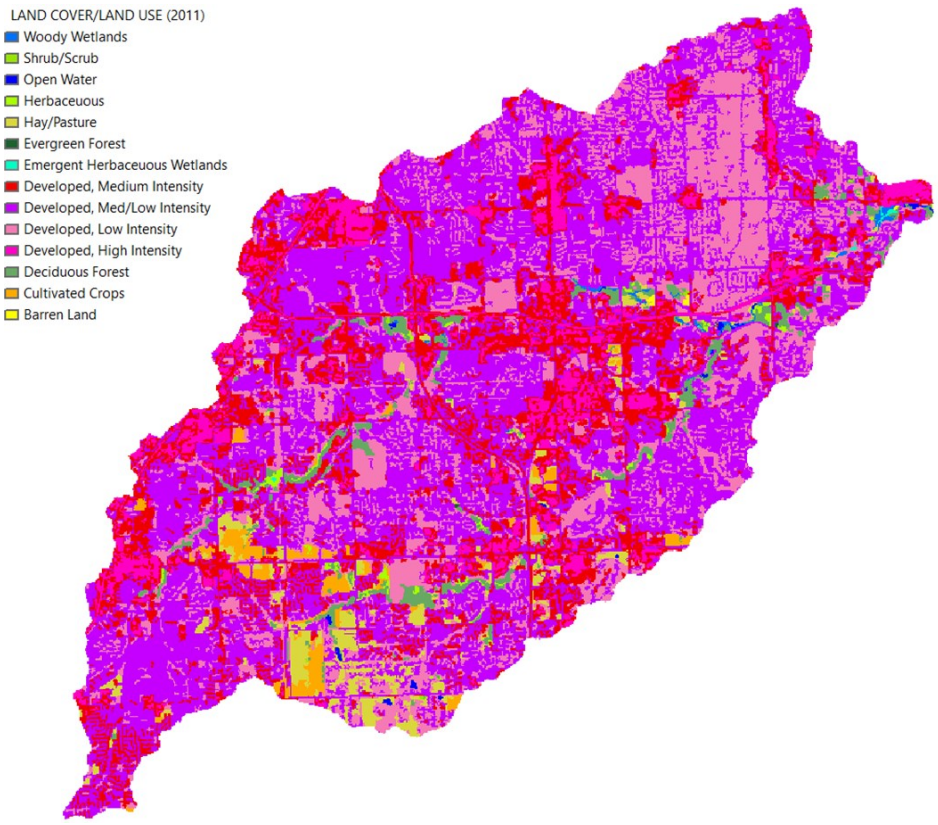

Figure 2. Land cover/Land use raster map depicts an approximate of 92% of land within urban developed areas (NLCD 2011).

CHAPTER 2

LITERATURE REVIEW

2.1 Urban Non-point Source Pollution

Urban non-point pollution is a topic very well known in scientific communities. Many studies have been made around the urban activities and the deterioration of the streams by mostly non-point sources of contamination (Basnyat et al., 2000; Brett et al., 2005; De Oliveira, Pinheiro Santos and Maillard, 2013; Maillard and Pinheiro Santos, 2008; Mitchell, 2005). The previous studies considered that land cover/land use (LULC) changes played a crucial role on the impairment of urban streams. The LULC determines the level of roughness in the surface, in a way that forest surfaces decrease the runoff rate, whereas urban surfaces increase it (De Oliveira, Pinheiro Santos and Maillard, 2013). Some authors such as Basnyat et al. (2000), Brett et al. (2005), De Oliveira, Pinheiro Santos and Maillard (2013), and Maillard and Pinheiro Santos (2008) consider the creation or adjustment of buffer zones, which are protection zones with the riparian vegetation around the streams. To delineate the buffer zones, we can perform the reclassification of LULC in order to improve the accuracy of the zones (Basnyat et al., 2000). Mitchell (2005) showed that one of the most efficient ways to reduce pollution in urban areas is the development of sustainable drainage systems in consolidated urban spaces.

Many recent studies started to adopt GIS and remote sensing technologies due to analytical and spatial visualization capabilities. These visualization systems help to identify diffuse contamination through the analysis of different parameters such as nitrate, phosphorus, and turbidity (Brett et al., 2005; De Oliveira, Pinheiro Santos and Maillard,

2013;Maillard and Pinheiro Santos, 2008). Mitchell (2005) suggested a concentration model called Event Mean Concentration (EMC), which is the total mass load of a chemical yielded from the storm, divided by the total storm discharge. This model was crossed reference with an annual runoff model taking into account different land use changes at sub-basin levels with the maximum unit area load. Basnyat et al. (2000) suggested that there is a strong relationship between nitrate concentrations and different land use types. Two key elements for their study was the delineation of a basin through Digital Elevation Model (DEM) and the development of an equation to calculate the efficiency of buffer zones:

$$\frac{B_b}{B_r} = \left(\frac{n_b}{n_r}\right)^{0.6} \left(\frac{L_b}{L_r}\right)^{2} \left(\frac{K_b}{K_r}\right)^{0.4} \left(\frac{S_b}{S_r}\right)^{-0.7} \left(\frac{C_b}{C_r}\right) \tag{1}$$

where B_b refers to the proposed buffer zone and B_r refers to the 'reference zone'; B_b/B_r is the 'buffer zone' effectiveness ratio; n is the Manning roughness coefficient (Engman, 1986); L is the buffer zone width (feet or meters); K is the saturated hydraulic conductivity (in./h or cm/h); S is the slope (%); and C is the soil moisture storage capacity (in. or cm) (Basnyat et al., 2000). It is important to note that Equation (1) does not take into account the precipitation, whereas Mitchell (2005) considers the rainfall for the calculation of the annual runoff volume. Other studies consider the influence of slope and roughness within the runoff calculation process as shown in De Oliveira, Pinheiro Santos and Maillard (2013). In De Oliveira, Pinheiro Santos and Maillard (2013), the base for the evaluation is the Manning equation that is directly proportional to slope (i) and inversely to the roughness (n) and the substituted equation to determine the influence of i and n in the overland flow time is:

$$T = \left(n \times \frac{L}{R_H^{2/3} \times i^{1/2}}\right) \tag{2}$$

where T is the overland flow time (s); R_H is the hydraulic radius (m); and L is the travel distance.

As mentioned in Brett et al. (2005), forest lands help stabilize nutrients by its transition to urban areas contributing to the contamination in the urban water system. In one of their conclusions turbidity shows high concentrations during winter seasons, whereas Maillard and Pinheiro Santos (2008) suggested that high turbidity values are shown in wet season, which is around January in Brazil.

In general, LULC is a big determination factor for the study of non-point source pollution in the urban area. Nitrate, phosphorus, and turbidity are the main parameters to analyze, and the use of GIS and remote sensing technologies help understand, visualize, and analyze physical factors contributing to the non-point source pollution and its spatial location in the urban areas.

2.2 Water Quality

Watershed management is part of the efforts to maintain and improve water quality in streams. In the studies of water quality, it is crucial to take into account spatio-temporal changes of physical, chemical, and physiographic characteristics that may be present in the dynamics of the basin (Xu et al., 2012). It is necessary to recognize water quality variations and the climate variations that affect the amount of pollutants in the streams (Bhat, et al. 2014). Hall and Ellis (1985) investigated water quality deterioration with the urbanization itself, suggesting that there is a direct relationship between the increase of impervious surface and the proliferation of the building construction business. Hall and Ellis (1985) also suggested that one of the factors to influence water quality is the changes in the precipitation regime that may regulate the water network design and the runoff of pollutants. Chang

(2008) showed that the greater the population the more the nutrients and non-point source pollutants into urban streams.

Gazzaz, et al. (2012) presented a water quality index (WQI), which is a numeric value that compares water quality variables and the water quality standards. The combined sewer overflow (CSO) on streams have been studied as well, due to its influence in water quality once the system is oversaturated, specially, in heavy rainfall events. Even, et al. (2007) presented PROSE, a model to simulate the storm water and waste water flow through the CSO. Xu, et al. (2012) and Chang (2008) introduced the concept of seasonal variation to define water quality parameters through the Mann-Kendall's Test. Davis, Traver and Hunt (2010) provided important concepts of stormwater control measures (SCMs) such as green roofs, vegetated swales, grassed filter strips, bioretention, and pervious pavements.

2.3 Snow and Times of Concentration

The relationship between runoff and snowmelt in urban areas is not well known so far. Many studies focus on the snowmelt characteristics rather than how the snowmelt would affect urban streams (Kronis 1978). Peterson, et al. (2005) studied snowmelt characteristics under alpine temperature. Martinec, Rango and Major (1983) developed a snowmelt-runoff model to explore potential factors to affect snowmelt rates such as precipitation, runoff coefficient, and topographic variations including peaks and valleys.

The estimation of overland flow and runoff requires conditions of surface roughness, rainfall intensity, and topographic slope and its length (Wong, 2005; Almeida et al., 2014; Wong and Li, 1998). Urban land surface produces faster runoff and less time of retention. In the same way, channels in the urban area change the flow characteristics by increasing overland flow and producing the same effects by reducing the surface roughness.

Topographic slope is very important in a runoff process; it will determine the transport rate of urban debris that would affect water structures such as storm sewers and street ditches (Cronshey, et al. 1986). Peters (2009) showed the relationship between the increase of specific conductance and the amount of chloride in the urban streams, but did not considered the use of deicing salt during snowfall. Finding the effect of deicing salt will provide an interesting insight of urban runoff and NPS pollution.

2.4 Statistical Analysis of Water Quality

Many statistical methods have been adopted for the analysis of water quality parameters. Yang and Jin (2010) used the traditional ordinary least square (OLS) method to relate basin characteristics with water quality. Cluster analysis (CA) or factor analysis (FA) are also widely used to determine spatio-temporal variations of water quality (Xu et al., 2012; Bhat et al., 2014; Shrestha and Kazama, 2007). Cluster analysis helps group data based on the differences and similarities regarding the characteristics of surface water quality (Shrestha and Kazama, 2007). Correlation coefficient is an effective statistical number to determine the relationship between two or more water quality parameters (Khatoon et al., 2013; Noori et al., 2010; Wilkison, Amstrong and Hampton, 2009). There are innumerable statistics to assess a hydrological model; the most common ones are Nash-Sutcliffe efficiency (NSE), Pearson's coefficient of determination (R^2), Slope and y-intercept, Persistence model efficiency (PME), Percent bias (PBIAS), and Daily root-mean square (DRMS) (Gupta, Sorooshian and Yapo, 1999; Jeong et al., 2010; Moriasi et al., 2007). Each of them has something specific to contribute to the calculation or evaluation of model performance. According to Gupta, Sorooshian and Yapo (1999), NSE is a measure of the relative degree of the residual variance or noise to the variance of the flows or observed data. Moriasi et al.

(2007), it shows the 1 to 1 line agreement between observed and simulated values. It indicates the performance of the model relative to a standard; being 1 an indicative of optimal model performance (Jeong et al., 2010). NSE is also defined as a calibration measurement to evaluate the precision of the models (Moriasi et al., 2007).

2.5 Geospatial Analysis of Water Quality

With the advancement of the spatial technology several tools and methodologies have been used to study runoff rates and discharge of water pollutants. Fitzgerald, et al. (2012) and Di Luzio, Arnold and Srinivasan (2005) conducted covariance analysis to clarify relationships between basin characteristics and pollutants discharge, and identified the source of pollutants. Besides the statistical methods, Easton et al. (2010), Kundzewicz and Krysanova (2010), Chinh et al. (2011), Yang and Jin (2010), Mouri, Shinoda and Oki (2012), and Chang (2008) addressed the importance of land cover change in urban water quality. The urbanization changes the LULC by destroying natural conditions of streams (Cruise, Laymon and Al-Hamdan 2010). The level of urbanization may depend upon stakeholders or landowners and its effect should be taken into account (Wilcove, 2014; Babbar-Sebens et al., 2015).

The spatial resolution of basin model plays a key role in the implementation of runoff assessment. Kundzewicz and Krysanova (2010), Di Luzio, Arnold and Srinivasan (2005), and Mouri, Shinoda and Oki (2012) showed that a basin level modelling provides good resolutions for water quality and runoff analysis.

2.6 Hydrological Modeling

The use of models for contamination is well known. Authors such as Koç (2010), Erturk et al. (2010), and Even et al. (2007), employed one-dimensional modelling techniques to measure contaminants. These modelling techniques use the concept of "mass balance" to determine levels of infiltration, evaporation, evapotranspiration, temporal storage, and runoff. The benefits of these models are that they can identify active elements in stream pollution and determine the degrees of influence of those elements in impaired streams, so that they can evaluate possible effects of future socio-economic developments.

Multiple software applications or add-ins for watershed modelling have been developed along the years improving in this way the one-dimensional modelling approach to more complex models. Among others are the Watershed REstoration using Spatio-Temporal Optimization of REsources (WRESTORE) (National Science Foundation, 2014), MIKE SHE (*Systeme Hydrologique European*) (Jeong et al., 2010, Sandu and Virsta, 2105), Watershed Characterization and Modeling System (WCMS) (Strager et al., 2010), Agricultural Policy/Environmental Extender (APEX) (Golmohammadi et al., 2014), Topography Based Hydrological Model (TOPMODEL) (Beven,1997; Devi, Ganasri and Dwarakish, 2015; Peng, Zhijia and Fan, 2008), Better Assessment Science Integrating Point and Non-point Sources (BASINS) (Mohamoud, Sigleo and Parmar, 2009; United States Environmental Protection Agency, 2016), and SWAT (Arnold, Moriasi et al., 2012; Daggupati et al., 2015; Debele, Srinivasan and Parlange, 2008; Kim et al., 2012; Maharjan et al., 2013; Malagó et al., 2017; Malunjkar et al., 2015; Sheshukov et al., 2011; Tian et al., 2012; Wang et al., 2016; Yang, Liu, et al., 2016; Zhang, Srinivasan and Van Liew, 2008). Some authors have written about the advantages and disadvantages of diverse hydrological models and concluded that

accuracy of the models depends upon the characteristics of the basin such as area, the simplicity of the set-up, the spatio-temporal resolution of the streamflow, and the type of analysis (Devi, Ganasri and Dwarakish, 2015; Golmohammadi et al., 2014). WRESTORE is a web-based application design to support the visualization of watersheds and their management components adding a runoff component with limited capabilities. MIKE SHE is a European Hydrological System Model developed by the Danish Hydraulic Institute (DHI), and it is a spatial model type that requires a lot of computation time and is not ideal for development of hydrological models with long records in time and large watersheds (Jeong et al., 2010; Sandu and Virsta, 2105). However, MIKE SHE is a fully integrated hydrological model capable of assessing the hydrological changes product of land cover, land use changes and it has been largely used in watershed studies.

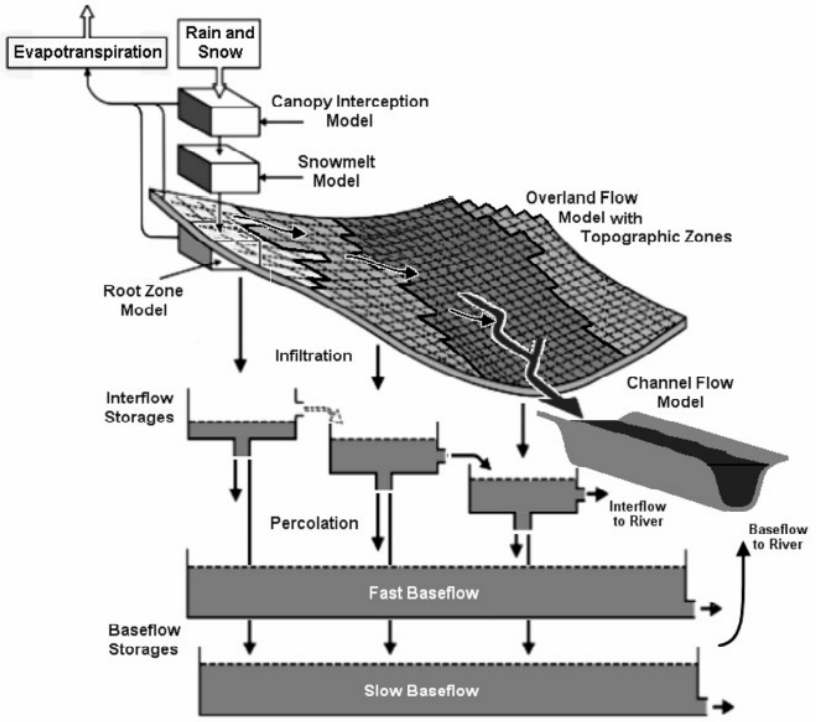

Figure 3. Schematic representation of the conceptual components in MIKE SHE - semi-distributed overland flow and linear reservoir groundwater models (Sandu and Virsta 2105).

Additional add-in for ArcGIS used by Strager et al. (2010), the WCMS, uses a spatial component dedicated to aim the analysis process and the prioritization of locations for remediation purposes. APEX is a watershed simulation application administered by the Texas A&M Agrilife Research. It has a wide range of hydrological and climate components and it can evaluate relationships among them (Golmohammadi, et al. 2014). APEX touches multiple topics such as climate predictions, hydrological cycles, land use administration, soil type modeling, and conservation (Texas A&M AgriLife Research 2016). There are multiple advantages that this software offers, however the lack of an extensive peer review articles bank is a decisive item. TOPMODEL is a hydrological software and a conceptual model that simulates all the components of the hydrological cycle through a basin. It was developed more than 40 years ago. The topography of the watershed is considered to generate runoff models. Among its advantages are the "simplicity and the possibility of visualizing the predictions of the model in a spatial context", turning it into a physically based model as well (Devi, Ganasri and Dwarakish, 2015; Beven, 1997; Peng, Zhijia and Fan, 2008). The model is simple because it uses a topographic index, however, it diminishes the flexibility of the basin dynamics (Beven, 1997). BASINS, developed by the USEPA, has been used widely for hydrological model development, integrating basin data for the whole USA continent, modeling tools, and GIS. The study of the effects of urbanization in the water quality and quantity can be well determined by the BASINS system, as demonstrated by Mohamoud, Sigleo and Parmar (2009). BASINS is a handy tool to model total maximum daily loads (TMDLs) and to reference non-point sources, however, the creation of snowmelt predictions has not been yet verified.

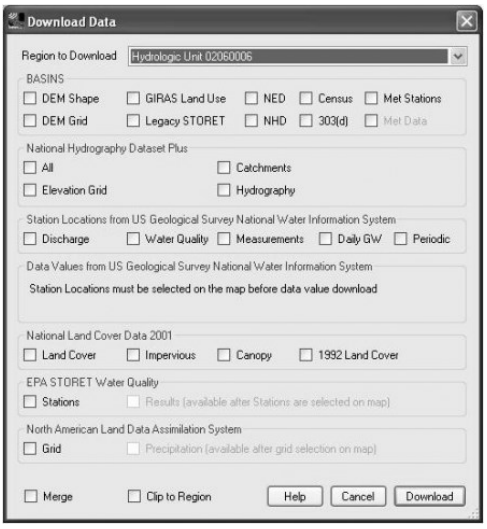

Figure 4. BASINS download module; this is one of the main modules of the software to download hydrologic, geological, and soil datasets (United States Environmental Protection Agency 2016).

The advantage of this software is the capacity to work independently from any commercial GIS platform allowing at the same time the migration to different formats. Also, the capacity to interact with different datasets such as the National Hydrography Dataset (NHD), USGS water stations, and National Land Cover Data among others, in just one module as shown above (United States Environmental Protection Agency, 2016). SWAT is a multi-spectral hydrological package, it has been used for many authors to solve multiple and complex hydrological and environmental issues. Dissolve Organic Carbon (DOC) is a fundamental component of a water natural system and hence it has been studied to understand the relationship between the natural balance and the environmental effects over stream flow. SWAT helped understand the relationship and determined the considerable elements impacting DOC balance such as streamflow, drainage area, and percentage of land cover (Tian et al., 2012). In contrast with Sheshukov et al., (2011), soil information is not a relevant data for the accurate analysis of DOC as found also by Kim et al., (2012) in its

research for the analysis of different datasets resolution in the accuracy of a SWAT model. In Sheshukov, et al. (2011), soil resolution is an important factor in hydrological models and ArcSWAT was a facilitator by the integration with the Soil Survey Geographic database (SSURGO) and the development of a tool using Visual Basic as a frame language. Soil erosion and GIS resolution for datasets is also a very good example of SWAT flexibility. Kim, et al. (2012) demonstrated that the runoff and the transport of suspended sediments generated by the SWAT model is directly connected to the quality and resolution of the GIS datasets entered into it. In Kim's final conclusion, the 30 m DEM was the one that produced the best model results in the SWAT outputs, however no relevant improvements were obtained by combining different resolutions of soil and land use, this reiterates the findings of the previous authors regarding, mainly, about soil datasets. SWAT can be defined in different temporal events, ranging from years, days, hours, and sub-hours scales. One of the hourly studies, Debele, Srinivasan and Parlange (2008), demonstrated that the disaggregation in daily runoff may improve the accuracy of SWAT models by implemented an enhanced SWAT variation for this purpose.

Different studies such as Yang, Liu et al., (2016) and Maharjan et al., (2013), have been developed regarding the temporal use of SWAT models into hourly or sub-hourly time lapses; some conclusions appointed that the hourly lapse is better than the sub-hourly lapse, even though the sub-hourly time lapse improves the prediction of high flows in comparison with daily SWAT models (Jeong et al., 2010). As we suggested previously, SWAT is a very versatile hydrological package that can be used in watersheds with scarce data availability, as demonstrated by Malunjkar et al., (2015), reaching high efficiency values in the calibration and validation cycles. Similarly, with the methodology for time lapses used by Malunjkar et

al., (2015), developing the SWAT model in different years for calibration and validation processes. Arnold, Moriasi et al., (2012), Daggupati et al., (2015), and Zhang, Srinivasan and Van Liew (2008) suggested that is a good practice to split the data in two different groups, one for calibration and the other for validation. These two processes are the core and the success of the hydrological model; it may be a very convoluted task. However, innovative ways for calibration and validation have been proposed by adding into the equation the calibration of crops, the traditional streamflow, sediments, and the incorporation of total nitrogen and total phosphorus for both processes in studies regarding nutrient flows into a basin (Malagó, et al. 2017). Few SWAT studies have been focused on evaluation of snowfall and snowmelt processes and parameters to increase the precision of the model using the snow variables. SWAT calculates snowmelt simulations by the study of the threshold temperatures, and in the case of snowpacks the calculation is given by the following equation:

$$T_{spi} = T_{spi-1}(1\text{-}TIMP) + T_{ai}TIMP \tag{3}$$

where TIMP is the snow temperature hysteresis factor that implicitly accounts for snowpack density, water content, and exposure; T_{spi} and T_{spi-1} are the snowpack temperature on the current day (i) and the previous day (i-1); and Tai is the mean air temperature on day 1 (Wang et al., 2016). Wang et al., (2016) demonstrated the sensitivity of certain parameters and the insensitivity of others and concluded that it was a complex process and the complete certainty regarding the snowmelt model was not obvious and it required further investigation.

SWAT is a resourceful solution for a wide spectrum of hydrological and environmental issues in the real world and it has been utilized for many years to predict runoff behaviors, water quality analysis, and entrance of pollutants into water systems. In

more recent years, the GIS-integrated model, ArcSWAT has transformed SWAT into a robust and dynamic modeling software.

CHAPTER 3

METHODOLOGY

3.1 Data Collection

The present research consists of three main components; the first one is the collection and analysis of initial datasets, the second one is the exploratory statistical relations among different physical and climatology datasets (shown in chapter 4), and the third one is the creation of a hydrological model to verify the findings during the statistical process. During the initial process, the selection of the weather and water stations was defined. The stations were selected based on two criteria: spatial locations and datasets availability. We adopted six water stations administered by the USGS, nine weather stations administered by the High Plains Regional Climate Center (HPRCC), and two weather stations administered by the University of Missouri Extension (UMOEXT). To see the initial analysis of all stations, go to appendix B. Table 1 shows the overall final selection of weather stations.

Table 1. Climate stations for the ArcSWAT model.

NAME	STATE	LATITUDE	LONGITUDE	BEGIN DATE	END DATE	STATION TYPE	PARAMETERS
OLATHE 3.3 ENE (KSJO0006)	KS	38.9049	-94.7569		Current	HPRCC	MXT,MT,P,S,SD
OLATHE JOHNSON CO EXEC AP (KOJC)	KS	38.85	-94.73917	2000-7-31	Current	HPRCC	MXT,MT,P,S,SD
OLATHE JOHNSON CO AP (KIXD)	KS	38.83167	-94.88972	2000-10-6	Current	HPRCC	MXT,MT,P,S,SD
OTTAWA (OTTK1)	KS	38.62	-95.28	1985-3-28	Current	HPRCC	MXT,MT,P,W,ST,SR,RH,ET
OVERLAND PARK S 87TH (OPSK1)	KS	38.9533	-94.7142	2000-1-4	Current	HPRCC	P,S,SD
SILVERLAKE (a147399)	KS	39.07	-95.77	1985-3-28	Current	HPRCC	MXT,MT,P,W,ST,SR,RH,ET
KANSAS CITY DOWNTOWN AP (KMKC)	MO	39.12	-94.6	2000-8-15	Current	HPRCC	MXT,MT,P,S,SD
KANSAS CITY WATTS MILL (KCWM7)	MO	38.9464	-94.6047	2006-4-23	Current	HPRCC	P,S,SD
LEES SUMMIT MUNI AP (KLXT)	MO	38.96	-94.37	2001-10-26	Current	HPRCC	MXT,MT,P,S,SD
BRUNSWICK (UMOBRUN)	MO	39.412667	-93.1965	2008-12-1	Current	UMOEXT	W,SR,ET
GREEN RIDGE (UMOGREEN)	MO	38.621147	-93.416652	2008-12-1	Current	UMOEXT	W,SR,ET

Average Relative Humidity (RH), Average Soil Temperature at 10 centimeters (ST), Evapotranspiration (ET), Global Solar Radiation (SR), Maximum Temperature (MXT), Minimum Temperature (MT), Precipitation (P), Snowfall (S), Snow Depth (SD), Winds (W)

To assign the most accurate value of snow to a certain sub-basin the Thiessen Method was used. It is well known that this technique should not be used if the terrain is mountainous. This technique creates polygons of influence based on the distance or weight to each of the stations within the basin; one polygon belongs to just one station (Fetter 2001). This information is essential when executing calculations within each of the sub-basins produced by SWAT in the Indian Creek. Figure 5 shows the water stations and seven of the weather stations administered by the HPRCC, and the Thiessen polygons indicating the distribution of the sub-basins related to the four weather stations, which are within the area of interest.

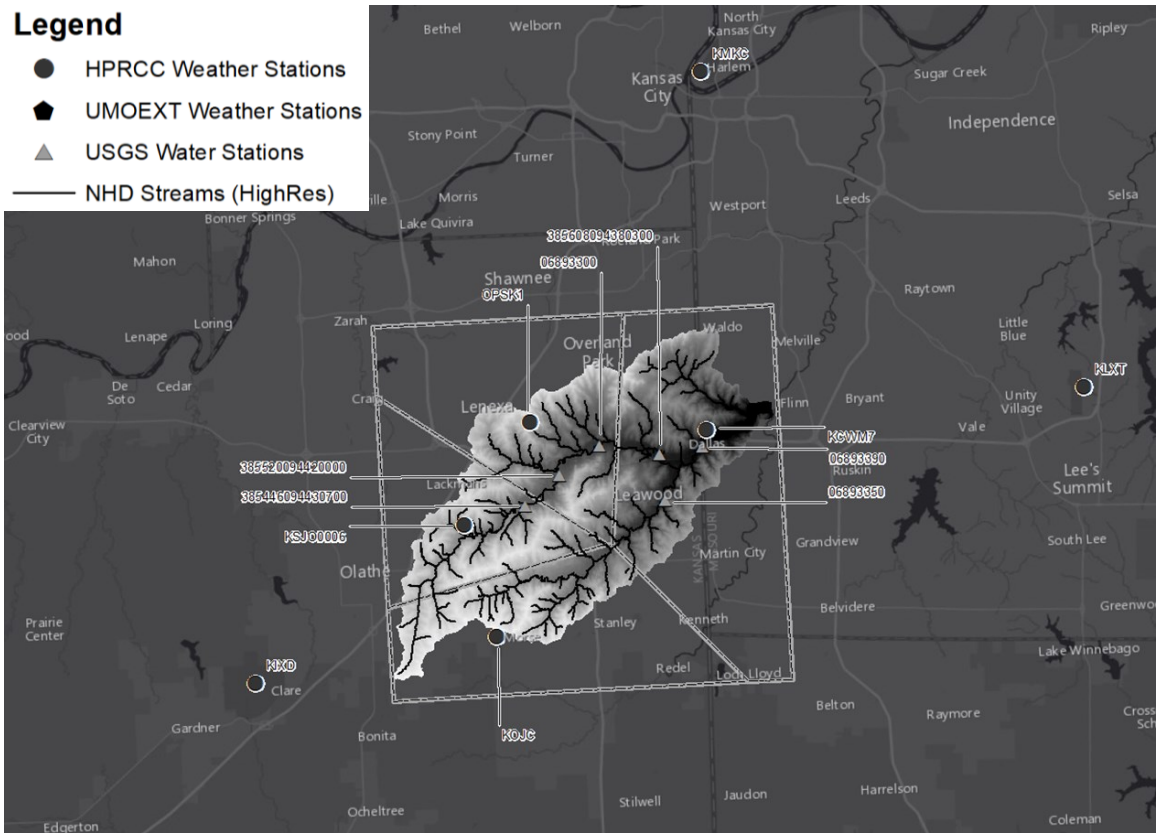

Figure 5. Thiessen polygons of influence based on climate stations within the watershed (AIMS 2014), (ESRI Data Maps 2016), (USGS NHD Data 2016).

Additional weather stations were selected due to the limitations of spatial coverage. All the stations that are more than 20 miles away from the study area provide the datasets for potential evaporation/evapotranspiration, relative humidity, solar radiation, and wind.

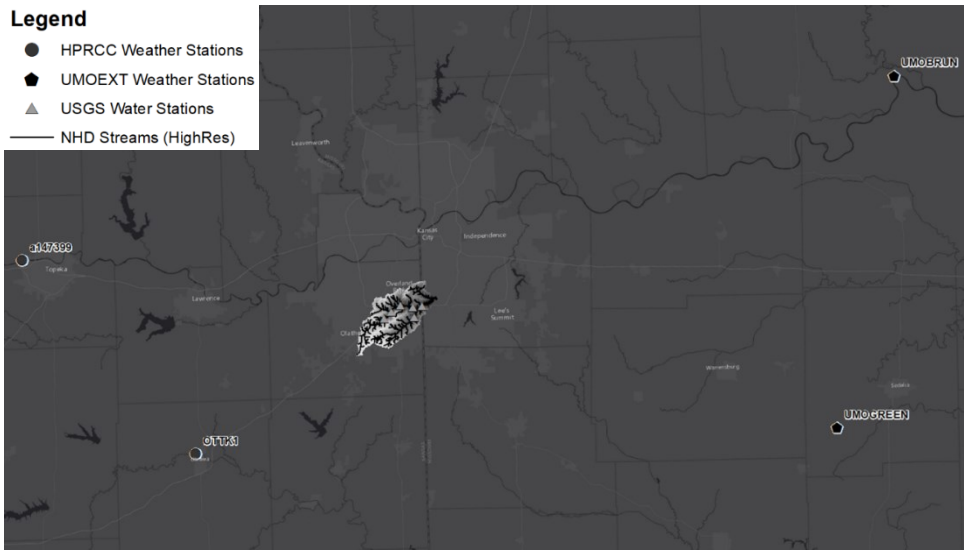

Figure 6. Distant weather stations containing ET, RH, SR, and W parameters (AIMS 2014), (ESRI Data Maps 2016), (USGS NHD Data 2016).

Once the weather and water stations were defined, the next step was to check the data quality and time interval.

Table 2. Time lapse and parameters availability by station.

PARAMETERS		DISCHARGE	CONDUCTANCE	TURBIDITY	PRECIPITATION	PET	REL HUMIDITY	SOLAR RAD	TEMPERATURE	WIND
USGS STATIONS	6893300	12/1/08 - 2/13/15	5/18/11 - 7/9/13	5/18/11 - 7/5/13						
	6893350	7/9/11 - 2/13/15	5/17/11 - 8/4/13	5/17/11 - 8/4/13						
	6893390	12/1/04 - 2/13/15	12/1/04 - 9/23/14	12/1/04 - 9/23/14						
	385446094430700	6/17/11 - 7/17/13	6/8/11 - 7/9/13	6/8/11 - 5/15/13						
	385520094420000	6/14/11 - 7/17/13	5/17/11 - 7/9/13	5/17/11 - 7/10/13						
	385608094380300	6/13/11 - 7/11/13	5/17/11 - 7/10/13	5/17/11 - 7/10/13						
HPRCC STATIONS	KCWM7				12/1/08 - 2/13/15					
	KOJC				12/1/08 - 2/13/15				12/1/08 - 2/13/15	
	OPSK1				12/1/08 - 2/13/15					
	KSJO0006				12/1/08 - 2/13/15					
	KIXD								12/1/08 - 2/13/15	
	KLXT								12/1/08 - 2/13/15	
	KMKC								12/1/08 - 2/13/15	

PARAMETERS		DISCHARGE	CONDUCTANCE	TURBIDITY	PRECIPITATION	PET	REL HUMIDITY	SOLAR RAD	TEMPERATURE	WIND
HPRCC STATIONS	OTTK1					12/1/08 - 2/13/15	12/1/08 - 2/13/15	12/1/08 - 2/13/15		12/1/08 - 2/13/15
	A147399					12/1/08 - 2/13/15	12/1/08 - 2/13/15	12/1/08 - 2/13/15		12/1/08 - 2/13/15
UMOEXT STATIONS	UMOBRUN					6/13/13 - 2/13/15		12/1/08 - 2/13/15		12/1/08 - 2/13/15
	UMOGREEN					6/4/13 - 2/13/15		12/1/08 - 2/13/15		12/1/08 - 2/13/15

After the analysis of the parameters, the development or scout for a high resolution DEM was necessary. The DEM was essential to produce a good result in the process of sub-basin delineation. The Automated Information Mapping System (AIMS) had the best DEM at resolutions of 3 feet (0.9411 m). A comparison between two different resolutions is shown in the figure below.

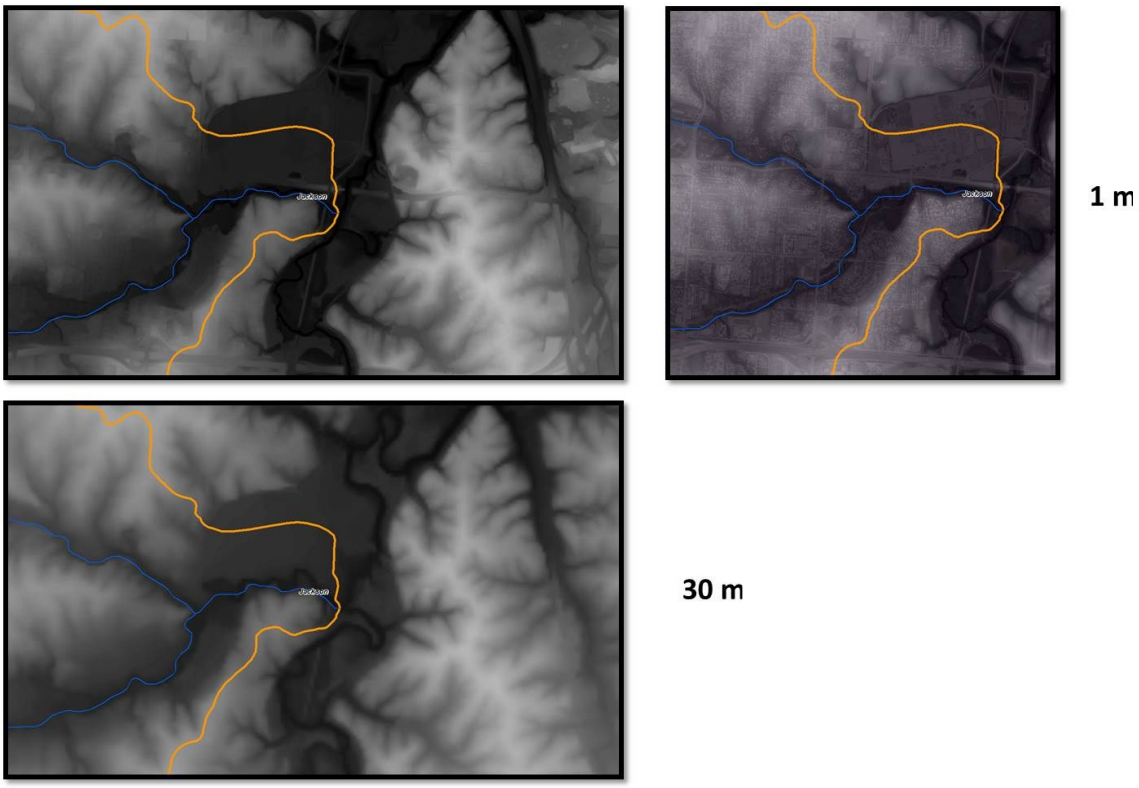

Figure 7. Comparison between 1 m DEM vs 30 m DEM (AIMS 2014), (USGS NHD Data 2016).

Because this is an urban landscape it is fundamental to define not just the stream path but also the roads that are routing the path of liquids and oils. The 1 meter DEM is a bare land DEM, so it means it has no canopy or building heights, so it can follow more accurately

the real earth's surface to improve the accuracy of the hydrological model. The DEM was improved by a process in which certain holes in the surface were filled out through a geospatial analysis method called 'fill', which basically fills sinks in a raster dataset to remove small imperfections on the data. Also, it was improved by a process that smooths the edges of a raster called 'filter' (Environmental Systems Research Institute (ESRI) 2016). ArcScene® by ESRI, helps visualize the differences in elevations even when the differences are not big or abundant. ArcScene has 3D visualization capabilities that allows creation of surfaces, rotation, augmentation, and other visual effects manipulations. Figures 8 and 9 show the DEMs before and after the fill and filter process created by ArcScene® showing the 3D effect with a vertical exaggeration of x10.

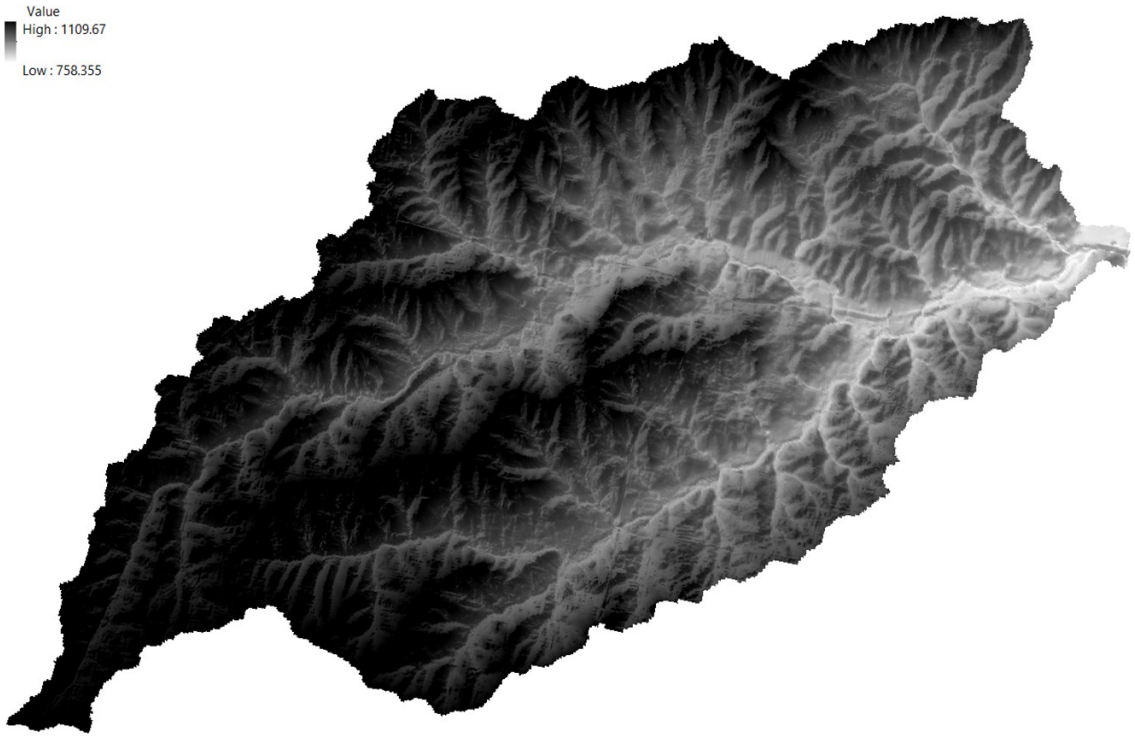

Figure 8. DEM before the filling and filtering process (AIMS 2014), (USGS NHD Data 2016).

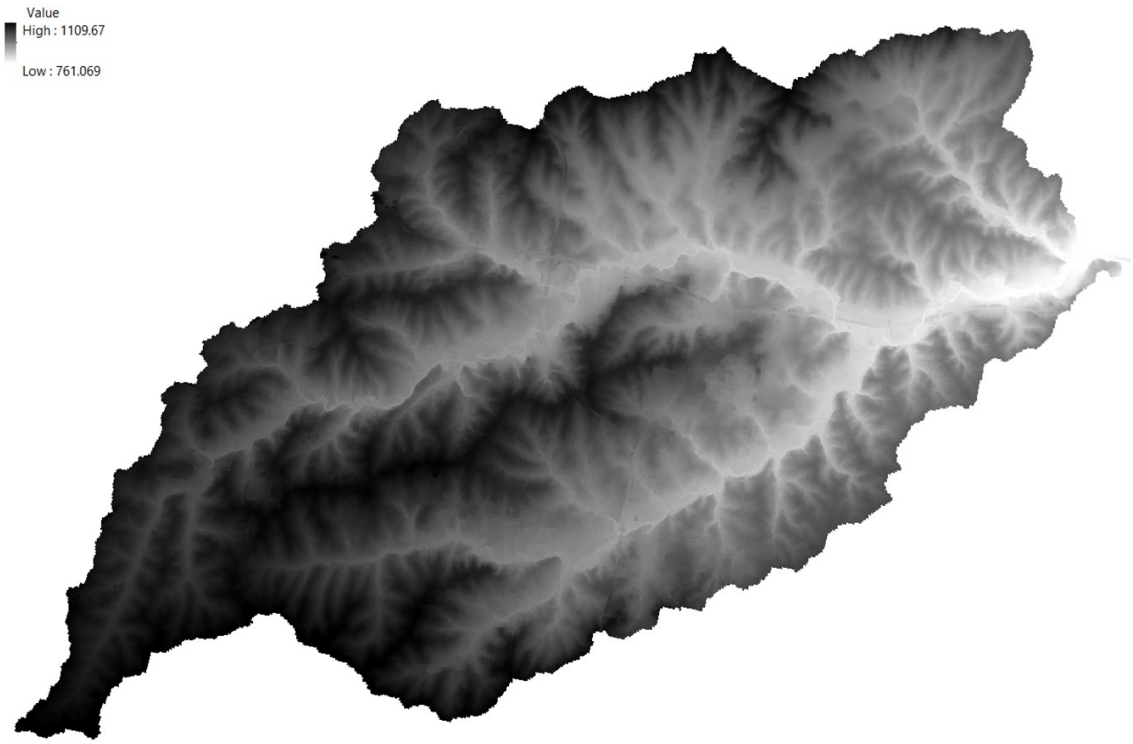

Figure 9. DEM after the filling and filtering process (AIMS 2014), (USGS NHD Data 2016).

Notice that the low elevation changed from 758.355 ft to 761.069 ft whereas the high elevation stayed the same; this is due to the filling process.

Besides the DEM, a soils and land use rasters were obtained from the USGS datasets. The soil raster was computed or merged because it had two parts, one for the Kansas portion of the basin and another for the Missouri portion of the basin. The table below shows the datasets that were collected and analyzed to prepare the statistical analysis and the hydrological model.

Table 3. Initial dataset's source information.

Dataset	Format	Source	Organization	Year
Flowlines	Vector	NHD	USGS - USEPA	2016
Waterbodies	Vector	NHD	USGS - USEPA	2016
Land Cover/Land Use	Raster	NLCD	USGS	2011 - 2012
DEM	Raster	AIMS	AIMS	2014
Soils	Raster	NRCS	USDA	2012 - 2013
HPRCC Weather Stations	Vector	HPRCC	HPRCC	2015 - 2016
UMOEXT Weather Stations	Vector	UMOEXT	UMOEXT	2015 - 2016

Dataset	Format	Source	Organization	Year
USGS Weather Stations	Vector	USGS	USGS	2015
Aerial Imagery	Raster	NAIP	USDA	2014
Golf Courses	Vector	AIMS	AIMS	2014
Counties	Vector	TIGER	USCB	2011

National Hydrography Dataset(NHD)
United States Environmental Protection Agency (USEPA)
National Land Cover Database (NLCD)
Natural Resources Conservation Service (NRCS)
National Agriculture Imagery Program (NAIP)
Topologically Integrated Geographic Encoding and Referencing (TIGER)
United States Census Bureau (USCB)

The flowlines, waterbodies, and golf courses were used to adjust the initial land cover/land use raster and improve the accuracy of the hydrological model.

3.2 Hydrological Model Development

SWAT is a hydrological model with an extensive number of parameters; it has been developed and successfully applied for more than 25 years to help understand the water cycles and land management practices. ArcSWAT is an add-in extension developed to integrate the SWAT capabilities with the power of GIS analysis. Initially, the hydrological tool was created to assist in the convoluted task of assess the consequences of land management practices in the soil and water (Dile, et al. 2016). The software allows introduction of multiple topographic, physical, and chemical parameters. It is a multi-purpose and sophisticated scientific tool that requires a substantial number of parameters to simulate the characteristics and complexities of the basins. One of the main keys of success in the analysis is the quality and quantity of the data entry process. In order to improve the initial modeling, it is essential to have calibration and validation processes with two different time steps. Figure 10 shows a general flow chart of the ArcSWAT processes.

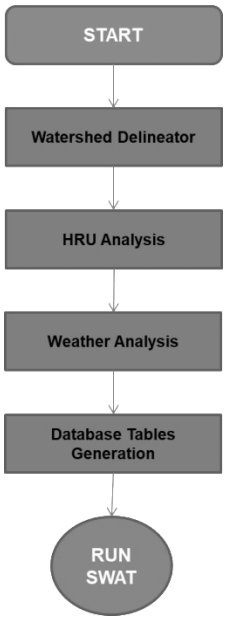

Figure 10. General flowchart of ArcSWAT as developed in this study.

SWAT employs variety of physical and climate parameters to predict runoff. SWAT runoff is determined by the SCS Curve Number estimated from DEM, soil data and land use among other elements. The ingredients of the runoff are determined by the following equation:

$$Q_{surf} = \frac{(R_{day} - 0.2S)^2}{(R_{day} + 0.8S)}, S = 25.4(\frac{1000}{CN} - 10) \quad (4)$$

where, Q_{surf} is the accumulated runoff or rainfall excess (mm H_2O), R_{day} is the rainfall depth for the day (mm H_2O) that varies spatially due to changes in soils, land use, and management, *CN* is the Curve Number for the day (Kim, et al. 2012).

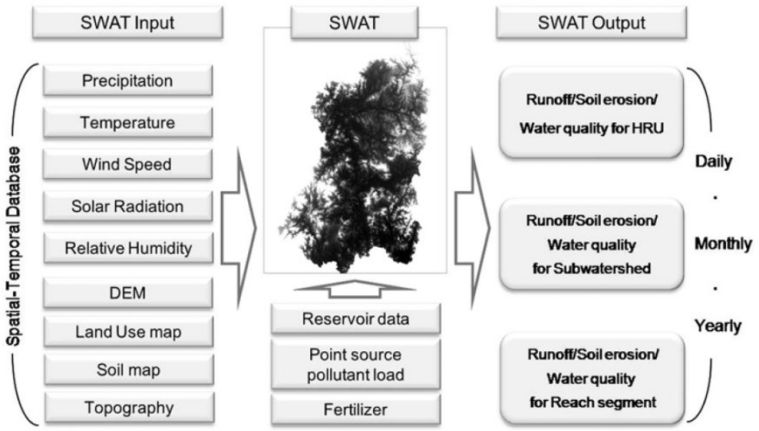

Figure 11. Input and output data structure for SWAT. This figure depicts the main input datasets, the running SWAT process, and the temporal output (Kim, et al. 2012)**.**

In Debele, Srinivasan and Parlange (2008), two methods of disaggregation were used: univariate assuming that there are no more than one rainfall event during a single day, and multivariate taking into account no only the datasets but also its spatio-temporal distribution for the disaggregation approach. In the final outcome of the model, the hypothesis of the use of disaggregation methods improved the final results (Debele, Srinivasan and Parlange 2008).

The research was developed over the ESRI software ArcGIS Advanced License, version 10.3.1 for Desktop and the ArcSWAT version 2012.10.0.9. Several processes were developed to obtain a hydrological model with satisfactory accuracy for future predictions. The hydrological data allow analyzing the basin at catchment levels. In this development, various water balance parameters such as velocity, drainage surface area, slope, vegetation index, soil, land use, imperviousness, evapotranspiration, filtration, rainfall, and runoff are simulated.

The amount of equations to analyze the transport times of pollutants may be overwhelming, but it is important to compare results and utilize the equation that better fits

the characteristics of the basin. (Wong 2005), (Almeida et al., 2014), (Wong and Li 1998) have dedicated investigations about the assessment of the time of concentrations in overland flow equations. Wong and Li (1998) suggested that there are two kinds of formulas, one that take into account the rain intensity and the other that does not. The study shows that the formulas employing the rainfall intensity as a parameter are more adjusted to the real values. Also, Wong and Li (1998) studied the effects of urbanization in the decrease of time of concentrations, assuming that the slope, roughness, and rain intensity are constant. Wong (2005) has evaluated overland flow equations developed during the last 70 years by different hydrology studies and has determined the efficiency of the equations through the R^2 function:

$$R^2 = 1 - \frac{\Sigma(t_{oo} - t_{oe})^2}{\Sigma(t_{oo} - t_{om})^2} \tag{5}$$

where t_{oo} is the observed overland time of concentration; t_{oe} is the estimated overland time of concentration; and t_{om} is the mean of all the observed overland times of concentration. The more accurate and interesting equations are the equation of the United States Army Corps of Engineers' (USACE) Formula (1954), the Kerby's Formula (1959), and the Chen and Wong's Formula (1993).

USACE's Formula

$$t_o = \left(10.57 + \frac{0.12}{S_o}\right)\left(\frac{L_o}{30.48}\right)^{0.55-(0.001/S_o)} \quad i_n^{-0.43} \tag{6}$$

where t_o (min) is the time of concentration overland, S_o (m m^{-1}) is the overland slope, L_o (m) is length of overland flow, and i_n (mm h^{-1}) is the net rainfall intensity. This equation was developed for concrete (typical urban surface) and in the assessment the R^2 equals 0.94; the highest accuracy value among the other equations (Wong 2005).

Kerby's Formula

$$t_o = 1.45(N_k L_o / S_o^{0.5})^{0.467} \quad (7)$$

where t_o (min) is the time of concentration overland, N_k is the retardance coefficient, L_o (m) is the length of overland flow, and S_o (m m^{-1}) is the overland slope. This equation is simple and represents one of the equations that do not use rainfall intensity as part of the components (Wong 2005).

Chen and Wong's Formula

$$t_o = \left(\frac{0.21(3.6\ x\ 10^6 v)^k C L_o^{2-k}}{S_o i_n^{1+k}} \right)^{1/3} \quad (8)$$

where t_o (min) is the time of concentration overland, C=3 and k=0.5 are constants, v=0.874x10^{-6} m^{2}s^{-1} for water at 26 ^{o}C, S_o (m m^{-1}) is the overland slope, L_o (m) is the length of overland flow, and i_n (mm h^{-1}) is the net rainfall intensity. The values for constants C and k are for the concrete and this equation gives better results for permeable and impermeable surfaces (Wong 2005).

Additionally, some studies describe the equations with limitations of use by dependencies on source (rural or urban), areas, lengths, and steepness (Almeida, et al. 2014). In the Almeida's study the equations for better adjustment in urban basins are the McCuen et al. Equation (1984), Carter Equation (1961), and Woolhiser&Liggett's Equation (1967).

McCuen et al. Equation

$$T_c = 2.2535 i^{-0.7164} L^{0.5552} S^{-0.2070} \quad (9)$$

where T_c (h) is the time of concentration, i (mm/h) is the rainfall intensity, L (km) is the length of the main stream in the watershed, and S (m/m) is the mean steepness. Although the

area is recommended for basins of maximum 16 km^2, it is originated from urban basins with moderate steepness ratio (Almeida, et al. 2014).

Carter Equation

$$T_c = 0.0977 L^{06} S^{-0.3} \tag{10}$$

where T_c (h) is the time of concentration, L (km) is the length of the main stream in the watershed, and S (m/m) is the mean steepness. Although the area is recommended for basins of maximum 20.72 km^2, it is originated from urban basins with moderate steepness ratio and does not account for rainfall intensity (Almeida, et al. 2014).

Woolhiser & Liggett's Equation

$$T_c = 7.3015 \left(\frac{nL}{S^{0.5}}\right)^{0.6} \quad i_n^{-0.4} \tag{11}$$

where T_c (h) is the time of concentration, n (m$^{-1/3}$s) is the Manning's roughness coefficient (see appendix C), L (km) is the length of the main stream in the watershed, S (m/m) is the mean steepness, and i (mm/h) is the rainfall intensity. This equation does not have restrictions in area or steepness and it is based on the theory of kinematic wave which take into consideration constant rainfall intensity, large canals as flowing surfaces, and is suitable for overland flow with great surface runoff and lateral recharges (Almeida, et al. 2014) and (Miller 1983).

The development of the hydrological model is the next step in the process. The very first step before the start of modeling was the project set-up. An *mxd* project was created over the ArcGIS interface with an option to create an initial *mdb* personal geodatabase to store vector data and an empty *mdb* personal geodatabase to store rasters and an *mdb* personal geodatabase for parameter setup. The overall work flow is shown in Figure 12.

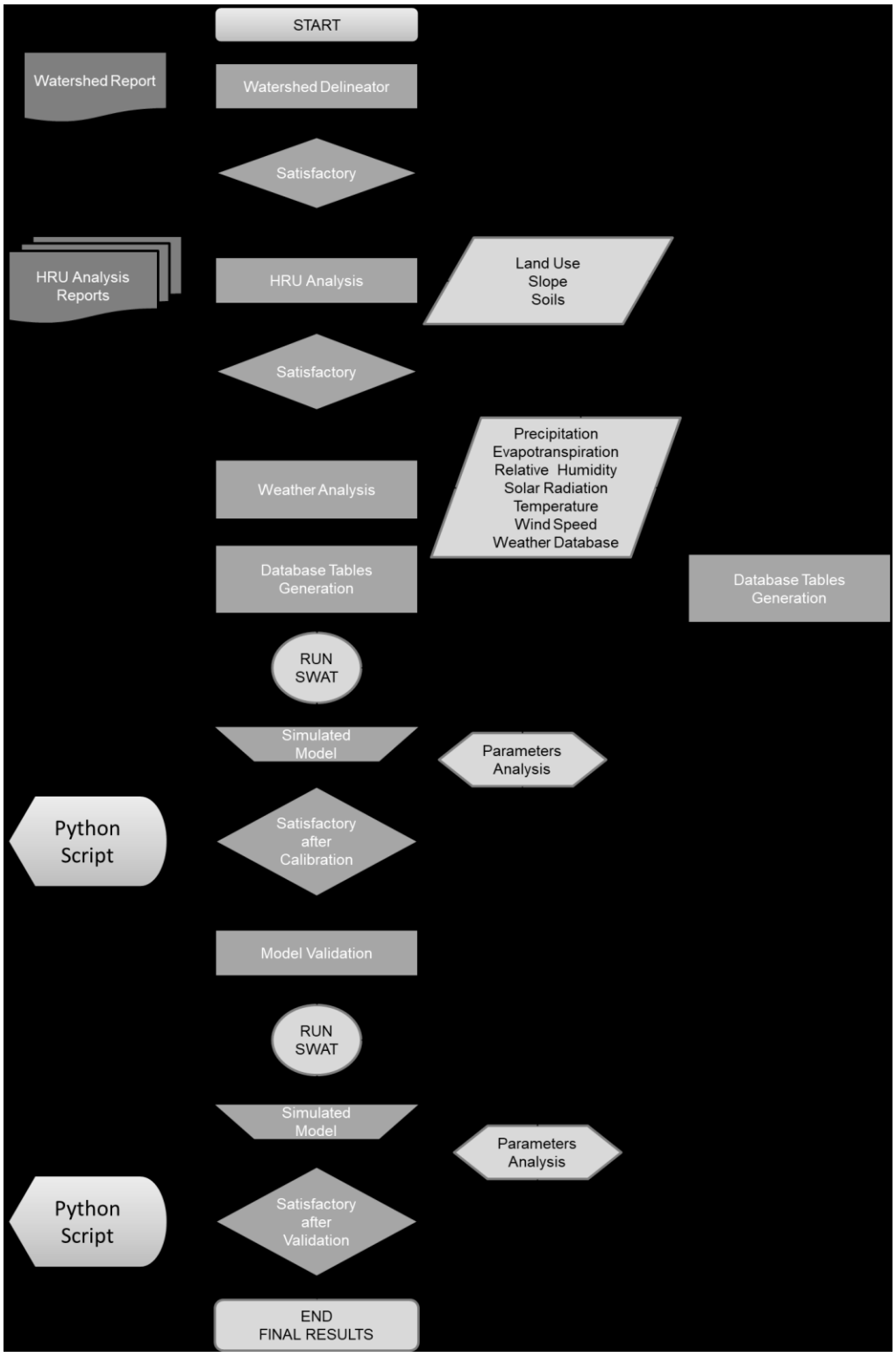

Figure 12. ArcSWAT Model specific work flow developed during the study.

The systematic order of the hydrological model development was as follows:

3.2.1 Watershed Delineator

The first step was to develop a watershed that may be added by user or created from scratch by ArcSWAT system. The tool uses the Spatial Analyst extension of ArcGIS (Winchell, et al. 2013). In this study the watershed sub-basins delineation was created by using the high resolution DEM (3 feet – 0.914 meters), a high resolution streams dataset, and a pre-determined watershed. The DEM was converted to meters with the spatial projection NAD 1983 State Plane Kansas North FIPS 1501. In the delineation process more layers were created, they were a selected number of streams called Reach, Outlets for each of the sub-basins, and Monitoring Points. Once the sub-basins were created, evaluation of them was performed. This is one of the many quality control (QC) stages in which the delineation of the sub-basins was evaluated. Basically, the process of evaluation was subjective to the number of sub-basins and the distribution and limits of each of them. The number of sub-basins was controlled by the number of segments of the streams layer. After running three watershed delineation processes a final sub-basin scheme was chosen. The basin system comprises 35 sub-basins, 35 monitoring points or outlets, and 35 reach segments. At this point, waterbodies were taken into account to add into the process features such as reservoirs; fundamental for sub-basin parameter estimation. One of the main characteristics of this step was that every single sub-basin should have one and just one reach segment. The other important part of the step was to verify whether water outlets correspond to the location of the water stations, because this will minimize the spatial error when comparing the observed discharge and the simulated runoff. In this process, the resolution of the DEM was a key factor because too much resolution implies more system processing time. Figure 13 shows the final watershed sub-basins delineation with the reaches and outlets.

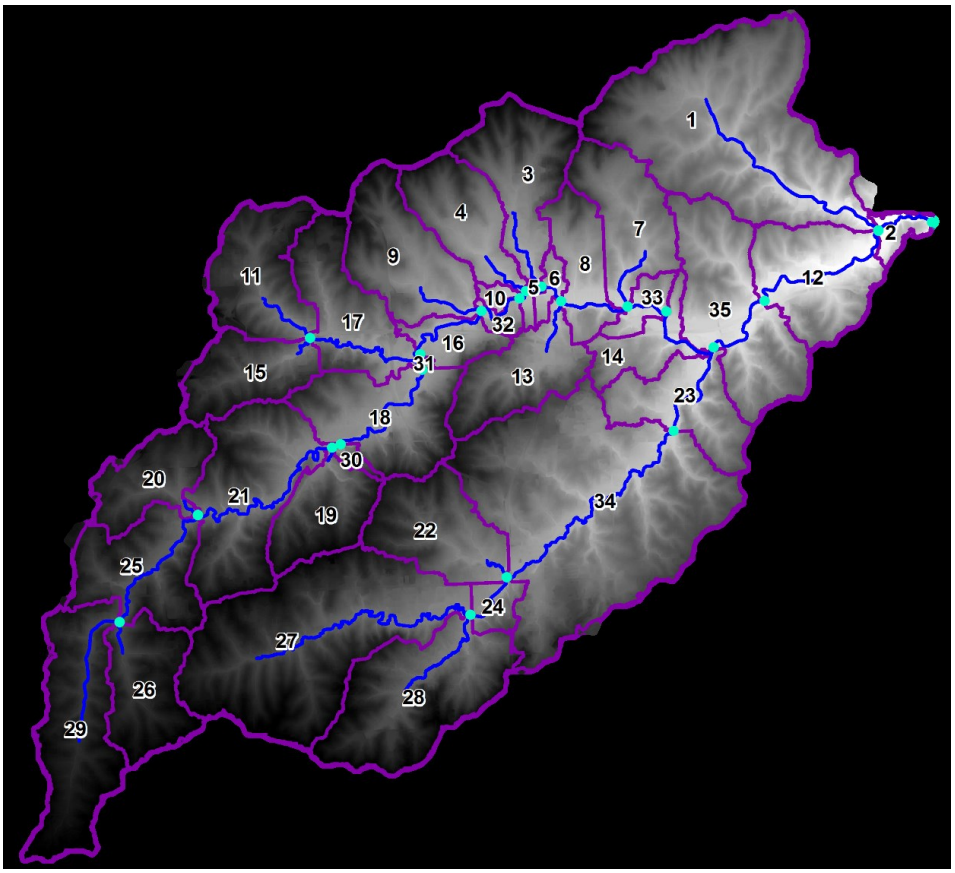

Figure 13. ArcSWAT Watershed and sub-basin model generated during the watershed delineation process (AIMS 2014), (USGS NHD Data 2016).

3.2.2 HRU Analysis

The Hydrologic Response Units (HRUs) are sub-sections of the sub-basins that were defined by differences in land use, soils, and slope (Winchell et al., 2013). The first step in the process was the addition of the land use into the model. LULC is a raster with classified land uses of the basin and it is necessary to re-classify the LULC to map out the dataset with a look-up table pre-existent in ArcSWAT. Also, it was necessary to validate the land use with the help of waterbodies datasets, streams datasets, and a recent high resolution imagery; for this research the chosen imagery was 2014. Below is the chart of the reclassification.

Table 4. LULC reclassification.

Land Use (Raw Data)	Description	Land Use (Re-classified)	Percentage	Description
11	Open Water	**11**	0.13	Open Water
21	Developed, Open Space	**21**	21.80	Developed, Low Intensity/Open Space
22	Developed, Low Intensity	**22**	46.63	Developed, Low/Medium Intensity
23	Developed, Medium Intensity	**23**	17.99	Developed, Medium Intensity
24	Developed, High Intensity	**24**	6.15	Developed, High Intensity
31	Barren Land	**31**	0.04	Barren Land
41	Deciduous Forest	**41**	2.45	Deciduous Forest
42	Evergreen Forest	**42**	0.01	Evergreen Forest
43	Mixed Forest			
52	Shrub/Scrub	**52**	0.04	Shrub/Scrub
71	Herbaceuous	**71**	0.40	Herbaceuous
81	Hay/Pasture	**81**	2.57	Hay/Pasture
82	Cultivated Crops	**82**	1.56	Cultivated Crops
90	Woody Wetlands	**90**	0.20	Woody Wetlands
95	Emergent Herbaceuous Wetlands	**95**	0.04	Emergent Herbaceuous Wetlands

As indicated in Table 4, this is an urban basin with approximately 92% corresponding to development areas.

The second step was to add the soils information into the model. The soil data has multiple classifications depending on the State. Therefore, some soils in Kansas has no matching classification in Missouri and vice versa. In order to minimize the disagreement between states and reclassify the soils, the acquired soil information was compared to the ArcSWAT SSURGO database to find the most similar designation corresponding to the characteristics of the soils in Kansas and Missouri. The key for the search in the SSURGO database was the Map Unit Key (MUKEY). However, not always was possible to match the soils for both states. Figure 14 depicts the entire soil map for the whole Indian Creek Basin with some disconnections between States.

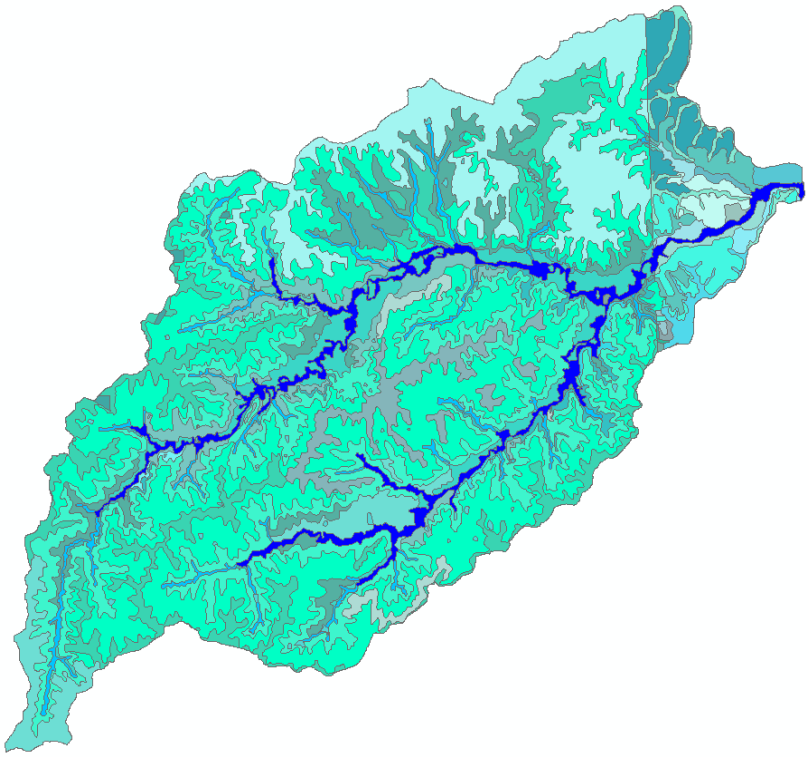

Figure 14. Soils structure for the Indian Creek Basin developed with a join tool for the KS and MO States (USDA 2012).

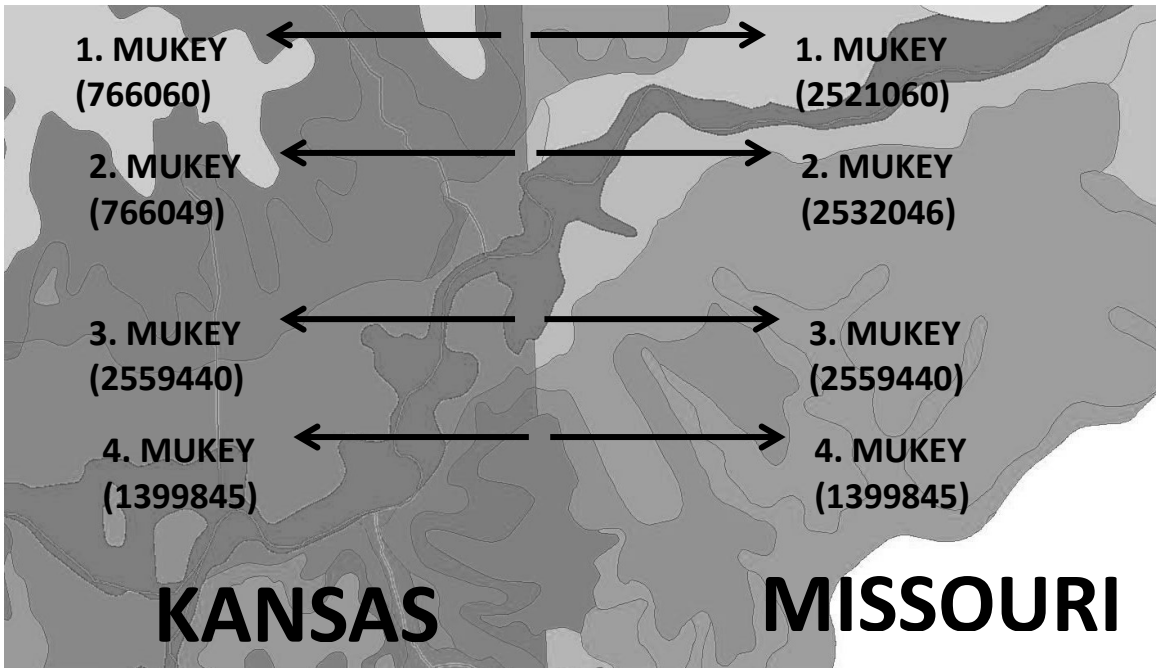

Figure 15. Similarities and differences in SSURGO state database soils (USDA 2012).

SSURGO is a reliable database developed for many years and is a representation of the characteristics of the soils with different physical aspects and properties (United States Department of Agriculture, Natural Resources Conservation Service, 2016). As a consequence, a comparison for four types of soil is shown in Figure 15, constituting an example of differences and similarities in both soil databases between Kansas and Missouri. The characteristics for each of the examples are as follow:

Example 1

Kansas

MUKEY: 766060
Map unit Name: Martin silty clay loam, 3 to 7 percent slopes
Flooding Frequency: None
Drainage Class: Moderately well drained
Hydrologic Group: D

Missouri

MUKEY: 2521060
Map unit Name: Greenton-Urban land complex, 5 to 9 percent slopes
Flooding Frequency: None
Drainage Class: Somewhat poorly drained
Hydrologic Group: D

Example 2

Kansas

MUKEY: 766049
Map unit Name: Chase silt loam, occasionally flooded
Flooding Frequency: Occasional
Drainage Class: Somewhat poorly drained
Hydrologic Group: D

Missouri

MUKEY: 2532046
Map unit Name: Bremer silt loam, 0 to 2 percent slopes, occasionally flooded
Flooding Frequency: Occasional
Drainage Class: Poorly drained

Hydrologic Group: C/D

Example 3

Kansas and Missouri

MUKEY: 2559440
Map unit Name: Kennebec silt loam, occasionally flooded
Flooding Frequency: Occasional
Drainage Class: Moderately well drained
Hydrologic Group: C

Example 4

Kansas and Missouri

MUKEY: 1399845
Map unit Name: Chillicothe silt loam, 2 to 5 percent slopes
Flooding Frequency: None
Drainage Class: Well drained
Hydrologic Group: C

As noticed in the previous cases, Examples 1 and 2 have different characteristics such as map unit name, slopes, drainage class, and hydrologic group. Also, Examples 3 and 4 have the same similarities in terms of map unit name, flooding frequency, drainage class, and hydrologic group.

The third step was to create a slope raster to add it into the model. The base of the slope raster was from DEM. During the data entry, the system required the entrance of either single or multiple slopes, for this particular research three classifications were chosen:

Slope 0 -3
Slope 3 – 10
Slope > 10

The last step in the HRU Analysis was the overlay of the land use, soil, and slope layers. In order to represent the different HRUs for each sub-basin it was crucial to define thresholds to filter information that was no representative in the sub-basin and to minimize

the amount of non-significant HRUs. The thresholds used in this research were 10%, 10%, and 20%, respectively, for the land use, soil class, and slope. It meant that, if one sub-basin had a land use percentage over a sub-basin area of less than 10%, then, it was taken out of the calculations to create the HRUs for this particular sub-basin because it was not representative of that sub-basin. After the thresholds were defined and the overlay was created, the accuracy of the model increased due to the different combinations that may influence in the evapotranspiration and the runoff calculations (Winchell et al., 2013). The final result of the overlay was a HRU Report that follows the scheme below:

		Area [ha]	Area[acres]	%Wat.Area	%Sub.Area	
SUBBASIN #	1	1800.7577	4449.7624	9.44		
LANDUSE:						
	Residential-Low Density --> URLD	832.3381	2056.7491	4.36	46.22	
	Residential --> URBN	966.8517	2389.1389	5.07	53.69	
SOILS:						
	1399845	287.3429	710.0387	1.51	15.96	
	766071	1069.6337	2643.1184	5.61	59.40	
	2521405	442.2132	1092.7309	2.32	24.56	
SLOPE:						
	3-10	1070.3974	2645.0054	5.61	59.44	
	10-9999	347.0770	857.6447	1.82	19.27	
	0-3	381.7154	943.2379	2.00	21.20	
HRUs						
1	Residential-Low Density --> URLD/1399845/3-10	185.8511	459.2473	0.97	10.32	1
2	Residential-Low Density --> URLD/1399845/10-9999	101.4918	250.7914	0.53	5.64	2
3	Residential-Low Density --> URLD/766071/3-10	380.8420	941.0796	2.00	21.15	3
4	Residential-Low Density --> URLD/766071/0-3	164.1532	405.6308	0.86	9.12	4
5	Residential --> URBN/2521405/10-9999	137.4437	339.6301	0.72	7.63	5
6	Residential --> URBN/2521405/0-3	95.2477	235.3618	0.50	5.29	6
7	Residential --> URBN/2521405/3-10	209.5218	517.7389	1.10	11.64	7
8	Residential --> URBN/766071/3-10	294.1824	726.9395	1.54	16.34	8
9	Residential --> URBN/766071/0-3	122.3145	302.2454	0.64	6.79	9
10	Residential --> URBN/766071/10-9999	108.1416	267.2232	0.57	6.01	10

Figure 16. Example of ArcSWAT HRU report scheme.

The hydrological model generated, as a result of the previous analysis, a total of 783 HRUs.

3.2.3 Weather Analysis

The weather analysis is a complex process that depends upon multiple parameters. At this point the hydrological model was divided in two time periods, one for the calibration of the model and the other for the validation of the model. For this study, we employed

precipitation, potential evapotranspiration, relative humidity, solar radiation, temperature, and wind speed as modeling parameters. Also, the time period for the calibration was from 12/1/2008 to 5/15/2012 and the one for the validation was from 5/16/2012 to 2/13/2015. Datasets of the modeling parameters were formatted into the ArcSWAT formats, then the weather source database was chosen. This weather source database was a focal point and it was a require information to process the rest of the parameters already collected. The Cooperative Observer Program (COOP) administered through the National Weather Service (NWS) database "WGEN_US_COOP_1960_2010" was chosen because the time period was very wide and it had the greater amount of stations around the United States, with 18,072 first order and second order climate stations (Winchell et al., 2013). After the database source was defined, the entry of the parameters was executed.

Parameters to enter for the weather information were as follow:

a. Rainfall data, it was entered in millimeters (mm) in a daily time step and calculated with the weather station dataset and the weather source database (see Table 2).
b. Temperature data, it was entered in Celsius degrees (C°) in a daily time step and calculated with the weather station dataset and the weather source database (see Table 2).
c. Relative Humidity data, it was entered in fraction in a daily time step and calculated with the weather station dataset and the weather source database (see Table 2).
d. Solar Radiation data, it was entered in megajoule per square meter per day (MJ/m2/day) in a daily time step and calculated with the weather station dataset and the weather source database (see Table 2).

e. Wind Speed data, it was entered in meters per second (m/s) in a daily time step and calculated with the weather station dataset and the weather source database (see Table 2).

3.2.4 Database Tables Generation

In this step different database tables were transferred to a central SWAT folder to manage the whole project input tables. Figure 17 shows the tables transferred to the central folder.

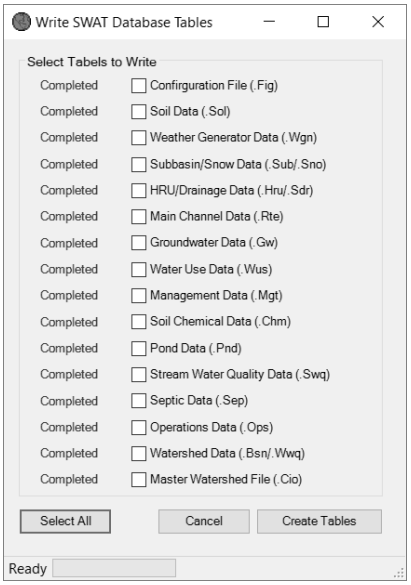

Figure 17. SWAT database tables transferred to the main database.

This is the standard transfer process from the shelf; the folder served as a collection point of the input tables that later will be transferred into a central SWAT database. The "Configuration File" contains the basic information for each of the sub-basins associating each of them to the respective file name and extension for sub-basin and route that will be created in the system. The "Soil Data" table was a table created for each of the HRUs; it contains physical characteristics of the soil present in the specific HRU. Figure 18 shows the scheme used for this type of dataset.

.Sol file Watershed HRU:782 Subbasin:35 HRU:13 Luse:URBN Soil: 766071 Slope: 3-10 08/31/2016 12:00:00 AM ArcSWAT 2012.10_0.9
Soil Name: Sharpsburg
Soil Hydrologic Group: C
Maximum rooting depth(m) : 1520.00
Porosity fraction from which anions are excluded: 0.500
Crack volume potential of soil: 0.500
Texture 1 : SIL-SICL-SICL-SICL

Depth [mm]:	230.00	330.00	890.00	1520.00
Bulk Density Moist [g/cc]:	1.33	1.38	1.38	1.43
Ave. AW Incl. Rock Frag :	0.22	0.19	0.19	0.19
Ksat. (est.) [mm/hr]:	32.40	32.40	10.80	32.40
Organic Carbon [weight %]:	1.74	1.16	0.87	0.29
Clay [weight %]:	26.00	30.00	38.00	30.00
Silt [weight %]:	70.00	67.00	59.00	64.00
Sand [weight %]:	4.00	3.00	3.00	6.00
Rock Fragments [vol. %]:	0.00	0.00	0.00	0.00
Soil Albedo (Moist) :	0.16	0.16	0.16	0.16
Erosion K :	0.32	0.43	0.43	0.43
Salinity (EC, Form 5) :	0.00	0.00	0.00	0.00
Soil pH :	6.20	5.60	5.60	6.30
Soil CACO3 :	0.00	0.00	0.00	0.00

Figure 18. Example of ArcSWAT soil tables transferred.

The "Weather Generator" tables show the information of the database chosen in the previous steps. The "Subbasin Data" table shows information such as area in square kilometers, latitude and longitude of the central point of the sub-basin, total HRUs, and the number of parameter records used within the sub-basin. Also the "Snow Data" table shows different parameters such as snowfall temperature (°C), snow melt base temperature (°C), melt factor for snow on June 21 (mmH_2O/°C-day), melt factor for snow on December 21 (mmH_2O/°C-day), and snow pack temperature lag factor. "HRU Data" table shows multiple HRU related characteristics such as average slope length, soil evaporation compensation factor (ESCO), and plant uptake compensation factor. "Drainage Data" table shows information such as effective radius of drains (mm), drainage coefficient (mm/day), pump capacity, and distance between two drain tubes or tiles (mm). "Main Channel Data" table refers to diverse properties of each reach within the sub-basin; it compiles physical characteristics of the channel affecting water processes. Some of the data related to the channel is the average width of main channel at top bank (m), depth of main channel from top of bank to bottom, average slope of main channel, and so forth (Arnold, Kiniry, et al. 2012).

3.2.5 Run SWAT (Creation of Hydrological Model for Calibration)

Once all the tables were transferred to the database, the next step was to setup and run the first SWAT Model Simulation. This simulation employed all the information coming from the central input database and the weather stations for prediction of the hydrologic processes in the watershed (see Figure 19 below).

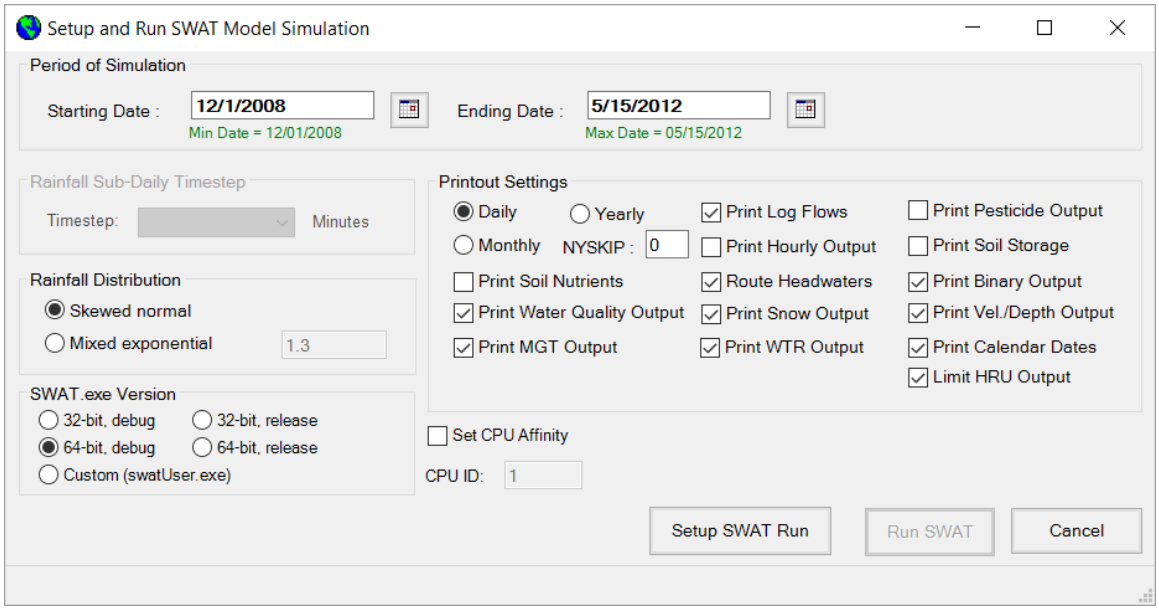

Figure 19. First set-up of ArcSWAT model simulation for calibration.

It is highly recommended to divide the time period of the simulations in two portions. One time period will be used for calibration of the model and the second time period will be used for validation of the model. The first simulation was run from December 1st, 2008 to May 15th, 2012 and the results were given in a daily time step. One of the factors taken into account was the data condition such as no data for a long time period, highly skewed information for zero rain days, 'skewed normal' rainfall distribution. Once the setup was done, the model creation was run to produce data outputs for the sub-basins, channels, and outlets. These outputs were the base for comparison between the observed data within the USGS water stations and the simulated data. A new simulation was created and the output

data was transferred to a new database through the "Read SWAT Output" option. SWAT produced a series of tables with relevant information; one of them was used to find the accuracy of the model. The "sub" and "vel" tables contain the runoff information and the channel velocity information needed to verify the accuracy of the model and the time period of snowmelt reaching the streams.

Before any calculation was made, it was imperative to separate the simulated surficial runoff from the baseflow. Several methods have been developed to do this, however, for this study the Web-based Hydrograph Analysis Tool (WHAT) developed by Purdue University was chosen. High accuracy results can be reached for calibration or validation of hydrological models (Lim, et al. 2005). The equation used for flow separation was the corresponding to the Eckhardt digital filter as follows:

$$b_t = \frac{(1 - BFI_{max}) \text{ x } \alpha + b_{t-1} + (1 - \alpha) \text{ x } BFI_{max} \text{ x } Q_t}{1 - \alpha \text{ x } BFI_{max}} \quad (12)$$

where b_t is the filtered base flow at the t time step; b_{t-1} is the filtered base flow at the t-1 time step; BFI_{max} is the maximum value of long term ratio of base flow to total streamflow; α is the filter parameter; and Q_t is the total streamflow at the t time step (Eckhardt 2005). For this research, a BFI_{max} of 0.80 was used. After the base flow was separated from the total runoff a surficial flow was found.

For verification of the model accuracy, we employed the Nash-Sutcliffe Coefficient (NSE), and the percent bias (PBIAS) as suggested by (Jeong et al., 2010), (Moriasi et al., 2007), and (Gupta, Sorooshian and Yapo 1999). The NSE was chosen because it represents the relative dimension between the residual variance and the measured data variance (Maharjan, et al. 2013), (Yang, Liu, et al. 2016), (Jeong, et al. 2010), (Saleh, et al. 2009), and

(Gupta, Sorooshian and Yapo 1999). The PBIAS was chosen because it represents the measurement of the tendency for over estimation or under estimation of simulated values compared with observed values, thus it is able to identify low quality model simulations (Jeong, et al. 2010), (Moriasi, et al. 2007), and (Gupta, Sorooshian and Yapo 1999). Results of the calibration model are shown in chapter 4.

3.2.6 Python Script Development

The development of a Python script was needed to integrate the outputs coming directly from the ArcSWAT model into the NSE and PBIAS model validation. (see appendix D). The preparation of the data for NSE and PBIAS is very expensive and tedious; it requires a lot of time to organize manually. However, with this automation by the Python script the computation time reduced more than 90% of the time; on average each simulation process requires 40 hours manually while the Python script does 2.5 hours. This same Python script will be used again to calculate the accuracy of the validation model as well. The main processes are defined in the following steps:

a. Variables Definition

The first step was to produce a geodatabase non-spatial table with the USGS discharge data and its fields and to create another file geodatabase non-spatial table with the data coming from the module *.sub* in the SWAT model. The module contains all the data of the sub-basin, physical and weather analysis; it is classified by day in time and sub-basin in space. The information in the USGS non-spatial table was developed by splitting the equations in mathematical portions (see equations 14 and 15 in chapter 4).

b. Fragmentation and Calculation

The second step was the dissolution of the data by the upstream sub-basins compounding the total area of the drainage to each of the USGS stations. In this step, the first transferring from the data coming from the hydrological model is produced. Also, the first calculations to organize the data by day and sub-basin are done here. Finally, the first calculation to find the accuracy of the model is developed; for this calculation NSE and PBIAS statistical methods were partially calculated.

c. Final Integration

The third step was the integration of all the statistical values for the data from each USGS station, into the central estimation of the NSE and PBIAS.

3.2.7 Run SWAT (Creation of Hydrological Model for Validation)

Once all the tables for the validation process were transferred to the database, the next step was to setup and run the SWAT Model Simulation. This simulation took all the data coming from the central input database and the weather stations, and predicted the hydrological processes in the watershed (see Figure 20 below).

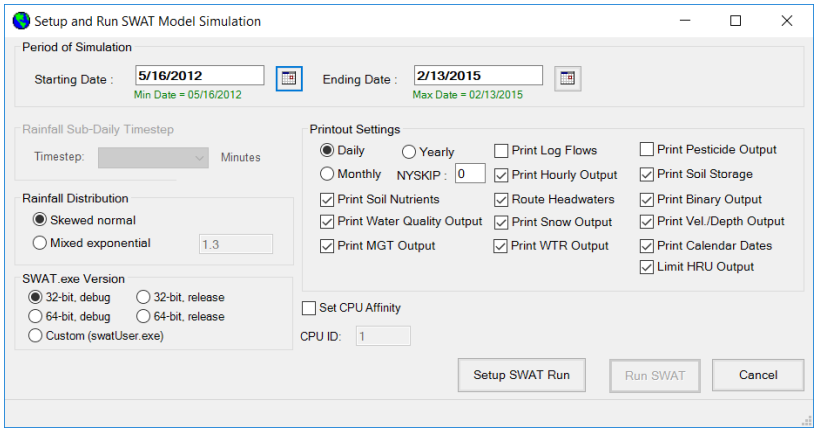

Figure 20. First set-up of ArcSWAT model simulation for validation.

The basic steps of validation is identical with the ones of calibration. The separation of the surficial runoff and the base flow was done with WHAT, and NSE and PBIAS were calculated. Results of the validation model are shown in chapter 4.

CHAPTER 4

RESULTS AND DISCUSSION

4.1 Cross Correlation Analysis

We performed cross-correlation analysis to investigate statistical relationships between water quality parameters and meteorological parameters with time lag of response. The basic concept of cross correlation is to determine the dependency of two variables with the time lapse between one event and the other (J. C. Davis 2002). Its mathematical equation is the same with the general correlation coefficient calculations, but we have a series of pairs with different time lags.

$$R(h) = \frac{\text{cov}\,[1(t), 2(t+h)]}{s[1(t)]s[2(t+h)]} \tag{13}$$

where *R(h)* is the correlation at the time lag interval, *h*, cov [1,2] is the covariance between the variables 1 and 2, and *s*[1(*t*)] and *s*[2(*t*+*h*)] are the corresponding standard deviations of each variables 1 and 2 with the time lag *h*. We adopted two statistical programs: The Statistical Package for the Social Sciences (SPSS) IBM (2015) and WinSTAT for Excel.

The initial analysis made with SPSS took into account 5 parameters as follows:

- Specific conductance (water unfiltered, uS/cm at 25 ºC)
- Evapotranspiration (Alfalfa base)
- Relative Humidity (%)
- Surface soil temperature at 4-inch depth
- Snowfall (snow accumulation in inches)

The time period of SPSS analysis is from Dec 1st, 2010 to May 15th, 2011, corresponding to a total number of 166 records in days.

Table 5 Correlation among parameters using SPSS.

Correlations

			SNOWFALL	RH	SURFACE_T	CONDUCTANCE	ET
Spearman's rho	SNOWFALL	Correlation Coefficient	1.000	.284**	-.264**	.252**	-.072
		Sig. (2-tailed)	.	.000	.001	.001	.357
		N	166	166	166	166	166
	RH	Correlation Coefficient	.284**	1.000	-.216**	-.351**	-.047
		Sig. (2-tailed)	.000	.	.005	.000	.546
		N	166	166	166	166	166
	SURFACE_T	Correlation Coefficient	-.264**	-.216**	1.000	-.587**	.276**
		Sig. (2-tailed)	.001	.005	.	.000	.000
		N	166	166	166	166	166
	CONDUCTANCE	Correlation Coefficient	.252**	-.351**	-.587**	1.000	.086
		Sig. (2-tailed)	.001	.000	.000	.	.270
		N	166	166	166	166	166
	ET	Correlation Coefficient	-.072	-.047	.276**	.086	1.000
		Sig. (2-tailed)	.357	.546	.000	.270	.
		N	166	166	166	166	166

**. Correlation is significant at the 0.01 level (2-tailed).

Table 5 indicates that the regular correlation coefficient, which is cross correlation with zero lag time, among the 5 parameters is not conclusive; the maximum correlation coefficient is 0.587 between conductance and surface temperature. To prove the hypothesis that there would be positive correlation between conductance and snowfall with a certain time lag, cross correlation would be a better way to find their relationship.

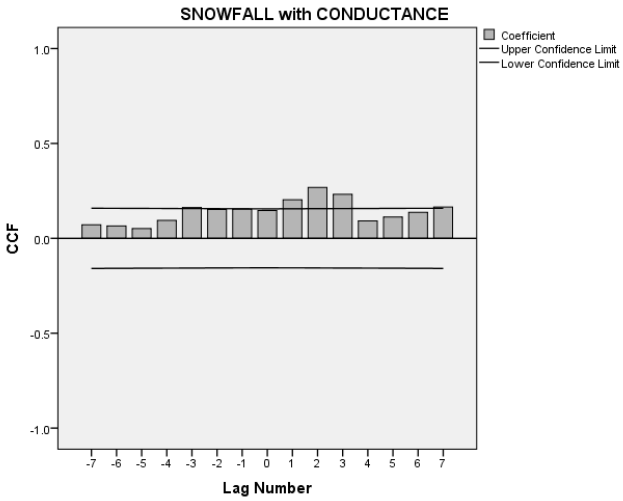

Figure 21. Cross correlation chart between conductance and snowfall developed with SPSS.

Figure 21 shows the cross correlation between snowfall and conductance. The maximum time lag of 2-3 days in the upper confidence limit, indicates that once the snowfall event occurs on the ground, the deicing salts in the melting snow reaches the streams in around 2-3 days. However, there is a weak correlation as indicated by the correlation coefficient equals 0.252; the test is not conclusive and hydrological models should be created in order to confirm this subtle relationship. Another interesting relationship is between conductance and surface temperature. Figure 22 shows a moderate correlation of -0.587 with 1-2 days of time lag between surface temperature and conductance, which indicates that a decrease in surface temperature leads to an increase of conductance. Also, it shows that the maximum correlation coefficient is around 1-2 lags or 1-2 days.

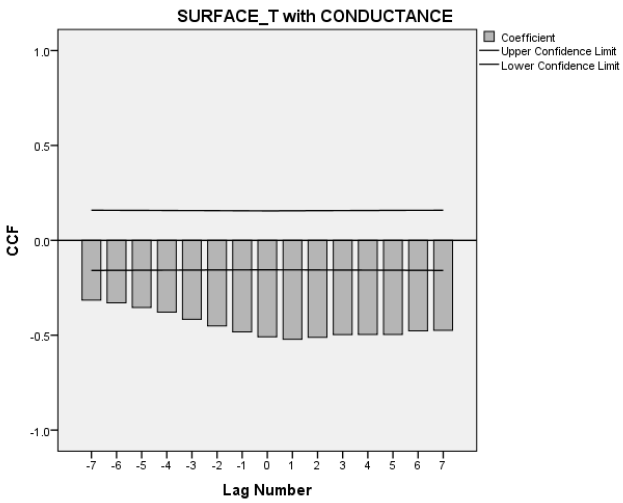

Figure 22. Cross correlation chart between conductance and surface temperature developed with SPSS.

The next analysis was to estimate the time lag of snowmelt by correlating snowfall and conductance in the Indian Creek. We adopted WinSTAT for this analysis. The analysis shows that for the majority of the years, the time lags are estimated to be 1-3 days. This finding concurs with the initial test developed with SPSS. Figures 23 through 25 are the cross correlation graphs for the downstream water station 6893390 in the Indian Creek.

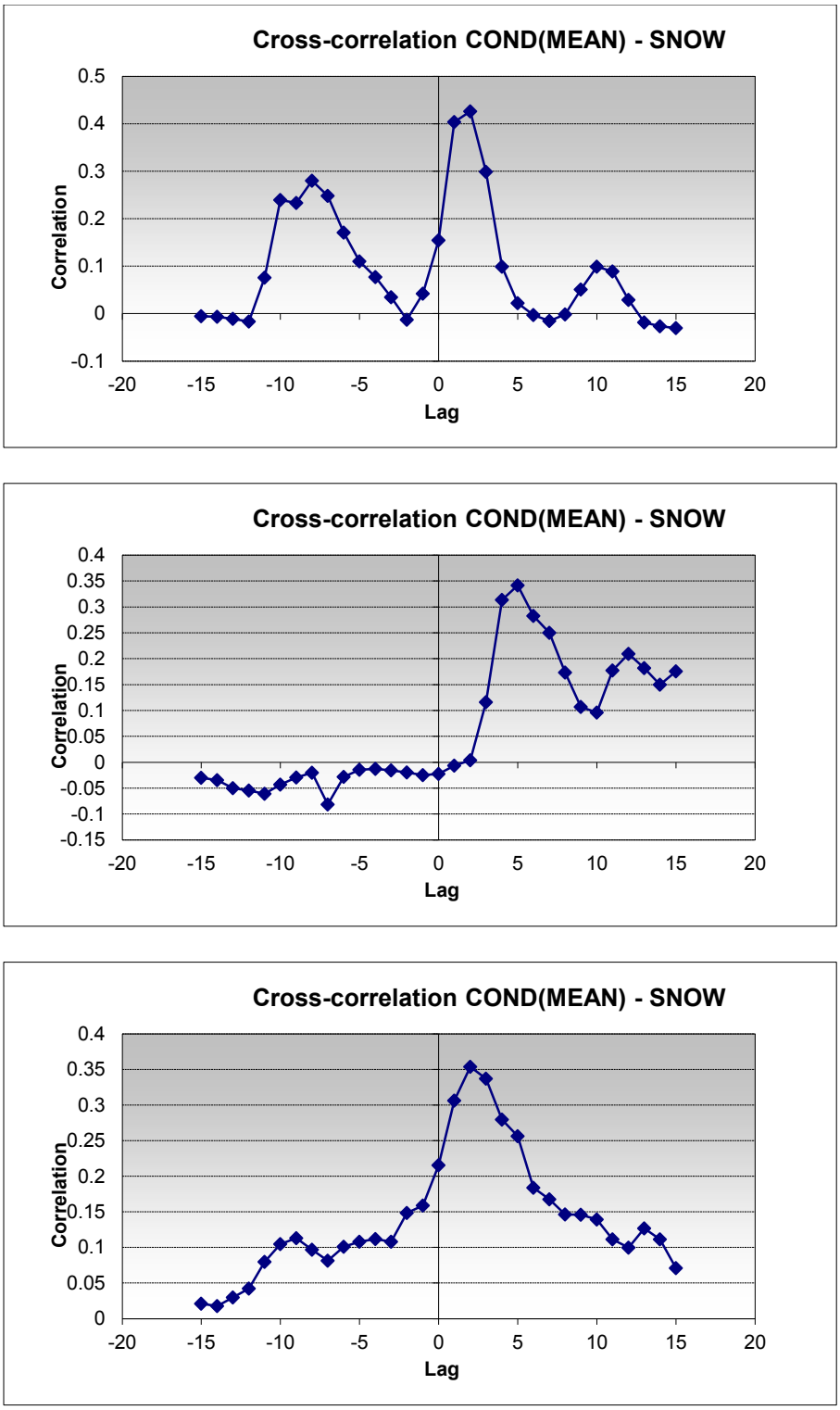

Figure 23. Cross correlation chart between conductance and snowfall for water station 6893390 for 2004, 2005, and 2006 respectively.

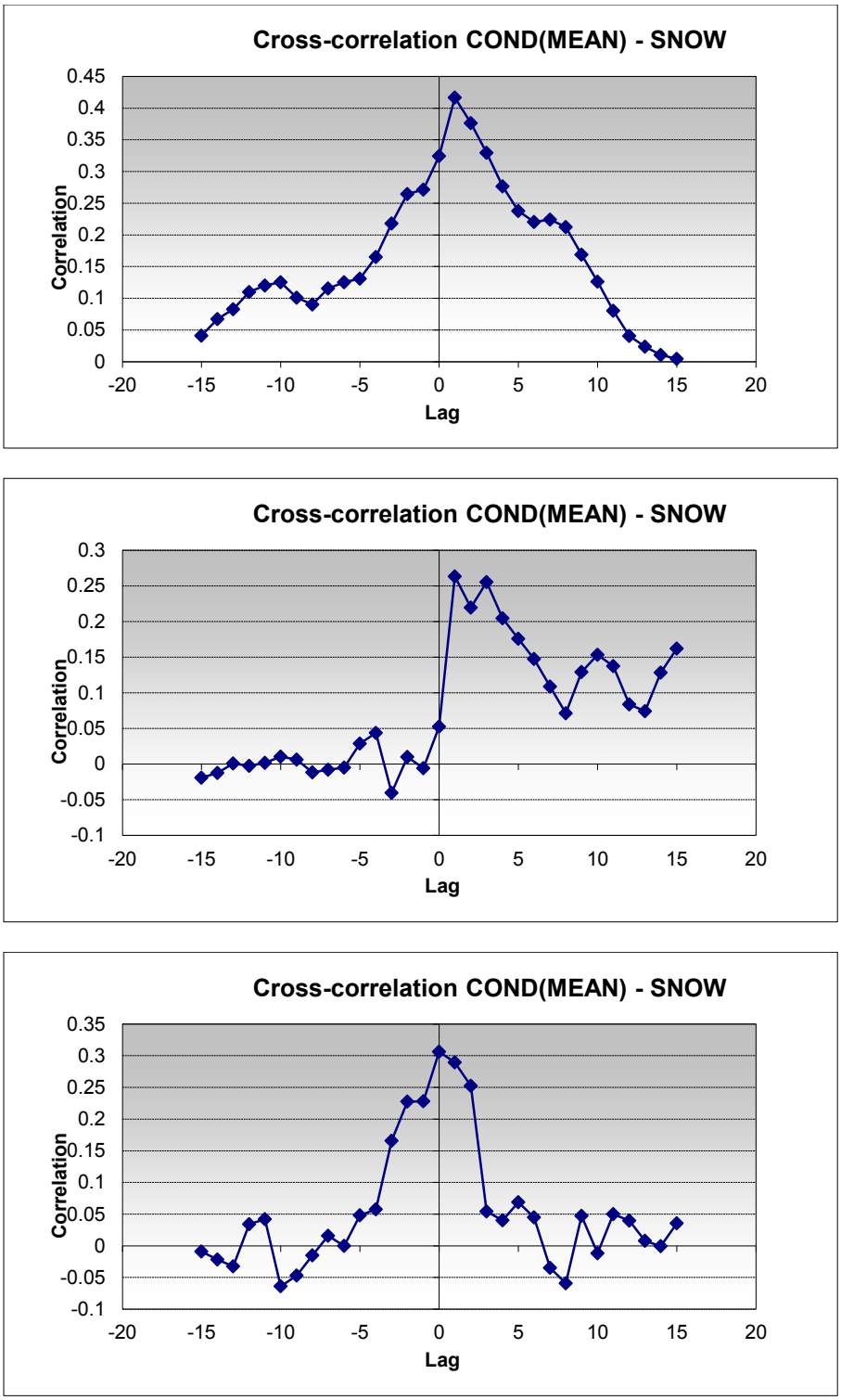

Figure 24. Cross correlation charts between conductance and snowfall for water station 6893390 for 2007, 2008, and 2009 respectively.

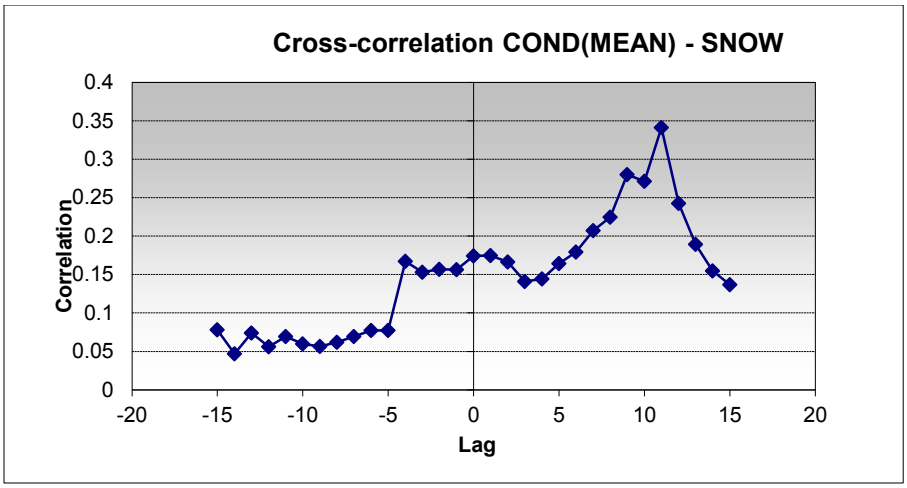

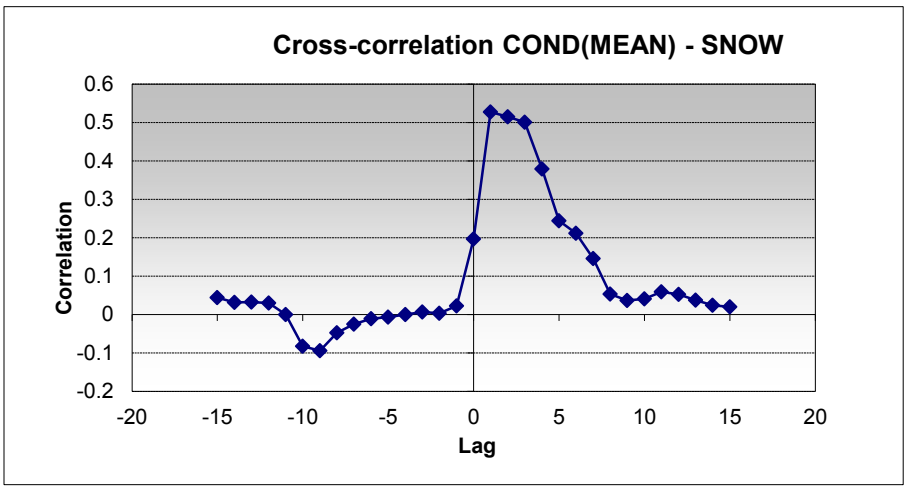

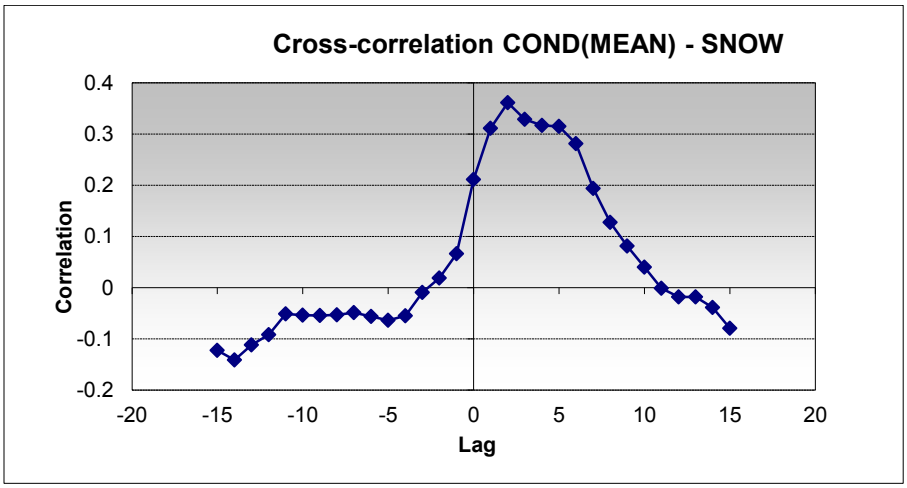

Figure 25. Cross correlation charts between conductance and snowfall for water station 6893390 for 2010, 2011, and 2012 respectively.

According to the previous statistical correlation for the most downstream water station, in the majority of the years the maximum correlation between conductance and snowfall was around 1 to 3 days with 78% of the values. However, there are some anomalies like the ones found in 2005 and 2010. Also, the table below shows that the majority of the lags are among 1, 2, and 3, being 2 the most predominant. Finally, due to the poor data quality, the majority of the 2011 values were out of these ranges and their correlation coefficients were very low, whereas the majority of the 2012 values were in these ranges and their correlation coefficients were a little higher overall.

Table 6. Correlation coefficients and lags for the 2011 and 2012 period years.

Station	2011 (Lags)	Correlation Coefficient	2012 (Lags)	Correlation Coefficient
6893390	1,2,3	0.53	2,3,4	0.361
6893350	0,1,2	0.487	2,1,3	0.271
385608094380300	10,13,12	0.105	2,3,1	0.43
6893300	11,10,13	0.117	2,1,3	0.42
385520094420000	5,6,4	0.187	2,4,1	0.425
385446094430700	0,10,13	0.122	2,4,3	0.26

The cross correlation analysis supports the hypothesis that the conductance would likely increase with snowfall after 1-4 days (mostly 2-3 days) due the deicing salts in the melting snow.

4.2 Hydrological Model Results

It was important to calibrate the model before proceeding with the validation process of the model (Arnold, Moriasi et al., 2012). The idea is to adjust the simulation as much as possible to the observed discharge in cubic meters per day (cmd) values for each of the USGS stations used in this research. For calibration we adopted SWATCup, a hydrological

model calibration software, and the 'Manual Calibration Helper' module from the ArcSWAT model. The initial accuracy of the model was as follow:

NSE = -0.04002

PBIAS = -49.0258

As shown above the accuracy was very low, taking into account that according to Moriasi, et al. (2007) satisfactory NSE > 0.0 and ideal NSE = 1, in the same way satisfactory PBIAS = +-25% and ideal PBIAS = 0. NSE equation used to determine the accuracy of the model was:

$$NSE = 1 - [\frac{\sum_{i=1}^{n}\left(Y_i^{obs} - Y_i^{sim}\right)^2}{\sum_{i=1}^{n}\left(Y_i^{obs} - Y^{mean}\right)^2}] \quad (14)$$

where Y^{obs} is the observed discharge, Y^{sim} is the simulated discharge, Y^{mean} is the mean of the observed records, and n is the total number of records. PBIAS equation used to determine the accuracy of the model was:

$$PBIAS = [\frac{\sum_{i=1}^{n}\left(Y_i^{obs} - Y_i^{sim}\right) * (100)}{\sum_{i=1}^{n}\left(Y_i^{obs}\right)}] \quad (15)$$

Multiple combinations were performed before the model reached the satisfactory values. SWATCup helped to identify the parameters to be adjusted. Some of the sensitive parameters used to calibrate the runoff hydrological model were CN2, ESCO, EPCO, SURLAG, GWQMN, GW_DELAY, Alpha_BF, and REVAPMN as suggested in Maharjan, et al. (2013) and Yang, Liu, et al. (2016) studies. In the initial simulations applying different parameters and supporting the findings with SWATCup, some of the parameters such as EPCO, SURLAG, GWQMN, Alpha_BF, and REVAPMN were taken out due to low influence in the NSE and PBIAS statistical evaluation of accuracy. After a careful analysis

and SWAT Google Group readings, three parameters were chosen as follow, CN2, ESCO, and GW_DELAY. CN2, initial SCS CN II value, is part of the general management parameters of SWAT; this parameter was very sensitive for runoff calibration. ESCO, the soil evaporation compensation factor, is part of the HRU analysis of SWAT; this parameter was also very sensitive for runoff calibration. GW_DELAY, groundwater delay in days, is part of the Groundwater analysis in SWAT; this parameter was not very sensitive for runoff calibration. Finally, the calibration model best simulation was reached combining or modifying the CN2 and ESCO parameters. The values of the modification in comparison with the initial model are:

Table 7. Parameters of modification for initial and final calibration models.

Hydrological Model	**CN2**	**ESCO**
Initial	No Modification	No Modification
Final Calibration	Multiply by 0.65	Multiply by 0.9

The model was calibrated after several attempts with different combinations of CN2 and ESCO. The statistical evaluation of the initial model and the final calibrated model shows a great improvement and fits the acceptable levels of accuracy for both parameters. The statistical evaluation of accuracy for the initial and final calibration model is shown in the table below:

Table 8. Statistical evaluation comparison for initial and final calibration models.

Hydrological Model	**NSE**	**PBIAS**
Initial Calibration	-0.4002	-49.0258
Final Calibration	0.183306	6.137551

The figures below show the final calibration time series curve of the observed and simulated discharges for all USGS chosen stations. Although the general pattern is of underestimation of the simulated values in higher discharges, the statistical evaluations and the time series curve represent a satisfactory accuracy according to the PBIAS values; being the USGS station 385520094420000 the most accurate with statistical evaluation NSE equals 0.411464 and the USGS station 385608094380300 the most accurate with statistical evaluation PBIAS equals 4.305814. For the calibration model comparison, the time lapse used was from July 2011 to May 2012. The stations were organized from the most upstream to the most downstream in the Indian Creek and the station of the Tomahawk Creek.

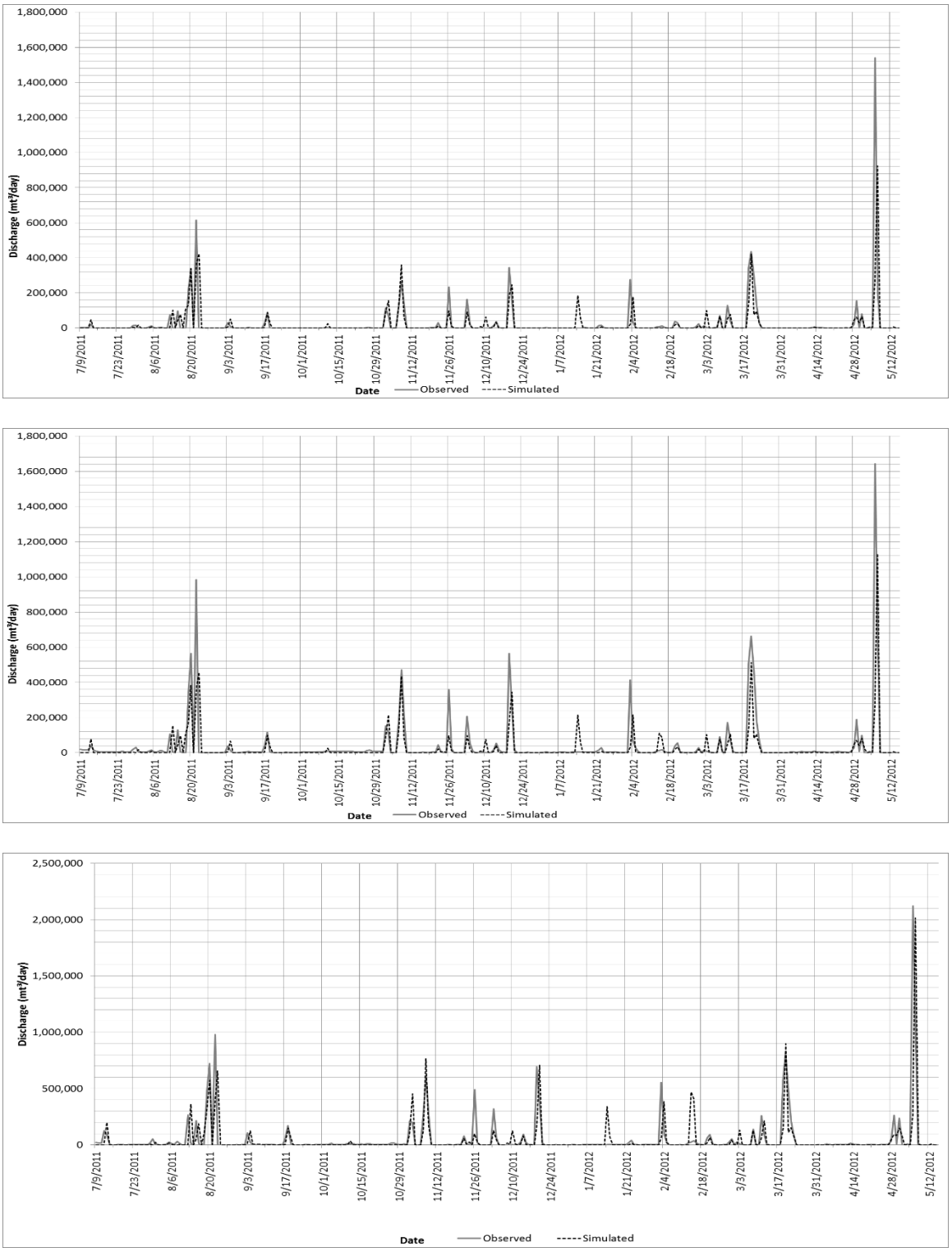

Figure 26. Final calibration model at USGS stations 385446094430700, 385520094420000, and 06893300 respectively.

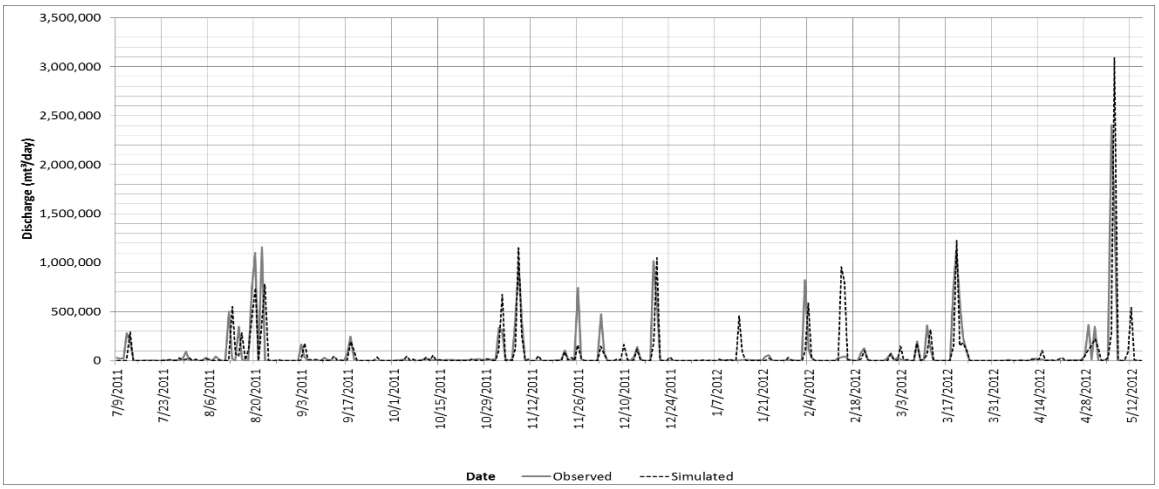

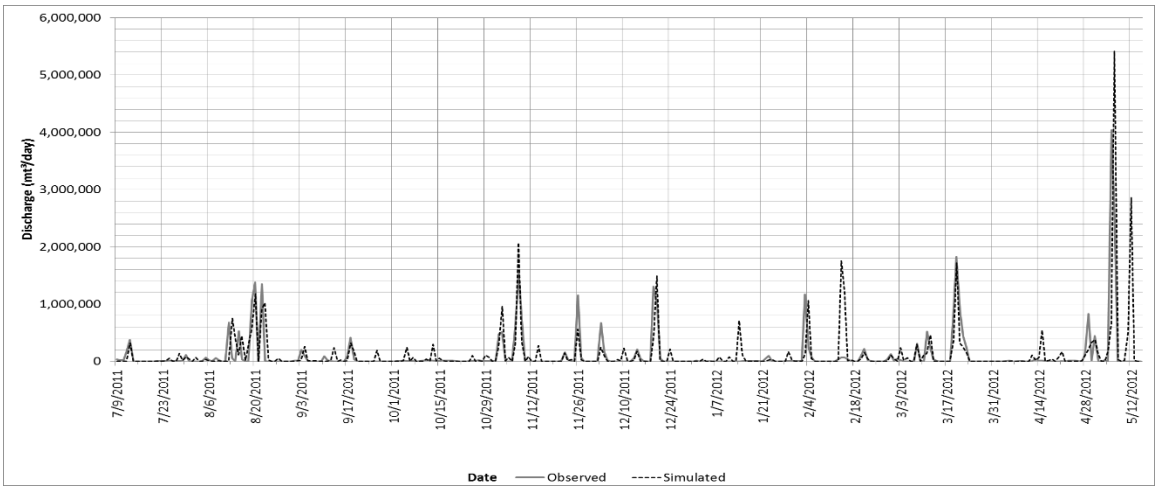

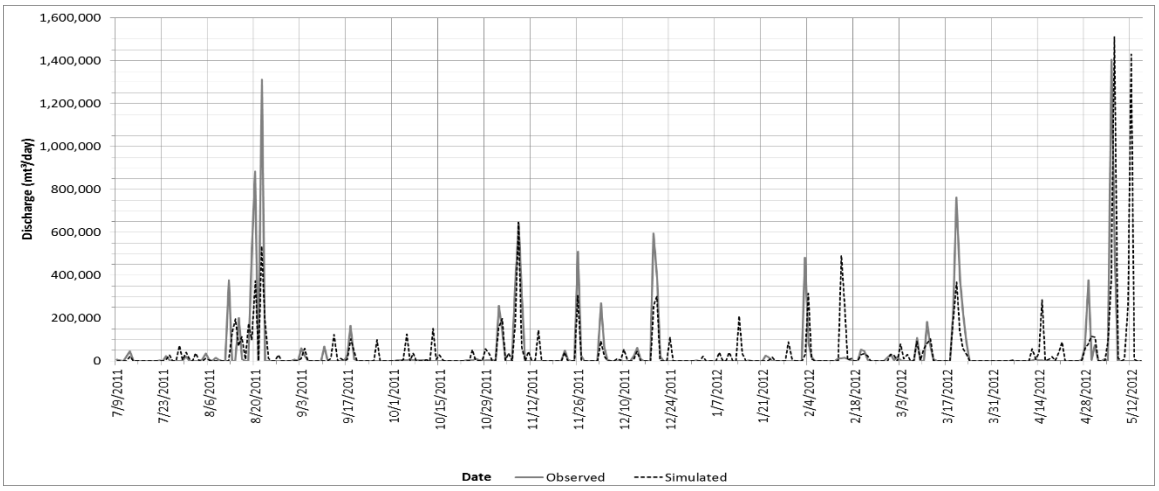

Figure 27. Final calibration model at USGS stations, and 385608094380300, 06893390, and 06893350 respectively.

The validation of the model was the last step in the hydrological modelling process. Applying the same values found in Table 7, for the final calibration model, CN2 multiply by 0.65 and ESCO multiply by 0.9; the model improved substantially as shown in Table 9.

Table 9. Statistical evaluation comparison for initial and final validation models.

Hydrological Model	NSE	PBIAS
Initial Validation	0.6189	-53.0888
Final Validation	0.77	-18.9050

Note that the calibration resulted in a significant increase of the NSE statistic while the NSE increase was not significant from the validation. The increase in the accuracy of the PBIAS statistic was as significant as the increase in the final model calibration. The general pattern was of overestimation according to the negative values of the PBIAS statistics; the statistical evaluations and the time series curve showed a satisfactory accuracy whatsoever; being the USGS station 385446094430700 the most accurate with statistical evaluation NSE equals 0.857836 and the USGS station 06893300 the most accurate with statistical evaluation PBIAS equals -13.2912. For the validation model comparison, the time lapse used was from July 2012 to March 2013.

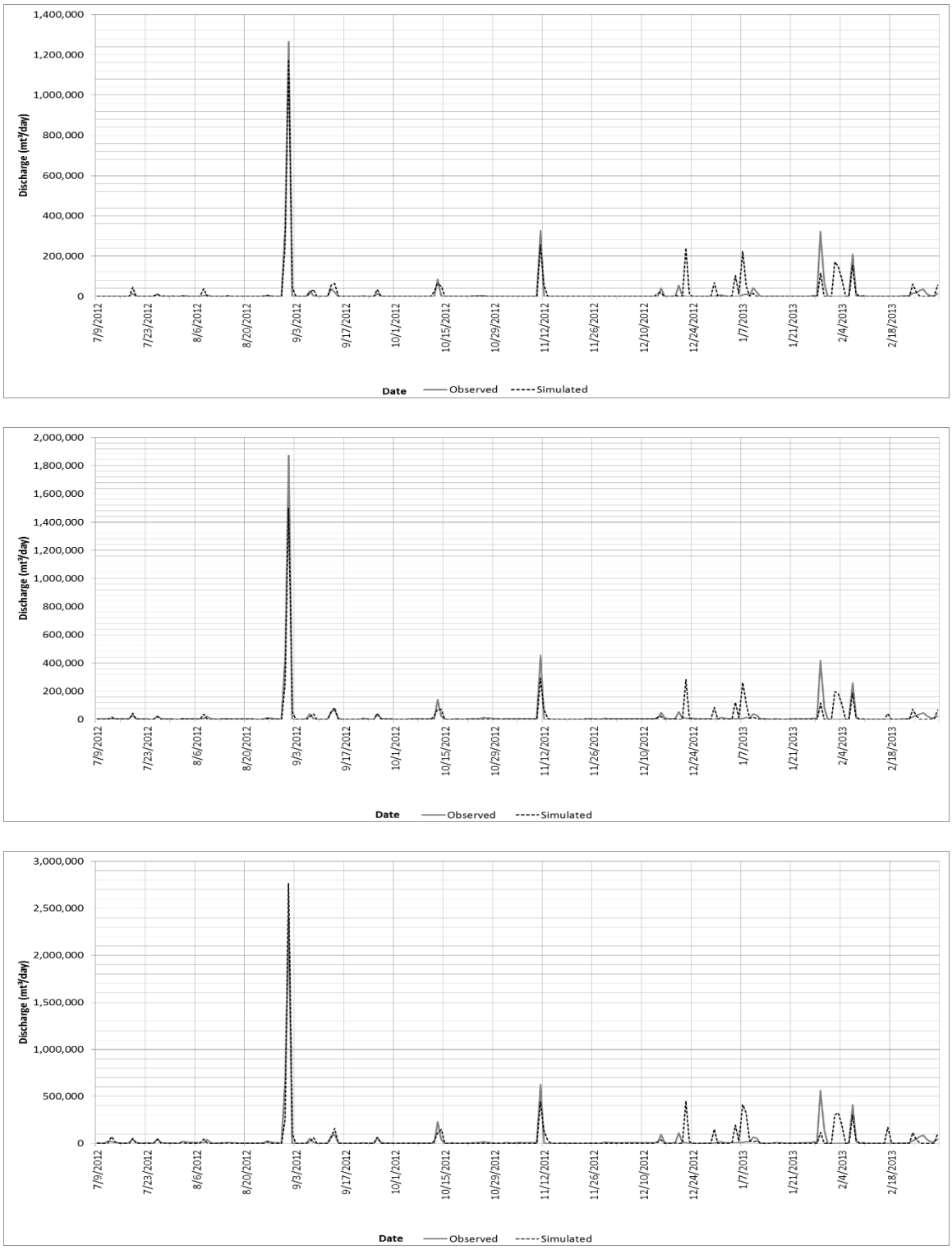

Figure 28. Final validation model at USGS station 385446094430700, 385520094420000, and 06893300 respectively.

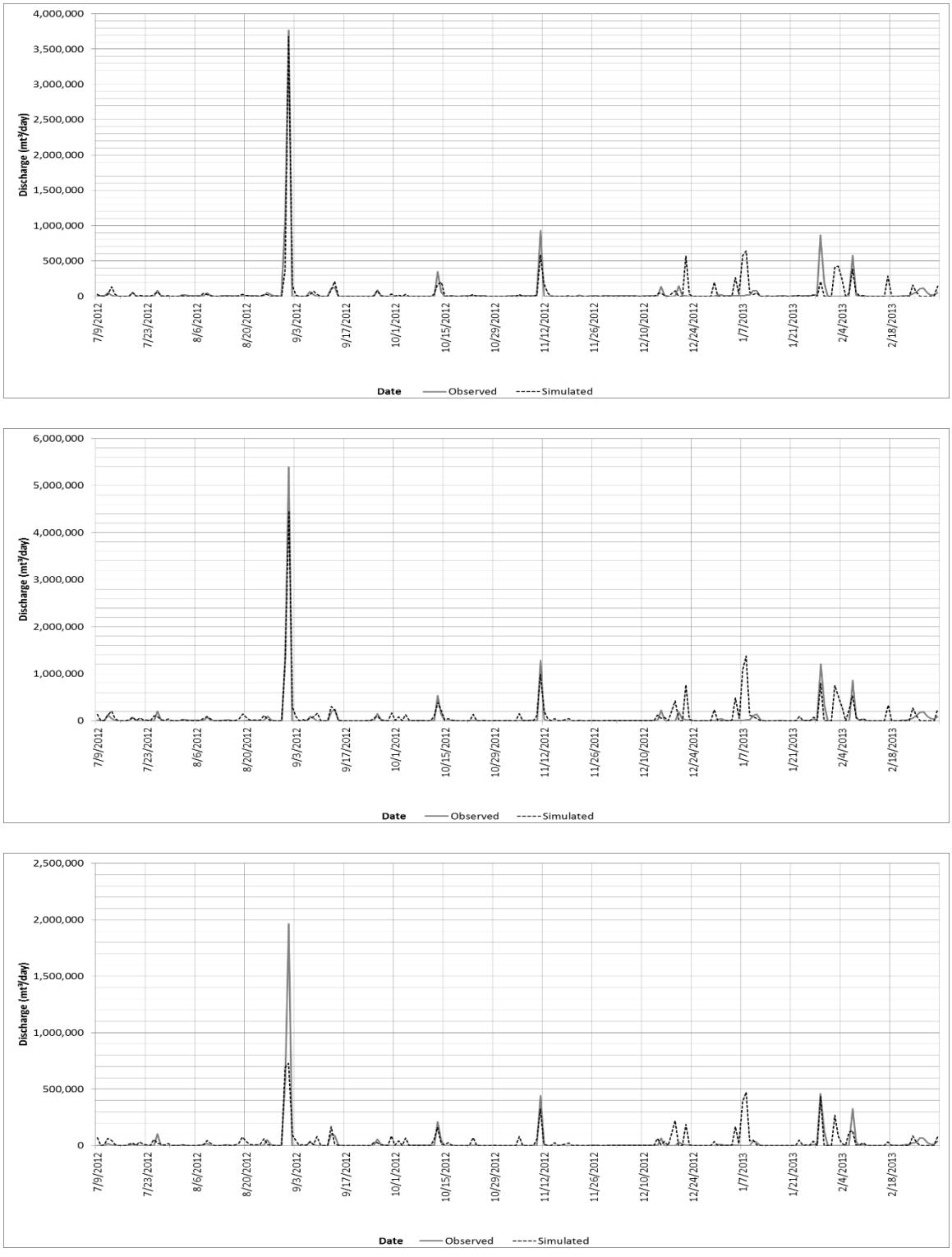

Figure 29. Final validation model at USGS stations 385608094380300, 06893390, and 06893350 respectively.

As presented in the previous paragraphs the final model accuracy was satisfactory, this means that the hydrological model does simulate the behavior of the water discharge. Taking into account the previous precedent, the results of the time lapse from snow melt to the closest reach for each sub-basin were found. Once the desired accuracy of the model was reached, the basis for calculation between snowfall and snow melt is consolidated. The table 10 and 11 show final results for both stages; calibration and validation.

Table 10. Final results for the calibration model.

STATION	(EVENT 1)	(EVENT 2)	(EVENT 3)	(EVENT 4)	AVE DAYS
385446094430700	1	2	5		2.7
385520094420000	1	2	1		1.3
06893300	1	2	1		1.3
385608094380300	1	2	3	1	1.8
06893390	2	3	1		2.0
06893350	1	2	3	1	1.8
				FINAL DAYS	**1.8**

Table 11. Final results for the validation model.

STATION	(EVENT 1)	(EVENT 2)	(EVENT 3)	(EVENT 4)	(EVENT 5)	(EVENT 6)	(EVENT 7)	(EVENT 8)	AVE DAYS
385446094430700	2	4	3	3	5	3			3.3
385520094420000	2	4	3	2	3	5	3		3.1
06893300	2	4	3	2	3	5	3		3.1
385608094380300	2	4	3	2	3	5	3		3.1
06893390	2	3	2	1	2	5	1	3	2.4
06893350	2	4	3	2	3	5	3		3.1
								FINAL DAYS	**3.0**

In these previous tables, each **EVENT** is defined by the subtraction of the first day of snowmelt occurrence minus the crest day of snowfall during the previous days. Figures 30 through 33 show the time series curves of the snowfall and snowmelt calculated by the ArcSWAT hydrological model.

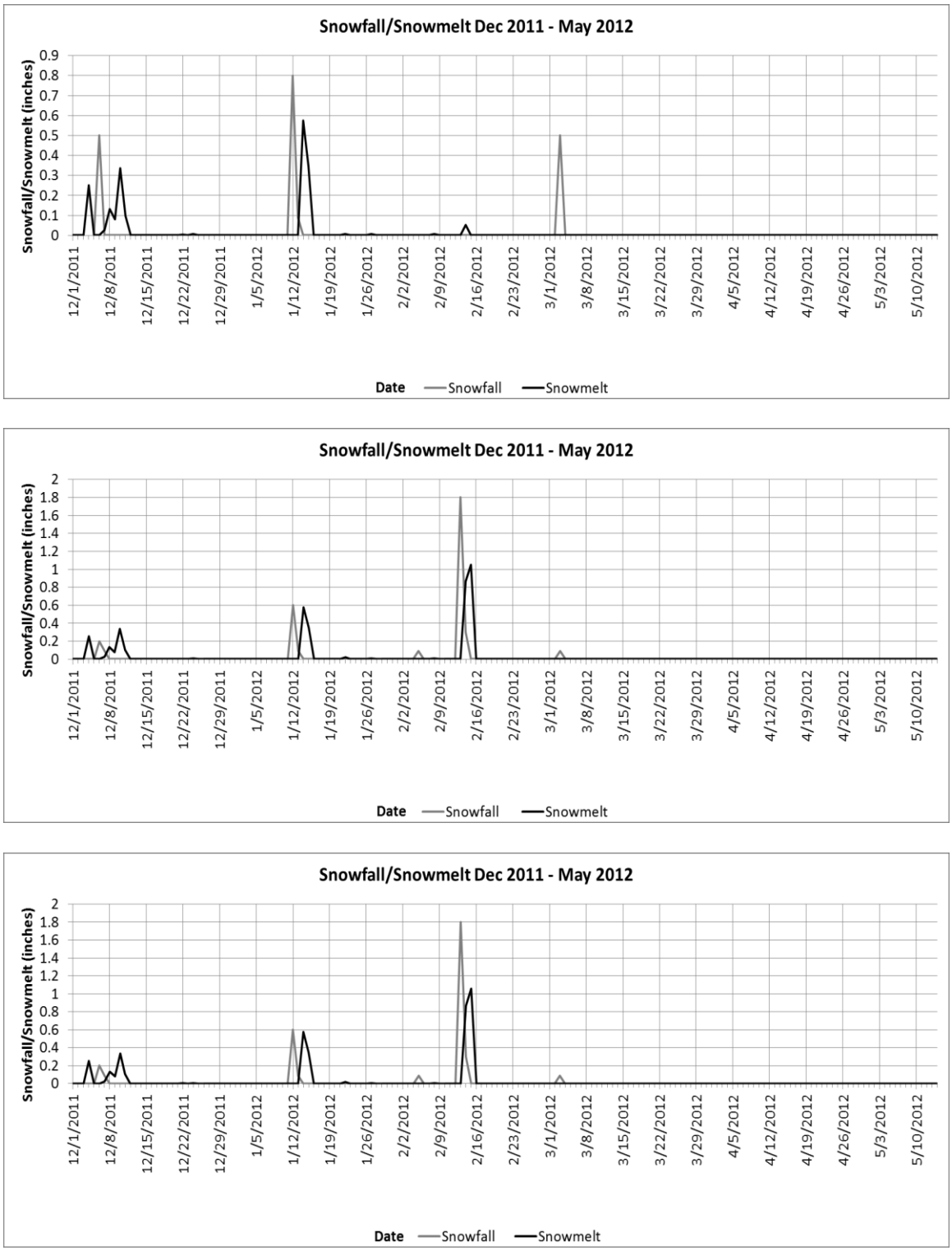

Figure 30. Snowfall and snowmelt calculation for calibration at USGS stations 385446094430700, 385520094420000, and 06893300 respectively.

Figure 31. Snowfall and snowmelt calculation for calibration at USGS stations, 385608094380300, 06893390, and 06893350 respectively.

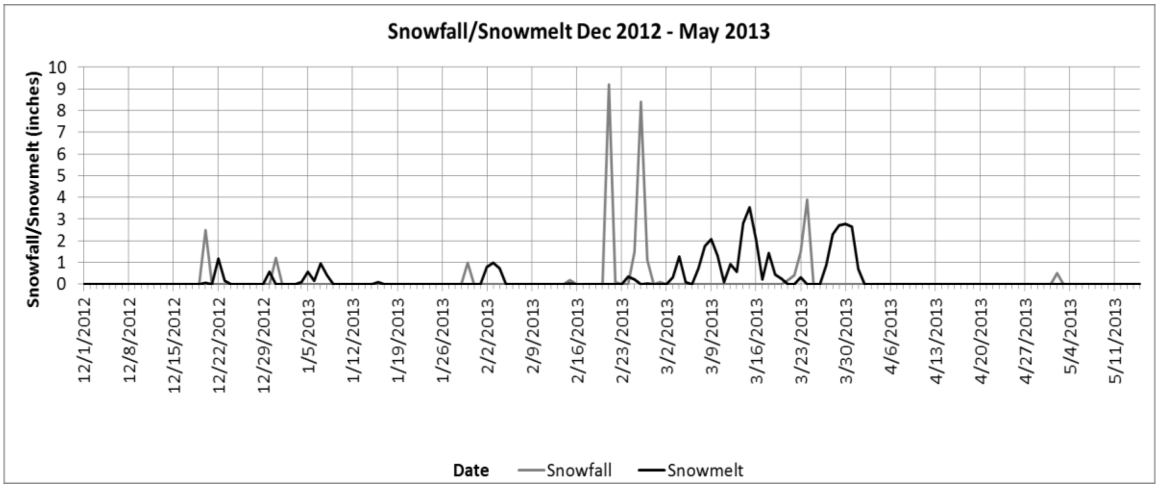

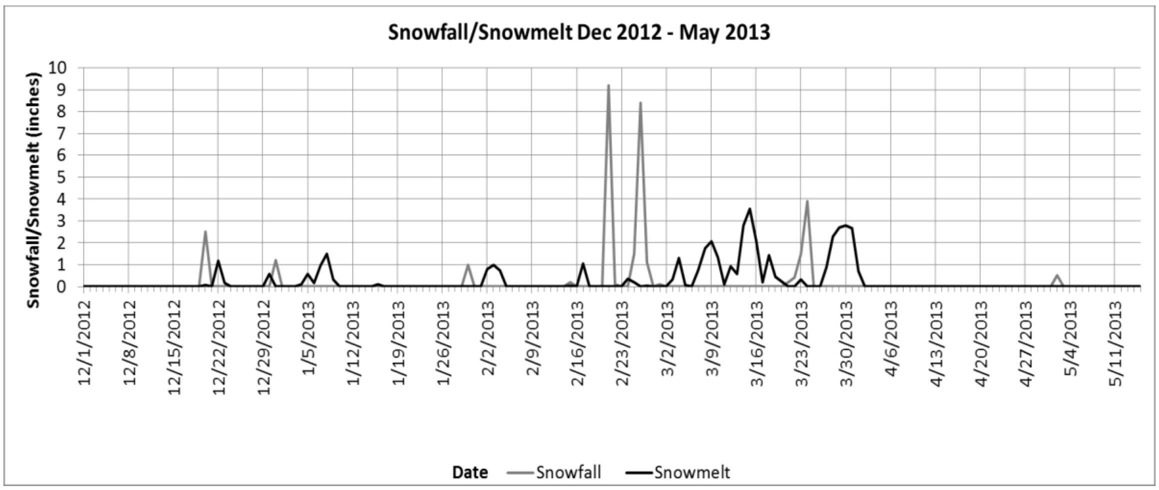

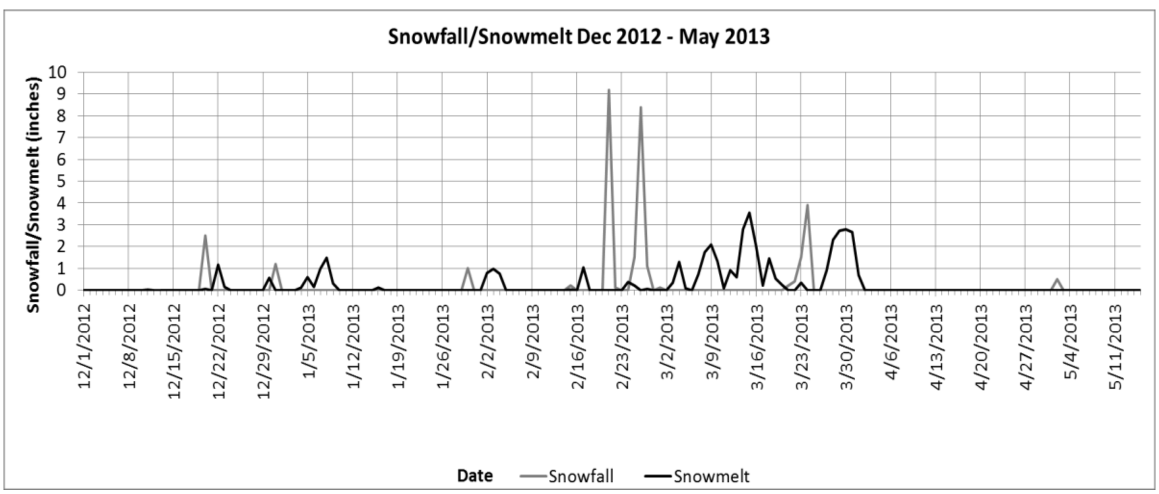

Figure 32 Snowfall and snowmelt calculation for validation at USGS stations 385446094430700, 385520094420000, and 06893300 respectively.

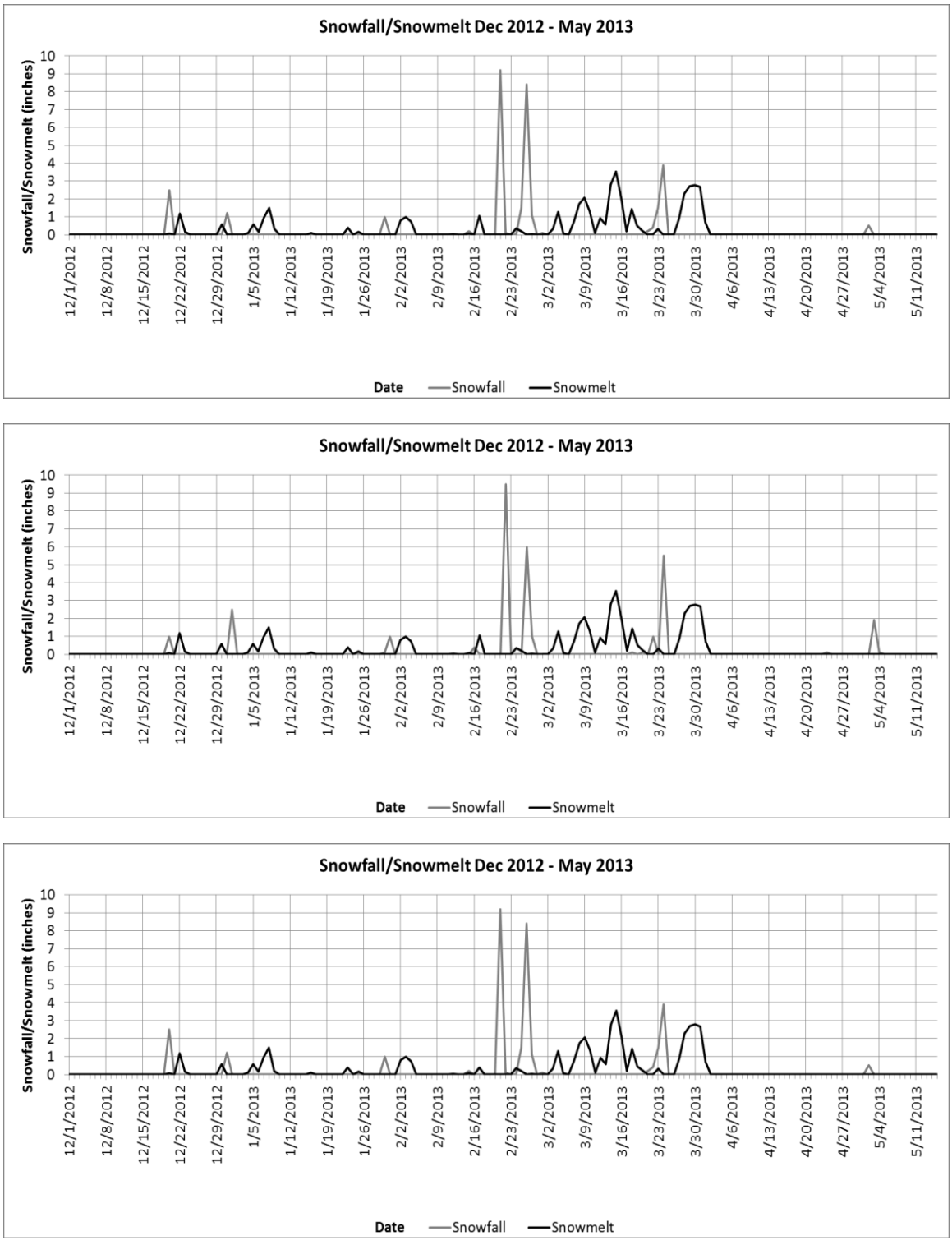

Figure 33. Snowfall and snowmelt calculation for validation at USGS stations, 385608094380300, 06893390, and 06893350 respectively.

The difference between the calibration and validation final values can be explain by the difference in the surface temperature for both periods of time. As noticed in Figure 34, the temperatures from December 2012 to May 2013 period were much lower than the temperatures from December 2011 to May 2012. Also, as shown in the trend lines accumulation, by the middle of May, there is a difference in temperatures of around 18 degrees.

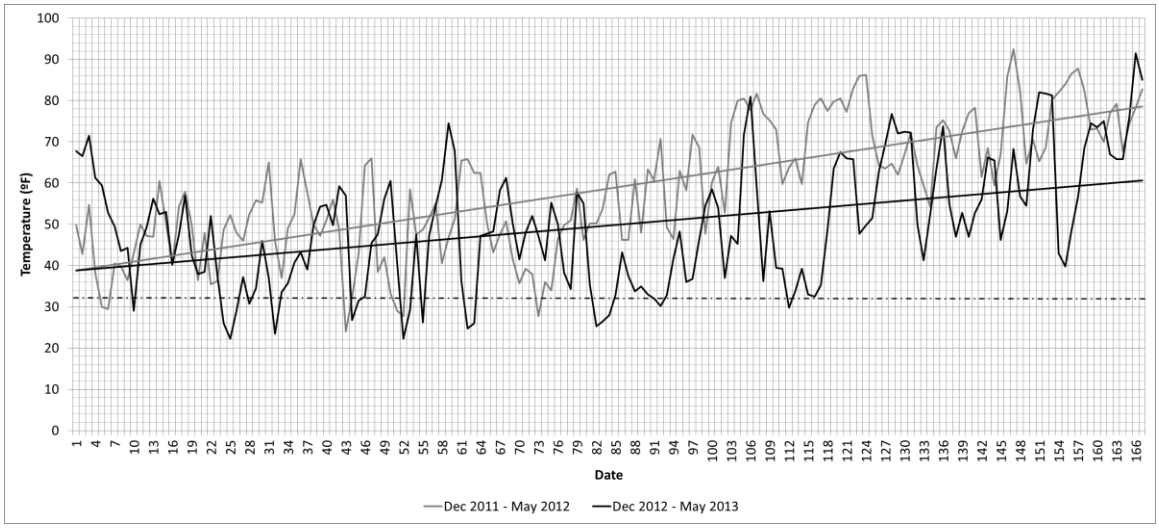

Figure 34. Temperature differences in Fahrenheit (ºF) between the calibration and the validation series.

The calibration and validation accuracies are affected by the drainage area differences between the USGS stations and the model sub-basin areas. In general, the difference between both sets of data is of approximate 2.33% (see table below).

Table 12. USGS areas and model areas comparison.

USGS STATION	USGS Area (sqmi)	Model Area (sqmi)	Difference
385446094430700 INDIAN C AT 119TH ST, OVERLAND PARK, KS	14.2	14	1.41%
385520094420000 INDIAN C AT COLLEGE BLVD, OVERLAND PARK, KS	15.8	16.59	5.00%
06893300 INDIAN C AT MARTY ST, OVERLAND PARK, KS	26.6	26.03	2.14%
385608094380300 INDIAN C AT INDIAN C PKWY, OVERLAND PARK, KS	36.6	36.36	0.66%
06893390 INDIAN C AT STATE LINE RD, LEAWOOD, KS	64.17	63.97	0.31%
06893350 TOMAHAWK C AT ROE AVE, LEAWOOD, KS	20.5	21.41	4.44%
		Average Area Differences	2.33%

Additional time could be added due to the overland flow of the snowmelt. The overland flow can be calculated from the most distant part of the sub-basins from any of the streams, and this is called 'time of concentration' (Fetter 2001). However, the additional time found was just for the overland flow, starting travel time on channel/stream is assume to start in the day that snow melt is beginning. In order to get the most distance hydraulic point in the sub-basins, visual observation and analysis was the first approach. Once the previous step was completed, GIS analysis was performed over the ArcGIS platform by converting the boundary of the sub-basins into points drawn for every vertex and by assigning geodesic distance values to a point, from the line stream until the chosen one. Four distant points were calculated and analyzed through the ArcGIS Online analysis tool "Trace Downstream". The figure below shows the farthest point and the path of overland calculation for the whole Indian Creek Basin.

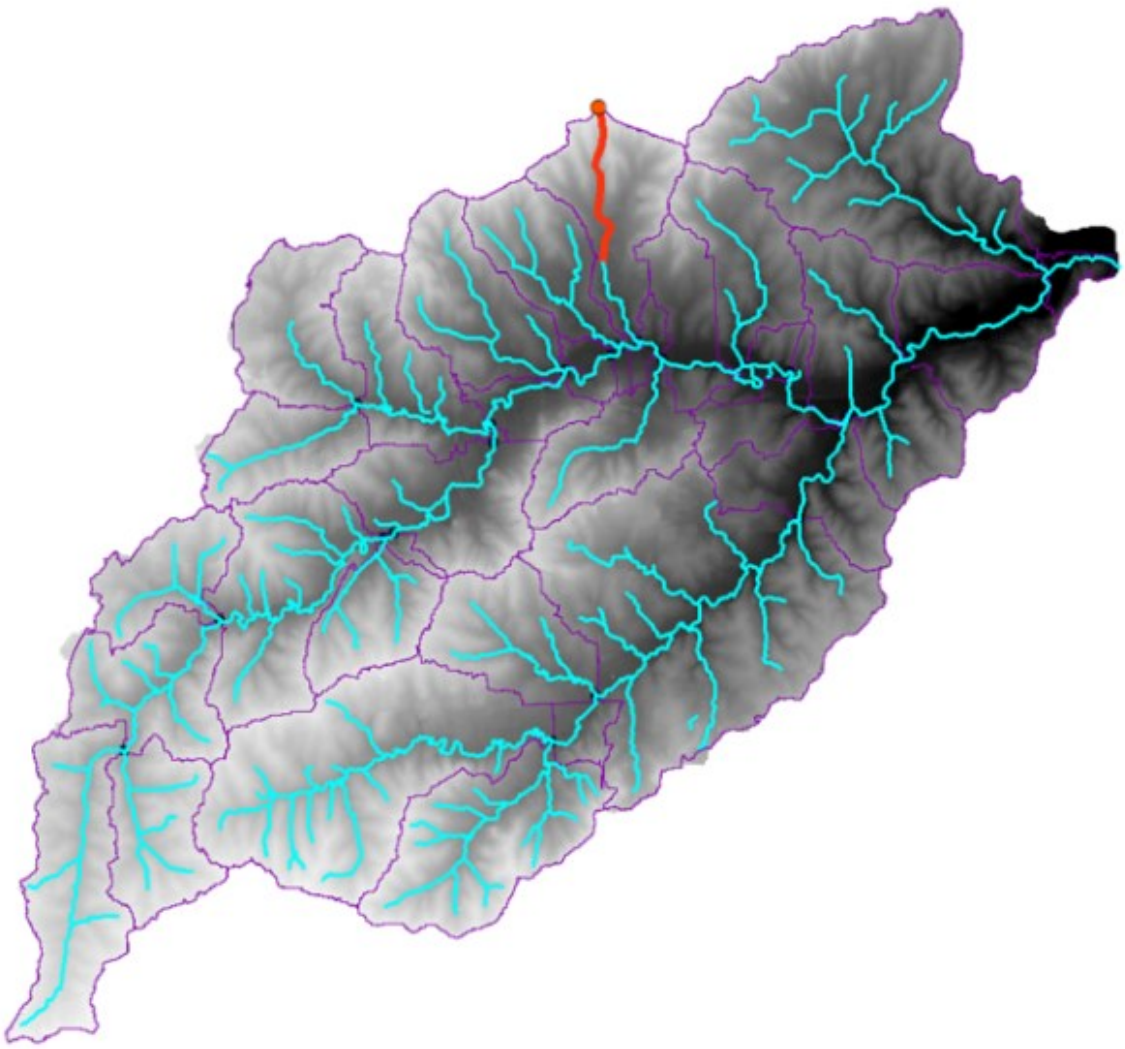

Figure 35. Downstream paths from farthest point in the watershed division (red path) and NHD high resolution streams (AIMS 2014), (USGS NHD Data 2016).

With the maximum overland flow point and the length of travel to the first stream, the overland flow calculation is developed after the evaluation of the more appropriate equations/formulas. According to chapter 2, section 2.6, there are many equations that fit the physical and meteorological characteristics of the Indian Creek Basin. In order to get the best result, six equations were developed for the maximum overland flow to get the time of concentration. The assumptions of constant rainfall and constant slope along the plane were implemented for all the equations/formulas. Also, the formulas presented below were developed for concrete/asphalt surfaces due to the high concentration of urban developments

in the basin and because it is evident that the time of concentration for grass or other surfaces is much higher.

The first equation is Equation (6) presented by Wong (2005). With S_o equals 0.017574 (m m^{-1}), L_o equals 3,056.46232 (m), and i_n equals 21.137738 (mmh^{-1}), then:

$$t_o = \left(10.57 + \frac{0.12}{0.017574}\right)\left(\frac{3{,}056.46232}{30.48}\right)^{0.55-(^{0.001}/_{0.017574})} \quad 21.137738^{-0.43}$$

t_o = 45 minutes

The second equation is Equation (7) presented by Wong (2005). With *Nk* equals 0.02 (imperviousness surface), L_o equals 3,056.46232 (m), and S_o equals 0.017574 (m m^{-1}), then:

$$t_o = 1.45(0.02x3{,}056.46232/0.017574^{0.5})^{0.467}$$

t_o = 25 minutes

The third equation is Equation (8) presented by Wong (2005). With constants (representing impervious surface – concrete) *C* equals *3* and *k* equals 0.5, *v* equals $0.874x10^{-6}$ m^2s^{-1} for water at 26 °C, S_o equals 0.017574 (m m^{-1}), L_o equals 3,056.46232 (m), and i_n equals 21.137738 (mmh^{-1}), then:

$$t_o = \left(\frac{0.21(3.6\ x\ 10^6 x\ 0.000000874)^{0.5}\ \ 3\ x\ 3{,}056.46232^{1.5}}{0.017574\ x\ 21.137738^{1.5}}\right)^{1/3}$$

t_o = 48 minutes

The fourth equation is Equation (9) presented by Almeida, et al. (2014). With *i* equals 21.137738 (mm/h), *L* equals 3.05646232 (km), and *S* equals 0.017574 (m/m), then:

$$T_c = 2.2535\ x\ 21.137738^{-0.7164}\ x\ 3.05646232^{0.5552}\ x\ 0.017574^{-0.2070}$$

Tc = 65 minutes

The fifth equation is Equation (10) presented by Almeida, et al. (2014). With L equals 3.05646232 (km), and S equals 0.017574 (m/m), then:

$$T_c = 0.0977\ x\ 3.05646232^{0.6}\ x\ 0.017574^{-0.3}$$

Tc = 39 minutes

The sixth equation is Equation (11) presented by Almeida, et al. (2014). With n equals 0.012 (see appendix C), L equals 3.05646232 (km), S equals 0.017574 (m/m), and in equals 21.137738 (mm/h), then:

$$T_c = 7.3015 \left(\frac{0.012\ x\ 3.05646232}{0.017574^{0.5}}\right)^{0.6} \quad 21.137738^{-0.4}$$

T_c = 60 minutes

The summary of the equations is presented below to illustrate the final decisions in choosing the time of concentration from the overland flow that better fitted the study.

Table 13. Summary of time of concentration equations/formulas.

Equation/Formula	USACE	Kerby	Chen and Wong	McCuen	Carter	Woolhiser & Liggett
Time Overland (min)	45	25	48	65	39	60
R^2 (Wong, 2005)	0.94	-0.8	0.92	No defined	No defined	No defined
Constraints/ Features	Better with i < 254	i value no taken into account	Kinematic k adjusted with flow regime	Urban, area 0.154 - 6.178 sqmi*, S 0.0007 - 0.03	Urban, area < 8 sqmi*, S < 0.005, i value no taken into account	Kinematic

Square miles*

Table 13 shows the influence of i on all the equations, the Kerby equation and the Carter equation were formulated without taking into account the rain intensity parameter, thus the overland time is shortest. The accuracy of the Kerby equation is very low. According to Wong (2005), the low accuracy may be affected by the lack of I, even though the accuracy of Carter equation is not defined. Additionally, Carter's constraints of area less than 8 square miles do not match the dimensions of the research area (73.64 square miles). McCuen's

Formula was generated through a study in the United States urban basins with smooth steepness, however, as in Carter's formula, constraints of area less than 6.178 square miles and the lack of accuracy suggests a low rank when choosing the right formula. USACE's equation has no area restrictions, thus it shows the highest accuracy with the time of overland flow close to the average time for the equations, which is 47 minutes. Additionally, USACE's equation considers the rainfall intensity parameter that helps reach one of the best fits for the Indian Creek basin. The Chen and Wong's formula and the Woolhiser & Liggett's formula both use the kinematic theory. The Chen and Wong's formula has a very high precision value whereas the Woolhiser & Liggett's formula does not have enough accuracy. The Chen and Wong's formula has a time of concentration overland very close to the average time of concentration. Furthermore, the Chen and Wong's formula has the advantage of the adjustment of the *k* variable. The Chen and Wong's formula has better accuracies for both concrete and grass (Wong, 2005). After all, the Chen and Wong's formula was the one that fitted the best in the basin.

The average and maximum time for snowmelt to reach any stream in the basin is the sum of the snow events in days (2.4 days) plus the t_o (48 minutes) that equals 2 days, 10 hours, and 24 minutes. This means that any liquid contaminant coming from snow melting processes within the basin may take, as a maximum, around 2-3 days.

It is indispensable at this point to see the interaction between conductance and turbidity, a closer look to the calibration period data indicates a great cross correlation on lag numbers zero and one, however, the validation period data does not indicate a great correlation and the predominant maximum lag is at -10. One of the reasons for the previous

statement may be that the periods of calibration and validation have different precipitation regimes. The statistical analysis of these two parameters is shown in the figures below.

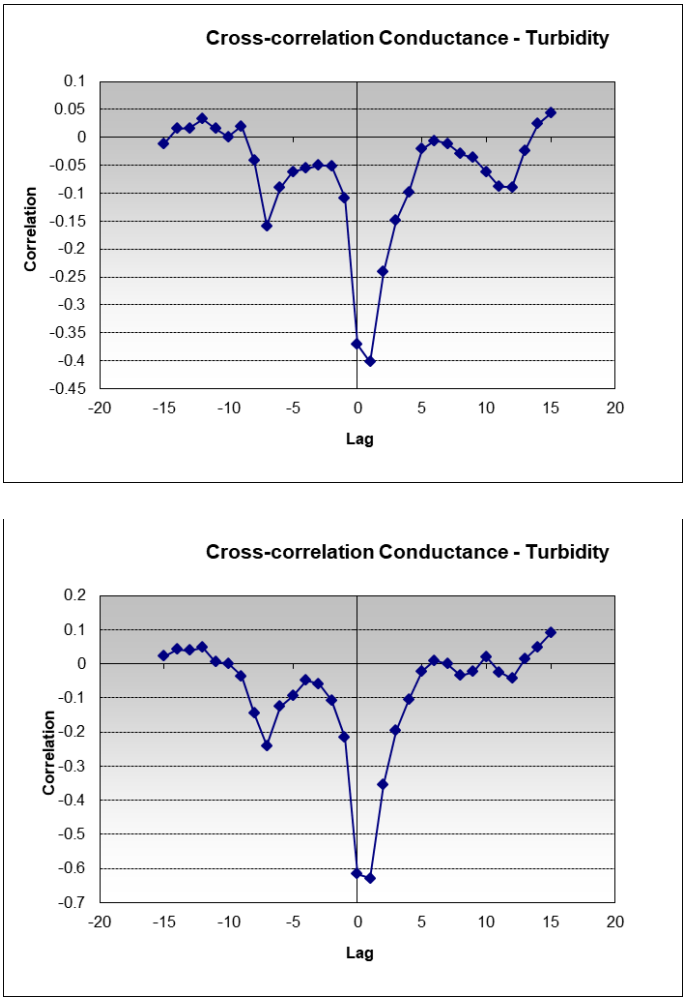

Figure 36. Cross-correlation conductance and turbidity for calibration at USGS stations 385446094430700 and 385520094420000 respectively (2011-2012).

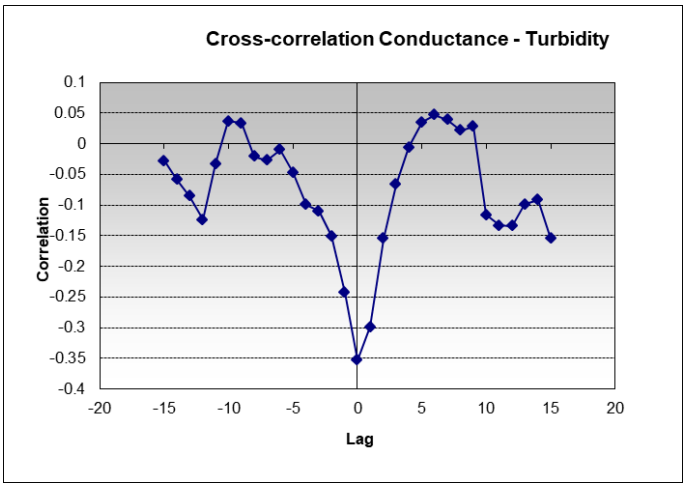

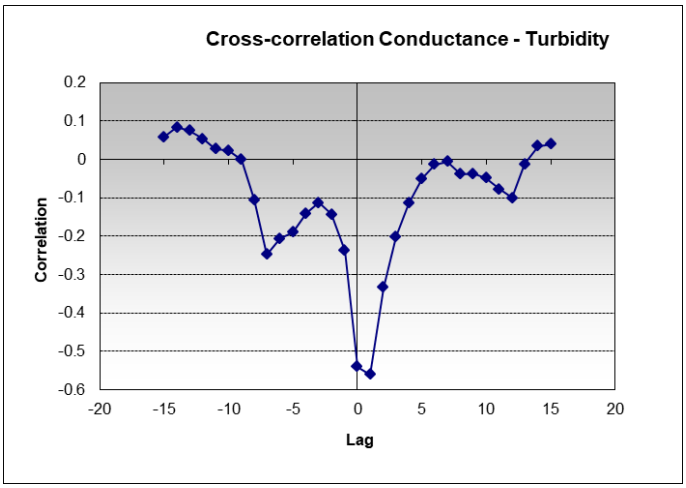

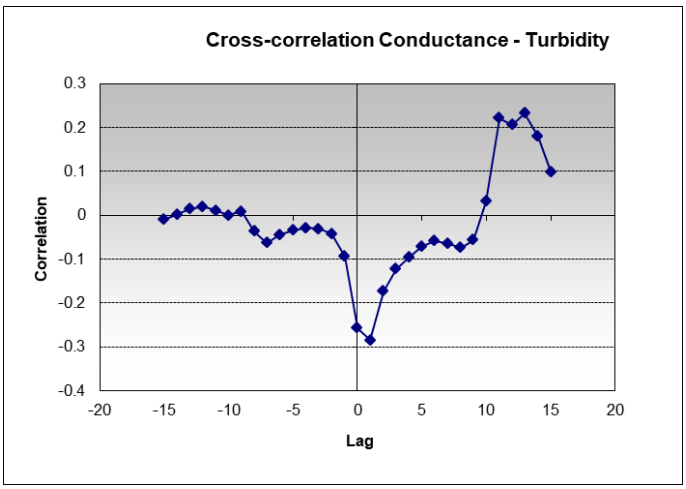

Figure 37. Cross-correlation conductance and turbidity for calibration at USGS stations 06893300, 385608094380300, 06893390, respectively (2011-2012).

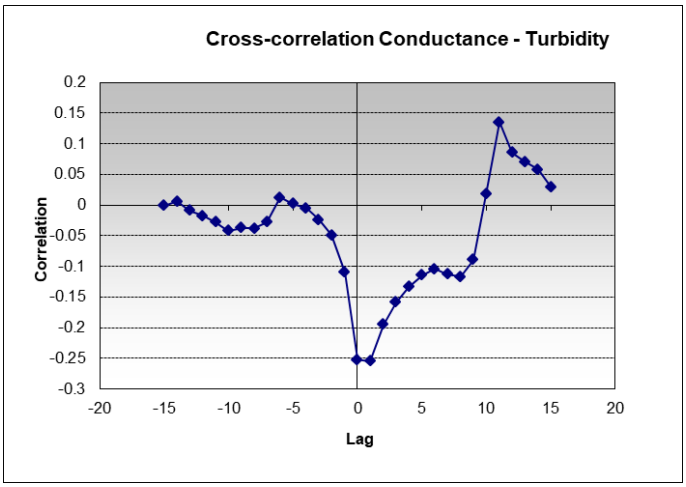

Figure 38. Cross-correlation conductance and turbidity for calibration at USGS station 06893350 (2011-2012).

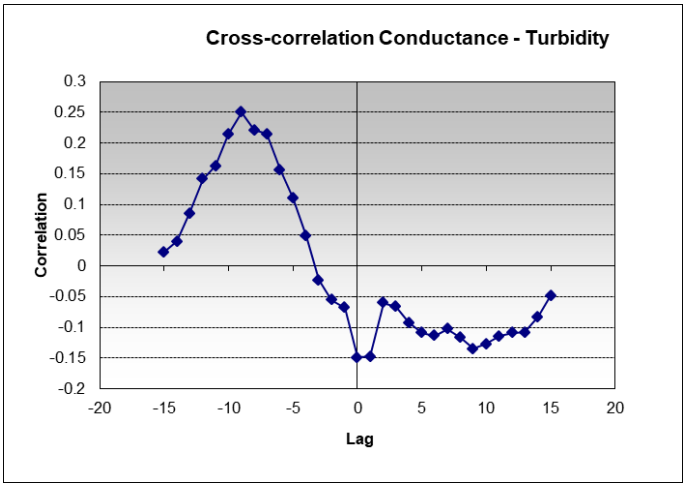

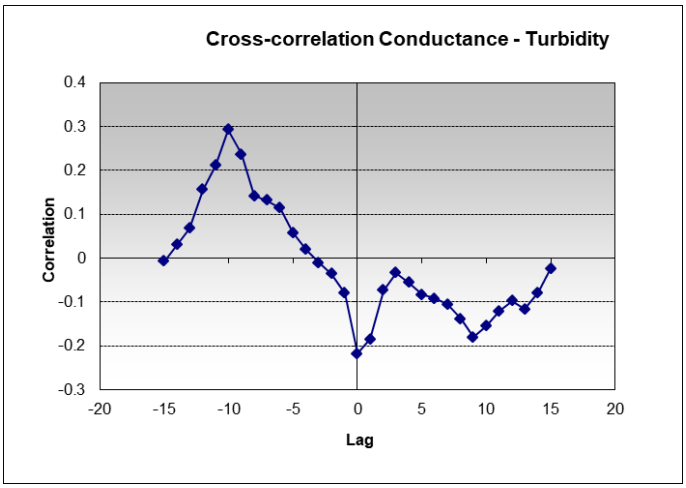

Figure 39. Cross-correlation conductance and turbidity for validation at USGS stations 385446094430700 and 385520094420000 respectively (2012-2013).

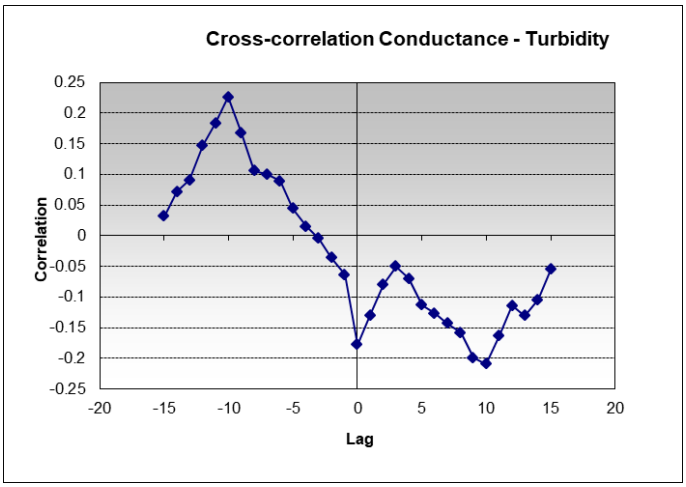

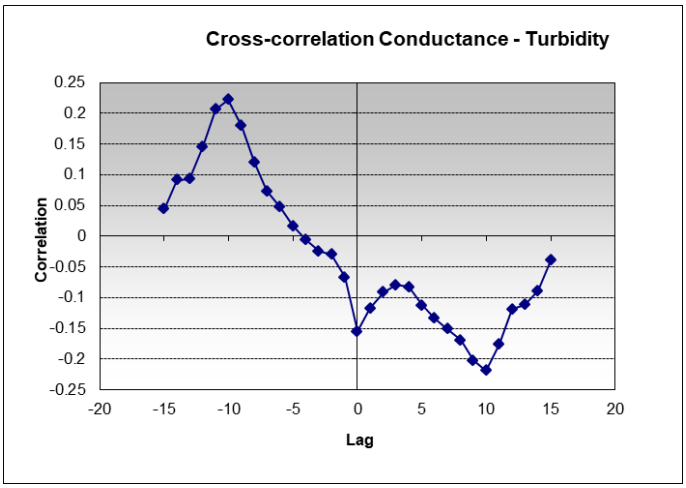

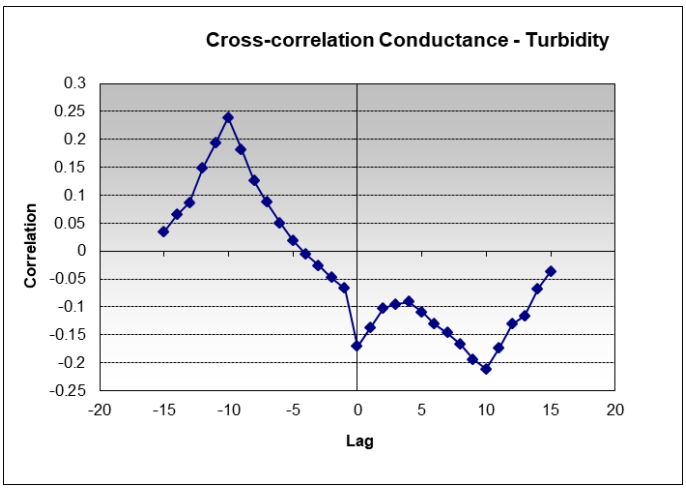

Figure 40. Cross-correlation conductance and turbidity for validation at USGS stations 06893300, 385608094380300, and 06893390 respectively (2012-2013).

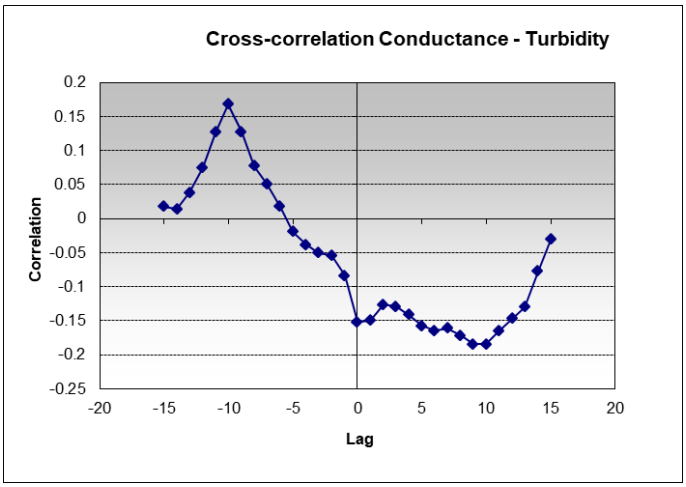

Figure 41. Cross-correlation conductance and turbidity for validation at USGS station 06893350 (2012-2013).

The following method of comparison among the four parameters may be misleading due to the arbitrary scale use to get the parameters to coincide. However, Figures 42 through 45 show series of representations among the snowfall, snowmelt, turbidity, and conductance, in which the evidence of the conductance disturbance due to the increase of salty solid matter into the streams is reflected in the turbidity as shown in the figures below.

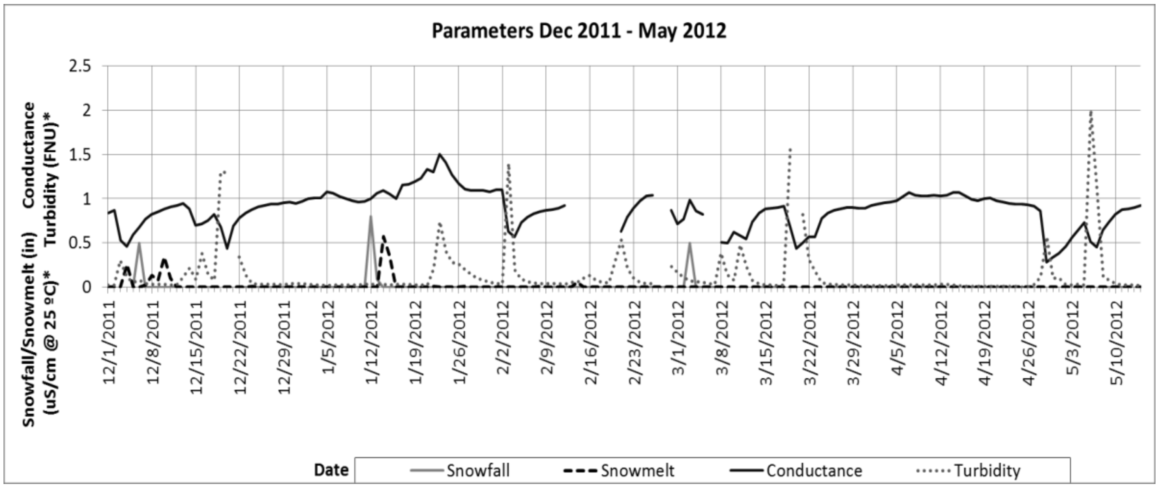

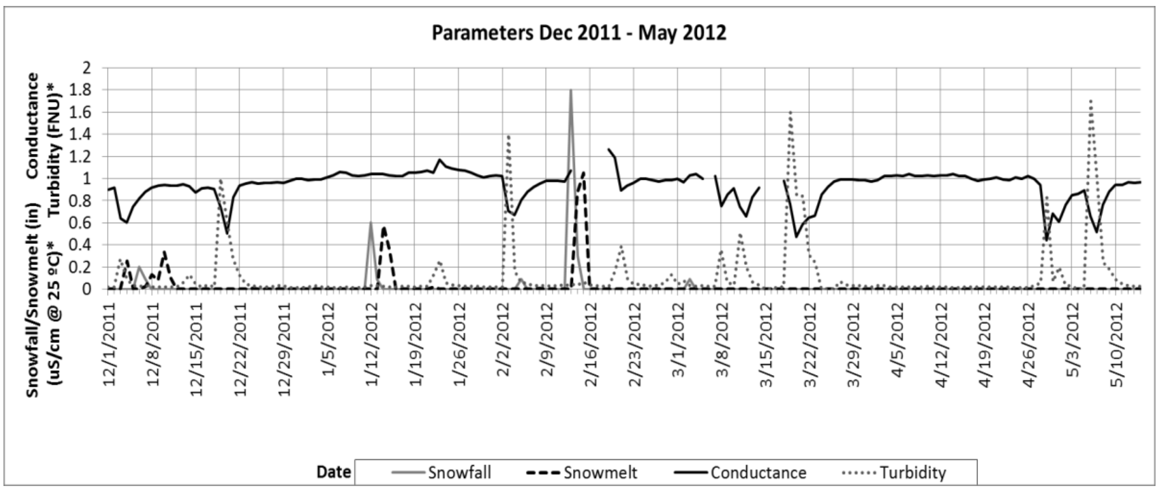

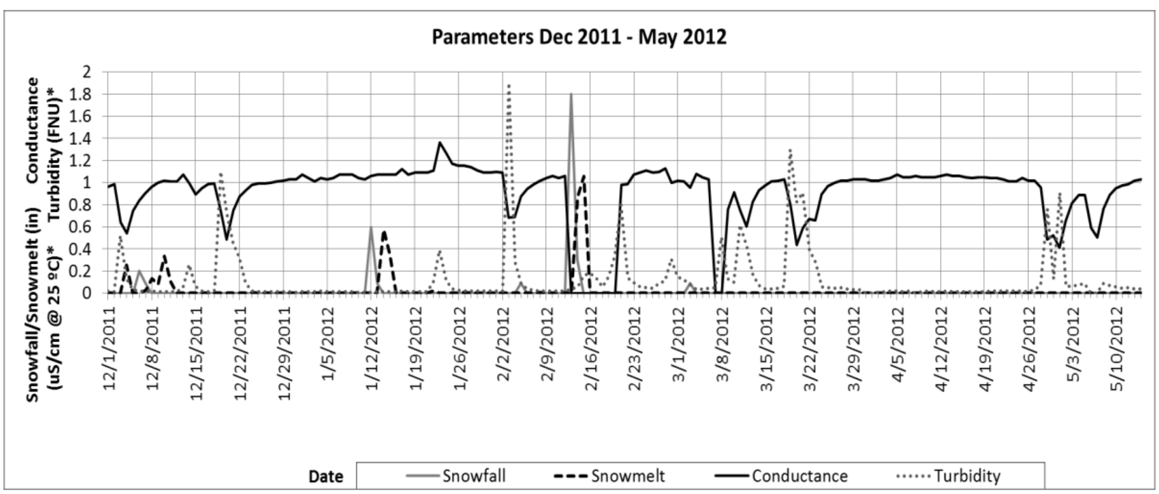

Figure 42 Snowfall, snowmelt, specific conductance, and turbidity for calibration at USGS stations 385446094430700, 385520094420000, and 06893300 respectively (2011 – 2012).

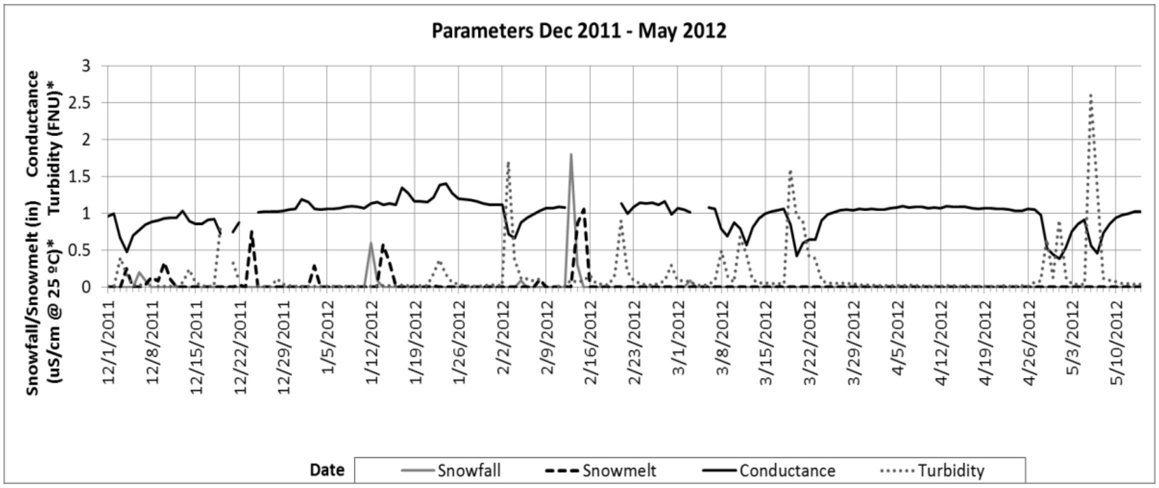

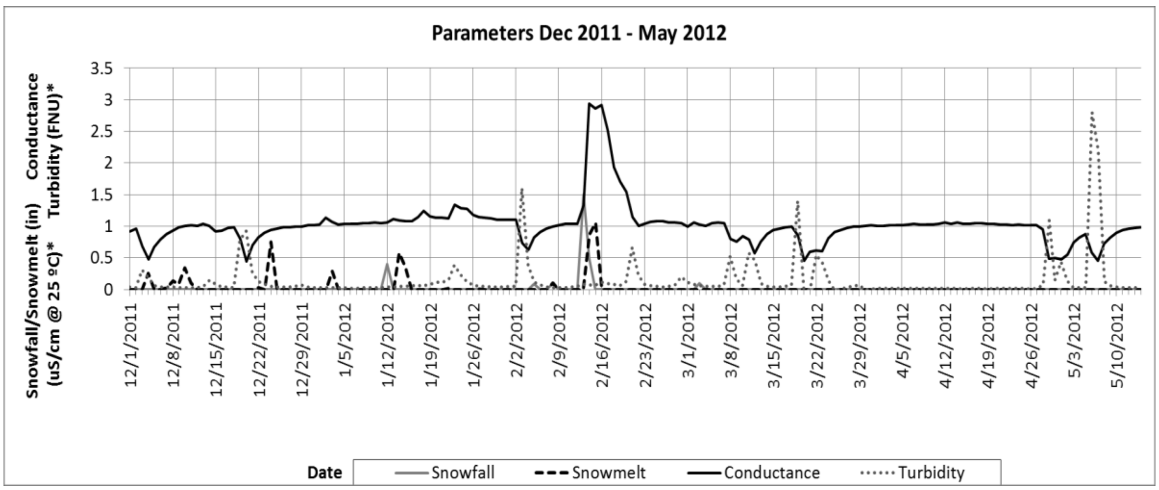

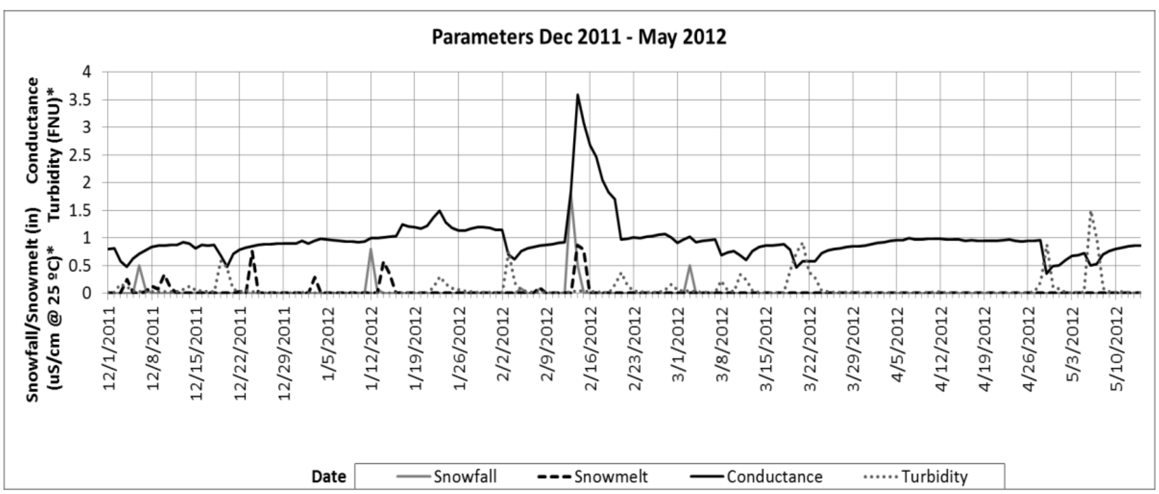

Figure 43. Snowfall, snowmelt, specific conductance, and turbidity for calibration at USGS stations 385608094380300, 06893390, and 06893350 respectively (2011 – 2012).

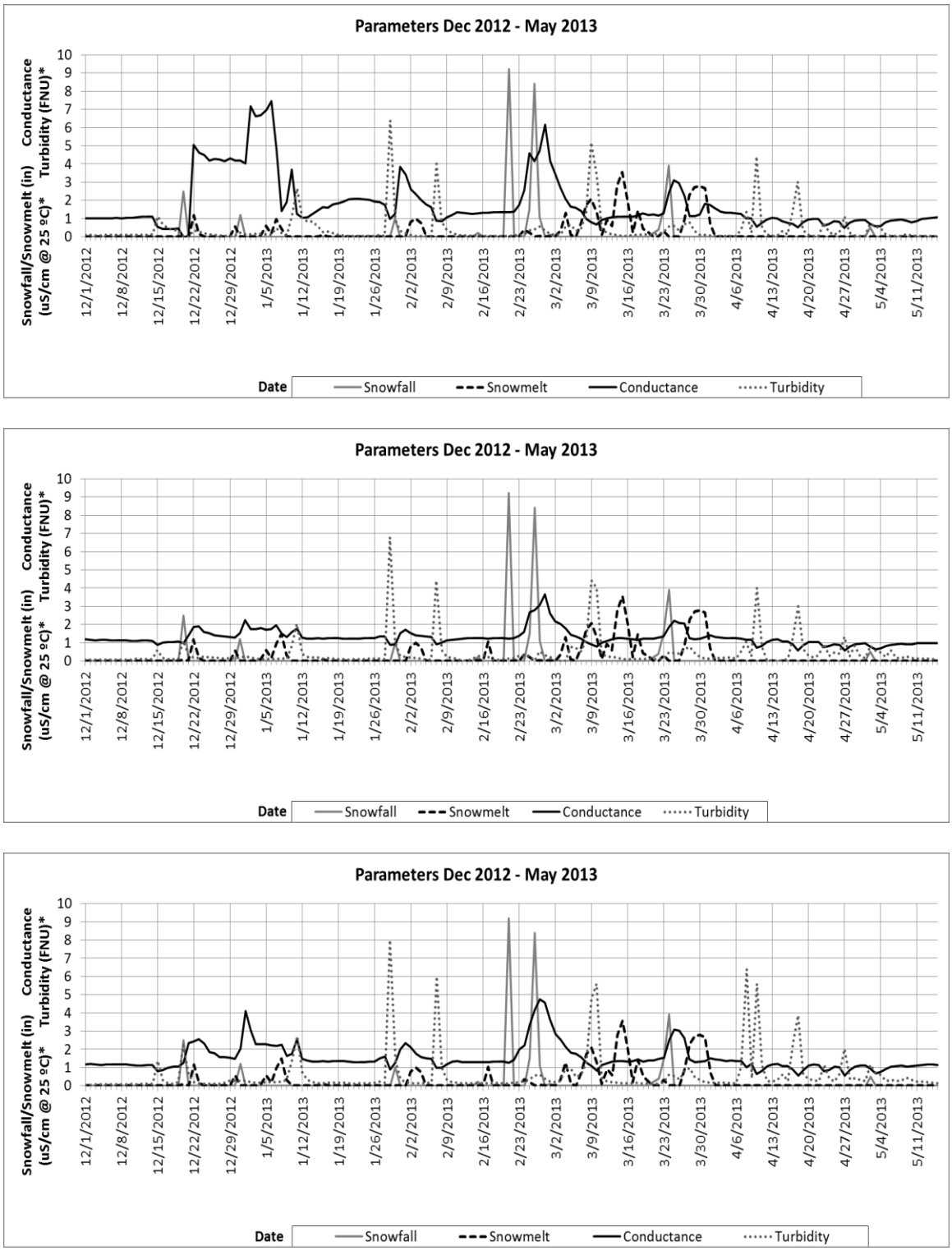

Figure 44. Snowfall, snowmelt, specific conductance, and turbidity for validation at USGS stations 385446094430700, 385520094420000, and 06893300 respectively (2012 – 2013).

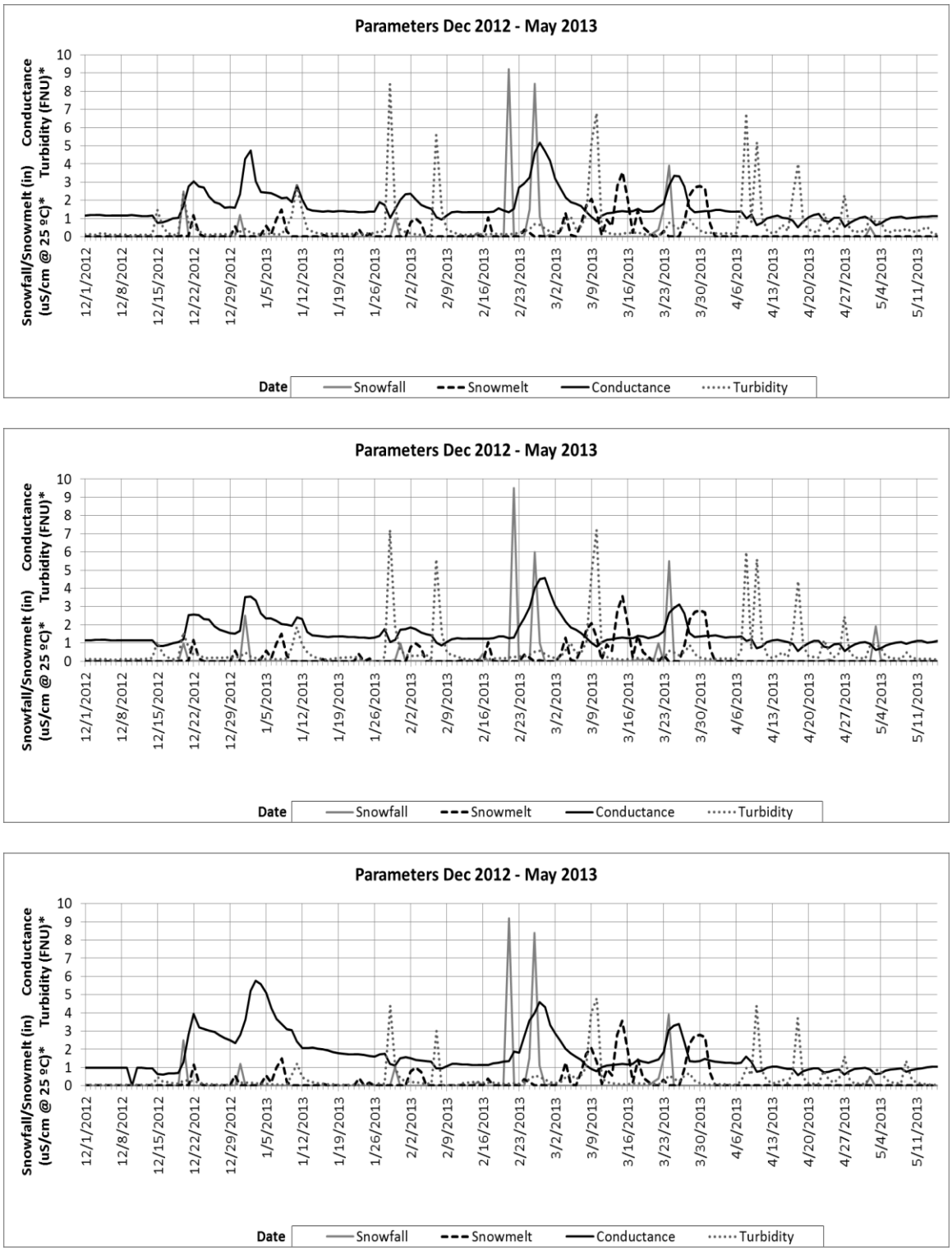

Figure 45. Snowfall, snowmelt, specific conductance, and turbidity for validation at USGS stations 385608094380300, 06893390, and 06893350 respectively (2012 – 2013).

The time series curves are a combination of different parameters and units that have been altered to accommodate the scale of snowfall and snowmelt in inches and to ease the visual interpretation of the data. For the calibration of the time series curves, specific conductance and turbidity where modified by the factor x 0.001 and x 0.01 respectively. For the validation of the time series curve, specific conductance and turbidity where modified by the factor x0.001 and x 0.05 respectively.

Although many thesis and papers have been written about the results with SWAT models, this research differs from those articles by making the runoff and snowmelt calculation an intermedia step to reach time lapse of this climatological process in a final step. The approach using snow fall information in mild winter locations as a media to scientifically calculate transport rates of contaminants may be found just in few other papers.

CHAPTER 5

CONCLUSION

It is fair to say that the initial hypothesis was valid since there is an agreement between the cross correlation analysis and the hydrological modeling results. The results in the hydrological model show a high dependency in relation with their spatiotemporal location.

The alteration between the results of calibration vs validation is highly due to the different precipitation and temperature values of both periods. One of the key components was the DEM and the resolution that affects the final model. It is essential to understand that the acquisition of the DEM may meet two criteria, the resolution must have a balance between accuracy and size, too much resolution implies more processing time and physical size in the machine. Nevertheless the 30 m resolution DEM was good in size the details were not enough to reach a good result in the development of the watershed and sub-basins. The ~1 m resolution DEM complied with both parameters and it has detailed information without being too bulky; approximately 1.82 GB.

ArcSWAT has proven the strength and versatility in hydrological forecasting and accuracy. Despite the lack of abundant information, SWAT calculated the runoff with a satisfactory accuracy serving as a base for the further analysis between snowfall and snowmelt processes. Some of the limitations were the lack of information for discharge values in the USGS stations, the time lapse was limited to the station with shortest dates. Even though the influence of the snow melt process in the conductance was evident, it was not strongly conclusive due to the high influence of the increase in salty solid matter

reflected in the turbidity, which diminishes the conductance values almost instantly; turbidity is a reflection of the possible increase of solid matter coming from sewer pipes that dilutes the salty water.

The limitation of the creation of a hydrological model with time lapse in hours, generates less precision of the final results. One of the most important conclusions was that the relationship between conductance and snowmelt is highly influence by physiographic and climatic factors, being turbidity a reflection of one of the most inferential parameters.

Due to the characteristics of the methodology and the support based on snow events, it is evident that this technique will not be the best choice for places in which snow events are very common because it will be extremely laborious to split the snowfall events to determine the source of snowmelt effects after the fall, when the snow events are typically happening in small periods of time among each other; the principal of the time lapse in places with heavy periods of snowfall is totally lost whatsoever.

The methodology of the research may open more spaces for watershed managers and stakeholders that have oversight the effects of snow melting salts in streams and the time lapses between snow fall and snow melt events and may help to examine or re-evaluate buffer zones in urban spaces.

CHAPTER 6

FUTURE RESEARCH

One of the disadvantages on selecting the Indian Creek as a case study was the lack of extensive time lapse data available to do the analysis during the hydrological modeling results and comparison; the time lapse must be sufficient to cover the calibration and validation of the model. Future research may include a case study with enough information to corroborate the influence of turbidity in the final results. Also, the case study will be chosen taking into account no just the time lapse but the spatial distance of weather station to the basin boundaries. Another point is the collection and analysis of waste water discharges to evaluate the effects of the components of such discharge mostly in the specific conductance and the turbidity. Although the configuration of the storm water system in the urban core was not necessary for this research, it will be taken into account for future developments. The storm water system may dissipate the effects of the salts entering the stream network. It is also important to bring into consideration the homogeneity of the climatology information incorporated within the model; initial parameters were collected from different stations instead of collecting all the datasets within the same climate stations and it may influenced the accuracy of the results as well.

The last improvement to incorporate in the research may be the development of the hydrological model following the same methodology and using hourly information instead of daily information to reach better accuracy on the prediction of snowmelt and the time lapse to reach the streams. Study of temporal resolution is necessary to measure the impacts in the SWAT model, especially for precipitation datasets (Yang, Liu, et al. 2016). Many researchers

have investigated this temporal resolution finding better performance on SWAT models for the sub-daily and sub-hourly analysis in comparison with traditional daily models (Yang, Liu, et al. 2016), (Maharjan, et al. 2013), and (Jeong, et al. 2010). Finally, the comparison among different software applications or add-ins for the development of hydrological models is a great option to find the most accurate software for this type of research.

APPENDICES

APPENDIX A

NOAA Climate Information

U.S. Department of Commerce
National Oceanic & Atmospheric Administration
National Environmental Satellite, Data, and Information Service

Global Summary of the Year 1997 - 2017

Generated on 08/15/2017

National Centers for Environmental Information
151 Patton Avenue
Asheville, North Carolina 28801

Current Location: Elev: 742 ft. Lat: 39.1208° N Lon: -94.5969° W
Station: **KANSAS CITY DOWNTOWN AIRPORT, MO US USW00013988**

Date	Liquid Precipitation (Inches)			Frozen Precipitation (Inches)					Number of Days		
Elem->	PRCP	EMXP		SNOW	EMSN		EMSD		DP01	DP05	DP10
Year	Total Liquid Content	Extreme Max Precip	Date of Occurrence	Snowfall	Extreme Max Snowfall	Date of Occurrence	Extreme Max Snow Depth	Date of Occurrence	Precip >= 0.01"	Precip >= 0.50"	Precip >= 1.00"
1997	33.24	1.64	Jul-12	22.0	5.5	Jan-27	3	Jan-09	74		57
1998	46.52	6.45	Jul-26	4.3	2.5	Mar-08	3	Mar-08	73		60
1999	38.30	3.00	Jun-27	4.6	1.5	Jan-02	0+	Feb-22	83		52
2000	43.27	5.25	Jun-20	6.3	2.2	Jan-28			70		58
2001	54.12	3.50	Jan-28	0.0T	0.0T	Jan-25	0+	Dec-31	73		62
2002	30.15	2.03	May-06						75		58
2003	37.03	5.60	Aug-31						72		55
2004											
2005	42.74	3.16	Aug-19						91		64
2006	28.70	2.00	Aug-27	2.0	1.5	Nov-30	2	Nov-30	65		50
2007	38.80	2.70	May-06	18.0	3.2	Jan-20			84		58
2008	51.88	4.84	Sep-12	14.6	3.0+	Dec-16	3+	Dec-17	105		80
2009	50.80	2.40	Aug-19	17.4	4.5	Dec-25	9	Dec-26	114		83
2010	40.31	2.02	Sep-18	11.8	4.0	Jan-06	5+	Jan-07	98		67
2011	29.26	2.25	Jul-07						81		48
2012	20.86	3.00	Aug-31						72		41
2013	30.31	2.91	Sep-19						91		50
2014	33.40	3.11	Aug-06						86		51
2015	34.13	2.91	May-16						94		57
2016	36.29	4.56	Aug-26						91		56
2017											

(blank) Data element not reported or missing.

+ Occurred on one or more previous dates during the month. The date in the Date field is the last day of occurrence.

A Accumulated amount.

T Trace amount

APPENDIX B

Initial Analysis of Suitable Climate Stations

NAME	STATE	LATITUDE	LONGITUDE	BEGIN DATE	END DATE	STATION TYPE	PARAMETERS
ATCHISON	KS	39.58	-95.11	2000-1-1	Current	HPRCC	MXT,MT,P,S,SD
ATCHISON 1S	KS	39.55	-95.12	2009-6-20	Current	HPRCC	MXT,MT,P,S,SD
BONNER SPRINGS	KS	39.06	-94.9	1964-4-1	Current	HPRCC	MXT,MT,P,S,SD
CENTERVILLE 4SW	KS	38.19	-95.07	1994-3-1	Current	HPRCC	P,S,SD
CLINTON LAKE	KS	38.94	-95.34	2001-7-17	Current	HPRCC	MXT,MT,P,S,SD
DE SOTO	KS	38.97	-94.98	2006-3-4	Current	HPRCC	P,S,SD
EASTON	KS	39.34	-95.12	2008-8-3	Current	HPRCC	P,S,SD
GARNETT 1 E	KS	38.28	-95.22	2009-11-1	Current	HPRCC	MXT,MT,P,S,SD
HILLSDALE LAKE	KS	38.66	-94.89	1986-4-1	Current	HPRCC	MXT,MT,P,S,SD
LANE	KS	38.44	-95.08	2009-2-10	Current	HPRCC	P,S,SD
LAWRENCE	KS	38.96	-95.25	2007-5-9	Current	HPRCC	MXT,MT,P,S,SD
LAWRENCE MUNI AP	KS	39.01	-95.21	2000-1-1	Current	HPRCC	MXT,MT,P,S,SD
LEAVENWORTH 3SW	KS	39.28	-94.95	2011-11-9	Current	HPRCC	MXT,MT,P,S,SD
LECOMPTON	KS	39.05	-95.39	1986-11-1	Current	HPRCC	P,S,SD
MANHATTAN	KS	39.2	-96.58	1984-6-28	Current	HPRCC	MXT,MT,P,W,ST,SR,RH,ET
MOUND CITY 1SSW	KS	38.13	-94.82	2008-4-1	Current	HPRCC	MXT,MT,P,S,SD
OLATHE 3.3 ENE	KS	38.9049	-94.7569		Current	HPRCC	MXT,MT,P,S,SD
OLATHE JOHNSON CO AP	KS	38.83167	-94.88972	2000-10-6	Current	HPRCC	MXT,MT,P,S,SD
OLATHE JOHNSON CO EXEC AP	KS	38.85	-94.73917	2000-7-31	Current	HPRCC	MXT,MT,P,S,SD
OSAWATOMIE	KS	38.5	-94.96	1998-11-1	Current	HPRCC	MXT,MT,P,S,SD
OTTAWA	KS	38.62	-95.28	1985-3-28	Current	HPRCC	MXT,MT,P,W,ST,SR,RH,ET
OVERBROOK 7SE	KS	38.73	-95.44	1996-9-1	Current	HPRCC	P,S,SD
OVERLAND PARK S 87TH	KS	38.9533	-94.7142	2000-1-4	Current	HPRCC	P,S,SD
PARSONS	KS	37.37	-95.28	1985-3-28	Current	HPRCC	MXT,MT,P,W,ST,SR,RH,ET
PERRY LAKE	KS	39.12	-95.41	2000-1-1	Current	HPRCC	MXT,MT,P,S,SD
POMONA LAKE	KS	38.65	-95.57	2002-12-27	Current	HPRCC	MXT,MT,P,S,SD
ROSSVILLE	KS	39.12	-95.92	1989-1-5	Current	HPRCC	MXT,MT,P,W,ST,SR,RH,ET
SILVERLAKE	KS	39.07	-95.77	1985-3-28	Current	HPRCC	MXT,MT,P,W,ST,SR,RH,ET
STANLEY 3S	KS	38.77	-94.67	2010-3-9	Current	HPRCC	P,S,SD
TONGANOXIE	KS	39.03	-95.05	2006-5-1	Current	HPRCC	P,S,SD
TOPEKA MUNI AP	KS	39.07	-95.63	1946-8-1	Current	HPRCC	MXT,MT,P,S,SD
VALLEY FALLS	KS	39.3	-95.49	2001-2-7	Current	HPRCC	MXT,MT,P,S,SD
APPLETON CITY	MO	38.19	-94.03	2000-1-1	Current	HPRCC	MXT,MT,P,S,SD
BUTLER 4W	MO	38.26	-94.41	1978-7-1	Current	HPRCC	MXT,MT,P,S,SD
CLINTON	MO	38.4	-93.77	1990-7-1	Current	HPRCC	MXT,MT,P,S,SD
DREXEL	MO	38.48	-94.61	2008-8-12	2013-12-19	HPRCC	P,S,SD
ELM	MO	38.87	-94.04	1997-9-1	Current	HPRCC	MXT,MT,P,S,SD
HARRISONVILLE	MO	38.65	-94.36	2005-5-1	Current	HPRCC	P,S,SD
HIGGINSVILLE	MO	39.07	-93.71	1991-11-1	Current	HPRCC	MXT,MT,P,S,SD
INDEPENDENCE	MO	39.06	-94.39	1992-6-1	Current	HPRCC	MXT,MT,P,S,SD
KANSAS CITY DOWNTOWN AP	MO	39.12	-94.6	2000-8-15	Current	HPRCC	MXT,MT,P,S,SD
KANSAS CITY INTL AP	MO	39.3	-94.73	1972-10-1	Current	HPRCC	MXT,MT,P,S,SD
KANSAS CITY NWSTC	MO	39.28	-94.66	2010-2-3	Current	HPRCC	MXT,MT,P,S,SD

NAME	STATE	LATITUDE	LONGITUDE	BEGIN DATE	END DATE	STATION TYPE	PARAMETERS
KANSAS CITY PLEASANT HILL	MO	38.81	-94.26	1995-7-1	Current	HPRCC	MXT,MT,P,S,SD
KANSAS CITY SOUTH	MO	38.93	-94.54	2009-4-1	Current	HPRCC	P,S,SD
KANSAS CITY STADIUM DR	MO	39.06	-94.51	2009-12-23	Current	HPRCC	P
KANSAS CITY WATTS MILL	MO	38.9464	-94.6047	2006-4-23	Current	HPRCC	P,S,SD
KEARNEY 3E	MO	39.37	-94.33	2009-7-1	Current	HPRCC	MXT,MT,P,S,SD
KINGSVILLE	MO	38.74	-94.07	2010-1-7	Current	HPRCC	P,S,SD
LEES SUMMIT MUNI AP	MO	38.96	-94.37	2001-10-26	Current	HPRCC	MXT,MT,P,S,SD
LEXINGTON 2SSW	MO	39.16	-93.89	2009-7-10	Current	HPRCC	MXT,MT,P,S,SD
POLO	MO	39.54	-94.04	2006-9-1	Current	HPRCC	MXT,MT,P,S,SD
RAYMORE	MO	38.8	-94.44	2000-1-1	Current	HPRCC	MXT,MT,P,S,SD
RAYTOWN #2	MO	38.97	-94.48	2005-2-6	Current	HPRCC	P,S,SD
RICHMOND 3 S	MO	39.24	-93.97	2000-5-9	Current	HPRCC	MXT,MT,P,S,SD
ROCKPORT	MO	40.47	-95.48	1991-1-1	Current	HPRCC	MXT,MT,P,W,ST,SR,RH,ET
SMITHVILLE LAKE	MO	39.39	-94.56	2000-1-1	Current	HPRCC	MXT,MT,P,S,SD
ST JOSEPH ROSECRANS AP	MO	39.77	-94.92	2000-7-31	Current	HPRCC	MXT,MT,P,S,SD
STJOE	MO	39.77	-94.92	1992-1-1	Current	HPRCC	MXT,MT,P,W,ST,SR,RH,ET
UNITY VILLAGE	MO	38.95	-94.4	2005-7-2	Current	HPRCC	P,S,SD
UNITY VILLAGE 2.6ESE	MO	38.94	-94.36	2008-1-31	Current	HPRCC	MXT,MT,P,S,SD
URICH 2 SW	MO	38.43	-94.03	2006-8-14	Current	HPRCC	P,S,SD
WARRENSBURG 4 NW	MO	38.78	-93.8	1998-2-1	Current	HPRCC	MXT,MT,P,S,SD
BRUNSWICK	MO	39.412667	-93.1965	2008-12-1	Current	UMOEXT	W,SR,ET
GREEN RIDGE	MO	38.621147	-93.416652	2008-12-1	Current	UMOEXT	W,SR,ET

APPENDIX C

Manning's Roughness Coefficients Table

Surface Material	Manning's Roughness Coefficient - *n* -
Asbestos cement	0.011
Asphalt	0.016
Brass	0.011
Brick	0.015
Canvas	0.012
Cast-iron, new	0.012
Clay tile	0.014
Concrete - steel forms	0.011
Concrete (Cement) - finished	0.012
Concrete - wooden forms	0.015
Concrete - centrifugally spun	0.013
Copper	0.011
Corrugated metal	0.022
Earth, smooth	0.018
Earth channel - clean	0.022
Earth channel - gravelly	0.025

Surface Material	Manning's Roughness Coefficient - *n* -
Earth channel - weedy	0.030
Earth channel - stony, cobbles	0.035
Floodplains - pasture, farmland	0.035
Floodplains - light brush	0.050
Floodplains - heavy brush	0.075
Floodplains - trees	0.15
Galvanized iron	0.016
Glass	0.010
Gravel, firm	0.023
Lead	0.011
Masonry	0.025
Metal - corrugated	0.022
Natural streams - clean and straight	0.030
Natural streams - major rivers	0.035
Natural streams - sluggish with deep pools	0.040
Natural channels, very poor condition	0.060

Surface Material	Manning's Roughness Coefficient - *n* -
Plastic	0.009
Polyethylene PE - Corrugated with smooth inner walls	0.009 - 0.015
Polyethylene PE - Corrugated with corrugated inner walls	0.018 - 0.025
Polyvinyl Chloride PVC - with smooth inner walls	0.009 - 0.011
Rubble Masonry	0.017
Steel - Coal-tar enamel	0.010
Steel - smooth	0.012
Steel - New unlined	0.011
Steel - Riveted	0.019
Vitrified Sewer	0.013 - 0.015
Wood - planed	0.012
Wood - unplaned	0.013
Wood stove pipe, small diameter	0.011 - 0.012
Wood stove pipe, large diameter	0.012 - 0.013

APPENDIX D

Python Script for Organization and Accuracy Calculation of the Model

Python Script for Organization and Accuracy Calculation of the Model

```
# import modules
import arcpy
import timeit
start = timeit.default_timer()
print start
# definition of variables
arcpy.env.workspace = r"C:\Student\UMKC\Thesis\GIS\gdb\RunoffCalculations.gdb"
Area3 = 5915254.356
Area4 = 4591190.379
Area5 = 83738.4863
Area6 = 686021.0045
Area7 = 5340452.947
Area8 = 3453069.307
Area9 = 6408876.615
Area10 = 643089.556
Area11 = 5666385.896
Area13 = 4865617.654
Area14 = 2604099.774
Area15 = 4178129.232
Area16 = 1926791.307
Area17 = 5584649.084
Area18 = 6697865.119
Area19 = 4111991.310048
```

Area20 = 3984365.116757

Area21 = 8727168.558616

Area22 = 5681126.827

Area23 = 4833588.421

Area24 = 1188413.48

Area25 = 5928141.65188

Area26 = 4985431.865367

Area27 = 16593174.38

Area28 = 9254653.359

Area29 = 8171853.186972

Area30 = 356311.231116

Area31 = 86246.10708

Area32 = 590864.6018

Area33 = 1182841.529

Area34 = 22731456.04

Area35 = 8637783.499839

FC1 = "Runoff_Data_26C"

#Where "YYYYMMDD" is [0],"SUB" is [1],"SURQmm" is [2]

FC1_Fields = ["YYYYMMDD","SUB","SURQmm"]

FC2 = "Runoff_Comp_Mod_26C"

#Where "YYYYMMDD" is [0],"SIM_30700" is [1],"SIM_20000" is [2],"SIM_93300" is [3],"SIM_80300" is [4],"SIM_93390" is [5],"SIM_93350" is [6],"OBS_30700"is [7],"OBS_20000" is [8],"OBS_93300" is [9],"OBS_80300" is [10],"OBS_93390" is [11],"OBS_93350" is [12]

"OBSSUM30700" is [13],"OBSAVE30700" is [14],"SIMSUM30700" is [15],"SIMAVE30700" is [16],"NSE30700_P1" is [17],"NSE30700_P2" is [18],"NSESUM30700_P1" is [19],"NSESUM30700_P2" is [20],"NSE_30700" is [21],"PBIAS30700_P1" is [22],"PBIAS_30700" is [23]

"R2_37000_P1" is [24],"R2_37000_P2" is [25],"R2SUM37000_P1" is [26],"R2SUM37000_P2" is [27],"R2_37000_P3" is [28],"R2_37000" is [29]

"OBSSUM20000" is [30],"OBSAVE20000" is [31],"SIMSUM20000" is [32],"SIMAVE20000" is [33],"NSE20000_P1" is [34],"NSE20000_P2" is [35],"NSESUM20000_P1" is [36],"NSESUM20000_P2" is [37],"NSE_20000" is [38],"PBIAS20000_P1" is [39],"PBIAS_20000" is [40]

"R2_20000_P1" is [41],"R2_20000_P2" is [42],"R2SUM20000_P1" is [43],"R2SUM20000_P2" is [44],"R2_20000_P3" is [45],"R2_20000" is [46]

"OBSSUM93300" is [47],"OBSAVE93300" is [48],"SIMSUM93300" is [49],"SIMAVE93300" is [50],"NSE93300_P1" is [51],"NSE93300_P2" is [52],"NSESUM93300_P1" is [53],"NSESUM93300_P2" is [54],"NSE_93300" is [55],"PBIAS93300_P1" is [56],"PBIAS_93300" is [57]

"R2_93300_P1" is [58],"R2_93300_P2" is [59],"R2SUM93300_P1" is [60],"R2SUM93300_P2" is [61],"R2_93300_P3" is [62],"R2_93300" is [63]

"OBSSUM80300" is [64],"OBSAVE80300" is [65],"SIMSUM80300" is [66],"SIMAVE80300" is [67],"NSE80300_P1" is [68],"NSE80300_P2" is [69],"NSESUM80300_P1" is [70],"NSESUM80300_P2" is [71],"NSE_80300" is [72],"PBIAS80300_P1" is [73],"PBIAS_80300" is [74]

"R2_80300_P1" is [75],"R2_80300_P2" is [76],"R2SUM80300_P1" is [77],"R2SUM80300_P2" is [78],"R2_80300_P3" is [79],"R2_80300" is [80]

"OBSSUM93390" is [81],"OBSAVE93390" is [82],"SIMSUM93390" is [83],"SIMAVE93390" is [84],"NSE93390_P1" is [85],"NSE93390_P2" is [86],"NSESUM93390_P1" is [87],"NSESUM93390_P2" is [88],"NSE_93390" is [89],"PBIAS93390_P1" is [90],"PBIAS_93390" is [91]

"R2_93390_P1" is [92],"R2_93390_P2" is [93],"R2SUM93390_P1" is [94],"R2SUM93390_P2" is [95],"R2_93390_P3" is [96],"R2_93390" is [97]

"OBSSUM93350" is [98],"OBSAVE93350" is [99],"SIMSUM93350" is [100],"SIMAVE93350" is [101],"NSE93350_P1" is [102],"NSE93350_P2" is [103],"NSESUM93350_P1" is [104],"NSESUM93350_P2" is [105],"NSE_93350" is [106],"PBIAS93350_P1" is [107],"PBIAS_93350" is [108]

"R2_93350_P1" is [109],"R2_93350_P2" is [110],"R2SUM93350_P1" is [111],"R2SUM93350_P2" is [112],"R2_93350_P3" is [113],"R2_93350" is [114],"NSE_AVE" is [115],"PBIAS_AVE" is [116],"R2_AVE" is [117]

FC2_Fields = ["YYYYMMDD","SIM_30700","SIM_20000","SIM_93300","SIM_80300","SIM_93390","SIM_93350","OBS_30700","OBS_20000","OBS_93300","OBS_80300","OBS_93390","OBS_93350","OBSSUM30700","OBSAVE30700","SIMSUM30700","SIMAVE30700","NSE30700_P1","NSE30700_P2","NSESUM30700_P1","NSESUM30700_P2","NSE_30700","PBIAS30700_P1","PBIAS_30700","R2_30700_P1","R2_30700_P2","R2SUM30700_P1","R2SUM30700_P2","R2_30700_P3","R2_30700",

"OBSSUM20000","OBSAVE20000","SIMSUM20000","SIMAVE20000","NSE20000_P1","NSE20000_P2","NSESUM20000_P1","NSESUM20000_P2","NSE_20000","PBIAS20000_P1","PBIAS_20000","R2_20000_P1","R2_20000_P2","R2SUM20000_P1","R2SUM20000_P2","R2_20000_P3","R2_20000",

"OBSSUM93300","OBSAVE93300","SIMSUM93300","SIMAVE93300","NSE93300_P1","NSE93300_P2","NSESUM93300_P1","NSESUM93300_P2","NSE_93300","PBIAS93300_P1","PBIAS_93300","R2_93300_P1","R2_93300_P2","R2SUM93300_P1","R2SUM93300_P2","R2_93300_P3","R2_93300",

"OBSSUM80300","OBSAVE80300","SIMSUM80300","SIMAVE80300","NSE80300_P1","NSE80300_P2","NSESUM80300_P1","NSESUM80300_P2","NSE_80300","PBIAS80300_P1","PBIAS_80300","R2_80300_P1","R2_80300_P2","R2SUM80300_P1","R2SUM80300_P2","R2_80300_P3","R2_80300",

"OBSSUM93390","OBSAVE93390","SIMSUM93390","SIMAVE93390","NSE93390_P1","NSE93390_P2","NSESUM93390_P1","NSESUM93390_P2","NSE_93390","PBIAS93390_P1","PBIAS_93390","R2_93390_P1","R2_93390_P2","R2SUM93390_P1","R2SUM93390_P2","R2_93390_P3","R2_93390",

"OBSSUM93350","OBSAVE93350","SIMSUM93350","SIMAVE93350","NSE93350_P1","NSE93350_P2","NSESUM93350_P1","NSESUM93350_P2","NSE_93350","PBIAS93350_P1","PBIAS_93350","R2_93350_P1","R2_93350_P2","R2SUM93350_P1","R2SUM93350_P2","R2_93350_P3","R2_93350","NSE_AVE","PBIAS_AVE","R2_AVE"]

 # start of the fragmentation process and the accuracy calculation

print 'Starting process for Station 30700'

Iter = 0.00

Simsum = 0.00

```
Simave = 0.00
cur2 = arcpy.da.UpdateCursor(FC2, FC2_Fields)
for row2 in cur2:
   cur = arcpy.da.SearchCursor(FC1, FC1_Fields, sql_clause=(None, 'ORDER BY
YYYYMMDD'))
   for row in cur:
            if row[0] == row2[0]:
             if row[1] == 19:
                Iter = Iter + 1
                row2[1] = ((row[2]*Area19)/1000)
             else:
                pass
             if row[1] == 20:
                Iter = Iter + 1
                row2[1] += ((row[2]*Area20)/1000)
             else:
                pass
             if row[1] == 21:
                Iter = Iter + 1
                row2[1] += ((row[2]*Area21)/1000)
             else:
                pass
             if row[1] == 25:
                Iter = Iter + 1
                row2[1] += ((row[2]*Area25)/1000)
```

```
            else:
                pass
            if row[1] == 26:
                Iter = Iter + 1
                row2[1] += ((row[2]*Area26)/1000)
            else:
                pass
            if row[1] == 29:
                Iter = Iter + 1
                row2[1] += ((row[2]*Area29)/1000)
            else:
                pass
            if row[1] == 30:
                Iter = Iter + 1
                row2[1] += ((row[2]*Area30)/1000)
            else:
                pass
    cur2.updateRow(row2)
    Simsum = Simsum + row2[1]
    Simave = Simsum/(Iter/7)
    arcpy.CalculateField_management(FC2, "SIMSUM30700", Simsum, "PYTHON_9.3", "")
    arcpy.CalculateField_management(FC2, "SIMAVE30700", Simave, "PYTHON_9.3", "")
    arcpy.CalculateField_management(FC2, "NSE30700_P1", "math.pow( !OBS_30700! -
!SIM_30700!,2 )", "PYTHON_9.3", "")
    arcpy.CalculateField_management(FC2, "PBIAS30700_P1", "(( !OBS_30700! -
!SIM_30700! ) * 100)/ !OBSSUM30700!", "PYTHON_9.3", "")
```

```
    arcpy.CalculateField_management(FC2, "R2_30700_P1", "(!OBS_30700! -
!OBSAVE30700! ) * (!SIM_30700! - !SIMAVE30700!)", "PYTHON_9.3", "")

    arcpy.CalculateField_management(FC2, "R2_30700_P2", "math.pow( !SIM_30700! -
!SIMAVE30700!,2 )", "PYTHON_9.3", "")


del cur, row, cur2, row2


NSESumP1 = 0.00

PBIAS = 0.00

R2SumP1 = 0.00

R2SumP2 = 0.00

cur2 = arcpy.da.SearchCursor(FC2, FC2_Fields)

for row2 in cur2:

    NSESumP1 = NSESumP1 + row2[17]

    PBIAS = PBIAS + row2[22]

    R2SumP1 = R2SumP1 + row2[24]

    R2SumP2 = R2SumP2 + row2[25]

arcpy.CalculateField_management(FC2, "NSESUM30700_P1", NSESumP1,
"PYTHON_9.3", "")

arcpy.CalculateField_management(FC2, "NSE_30700","(!NSESUM30700_P2! -
!NSESUM30700_P1!)/!NSESUM30700_P2!", "PYTHON_9.3", "")

arcpy.CalculateField_management(FC2, "PBIAS_30700", PBIAS, "PYTHON_9.3", "")

arcpy.CalculateField_management(FC2, "R2SUM30700_P1", R2SumP1, "PYTHON_9.3",
"")

arcpy.CalculateField_management(FC2, "R2SUM30700_P2", R2SumP2, "PYTHON_9.3",
"")

arcpy.CalculateField_management(FC2, "R2_30700_P3", "math.sqrt( !NSESUM30700_P2!
* !R2SUM30700_P2! )", "PYTHON_9.3", "")
```

```
arcpy.CalculateField_management(FC2, "R2_30700", "math.pow( !R2SUM30700_P1! /
!R2_30700_P3!,2 )", "PYTHON_9.3", "")

del cur2, row2

print 'Finished process for Station 30700'


print 'Starting process for Station 20000'

Iter = 0.00

Simsum = 0.00

Simave = 0.00

cur2 = arcpy.da.UpdateCursor(FC2, FC2_Fields)

for row2 in cur2:

   cur = arcpy.da.SearchCursor(FC1, FC1_Fields, sql_clause=(None, 'ORDER BY
YYYYMMDD'))

   for row in cur:

            if row[0] == row2[0]:

              if row[1] == 18:

                 Iter = Iter + 1

                 row2[2] = ((row[2]*Area18)/1000)

              else:

                 pass

              if row[1] == 19:

                 Iter = Iter + 1

                 row2[2] += ((row[2]*Area19)/1000)

              else:

                 pass

              if row[1] == 20:
```

```
        Iter = Iter + 1
        row2[2] += ((row[2]*Area20)/1000)
    else:
        pass
    if row[1] == 21:
        Iter = Iter + 1
        row2[2] += ((row[2]*Area21)/1000)
    else:
        pass
    if row[1] == 25:
        Iter = Iter + 1
        row2[2] += ((row[2]*Area25)/1000)
    else:
        pass
    if row[1] == 26:
        Iter = Iter + 1
        row2[2] += ((row[2]*Area26)/1000)
    else:
        pass
    if row[1] == 29:
        Iter = Iter + 1
        row2[2] += ((row[2]*Area29)/1000)
    else:
        pass
    if row[1] == 30:
```

```
                Iter = Iter + 1
                row2[2] += ((row[2]*Area30)/1000)
            else:
                pass
    cur2.updateRow(row2)
    Simsum = Simsum + row2[2]
    Simave = Simsum/(Iter/8)
    arcpy.CalculateField_management(FC2, "SIMSUM20000", Simsum, "PYTHON_9.3", "")
    arcpy.CalculateField_management(FC2, "SIMAVE20000", Simave, "PYTHON_9.3", "")
    arcpy.CalculateField_management(FC2, "NSE20000_P1", "math.pow( !OBS_20000! -
!SIM_20000!,2 )", "PYTHON_9.3", "")
    arcpy.CalculateField_management(FC2, "PBIAS20000_P1", "(( !OBS_20000! -
!SIM_20000! ) * 100)/ !OBSSUM20000!", "PYTHON_9.3", "")
    arcpy.CalculateField_management(FC2, "R2_20000_P1", "(!OBS_20000! -
!OBSAVE20000! ) * (!SIM_20000! - !SIMAVE20000!)", "PYTHON_9.3", "")
    arcpy.CalculateField_management(FC2, "R2_20000_P2", "math.pow( !SIM_20000! -
!SIMAVE20000!,2 )", "PYTHON_9.3", "")


del cur, row, cur2, row2


NSESumP1 = 0.0
PBIAS = 0.0
R2SumP1 = 0.0
R2SumP2 = 0.0
cur2 = arcpy.da.SearchCursor(FC2, FC2_Fields)
for row2 in cur2:
    NSESumP1 = NSESumP1 + row2[34]
```

```
    PBIAS = PBIAS + row2[39]

    R2SumP1 = R2SumP1 + row2[41]

    R2SumP2 = R2SumP2 + row2[42]

arcpy.CalculateField_management(FC2, "NSESUM20000_P1", NSESumP1,
"PYTHON_9.3", "")

arcpy.CalculateField_management(FC2, "NSE_20000","(!NSESUM20000_P2! -
!NSESUM20000_P1!)/!NSESUM20000_P2!", "PYTHON_9.3", "")

arcpy.CalculateField_management(FC2, "PBIAS_20000", PBIAS, "PYTHON_9.3", "")

arcpy.CalculateField_management(FC2, "R2SUM20000_P1", R2SumP1, "PYTHON_9.3",
"")

arcpy.CalculateField_management(FC2, "R2SUM20000_P2", R2SumP2, "PYTHON_9.3",
"")

arcpy.CalculateField_management(FC2, "R2_20000_P3", "math.sqrt( !NSESUM20000_P2!
* !R2SUM20000_P2! )", "PYTHON_9.3", "")

arcpy.CalculateField_management(FC2, "R2_20000", "math.pow( !R2SUM20000_P1! /
!R2_20000_P3!,2 )", "PYTHON_9.3", "")

del cur2, row2

print 'Finished process for Station 20000'


print 'Starting process for Station 93300'

Iter = 0.00

Simsum = 0.00

Simave = 0.00

cur2 = arcpy.da.UpdateCursor(FC2, FC2_Fields)

for row2 in cur2:

    cur = arcpy.da.SearchCursor(FC1, FC1_Fields, sql_clause=(None, 'ORDER BY
YYYYMMDD'))

    for row in cur:
```

```
if row[0] == row2[0]:
  if row[1] == 9:
     Iter = Iter + 1
     row2[3] = ((row[2]*Area9)/1000)
  else:
     pass
  if row[1] == 11:
     Iter = Iter + 1
     row2[3] += ((row[2]*Area11)/1000)
  else:
     pass
  if row[1] == 15:
     Iter = Iter + 1
     row2[3] += ((row[2]*Area15)/1000)
  else:
     pass
  if row[1] == 16:
     Iter = Iter + 1
     row2[3] += ((row[2]*Area16)/1000)
  else:
     pass
  if row[1] == 17:
     Iter = Iter + 1
     row2[3] += ((row[2]*Area17)/1000)
  else:
```

```
    pass
if row[1] == 18:
    Iter = Iter + 1
    row2[3] += ((row[2]*Area18)/1000)
else:
    pass
if row[1] == 19:
    Iter = Iter + 1
    row2[3] += ((row[2]*Area19)/1000)
else:
    pass
if row[1] == 20:
    Iter = Iter + 1
    row2[3] += ((row[2]*Area20)/1000)
else:
    pass
if row[1] == 21:
    Iter = Iter + 1
    row2[3] += ((row[2]*Area21)/1000)
else:
    pass
if row[1] == 25:
    Iter = Iter + 1
    row2[3] += ((row[2]*Area25)/1000)
else:
```

```
    pass
if row[1] == 26:
    Iter = Iter + 1
    row2[3] += ((row[2]*Area26)/1000)
else:
    pass
if row[1] == 29:
    Iter = Iter + 1
    row2[3] += ((row[2]*Area29)/1000)
else:
    pass
if row[1] == 30:
    Iter = Iter + 1
    row2[3] += ((row[2]*Area30)/1000)
else:
    pass
if row[1] == 31:
    Iter = Iter + 1
    row2[3] += ((row[2]*Area31)/1000)
else:
    pass
if row[1] == 32:
    Iter = Iter + 1
    row2[3] += ((row[2]*Area32)/1000)
else:
```

```
                pass
    cur2.updateRow(row2)
    Simsum = Simsum + row2[3]
    Simave = Simsum/(Iter/15)
    arcpy.CalculateField_management(FC2, "SIMSUM93300", Simsum, "PYTHON_9.3", "")
    arcpy.CalculateField_management(FC2, "SIMAVE93300", Simave, "PYTHON_9.3", "")
    arcpy.CalculateField_management(FC2, "NSE93300_P1", "math.pow( !OBS_93300! -
!SIM_93300!,2 )", "PYTHON_9.3", "")
    arcpy.CalculateField_management(FC2, "PBIAS93300_P1", "(( !OBS_93300! -
!SIM_93300! ) * 100)/ !OBSSUM93300!", "PYTHON_9.3", "")
    arcpy.CalculateField_management(FC2, "R2_93300_P1", "(!OBS_93300! -
!OBSAVE93300! ) * (!SIM_93300! - !SIMAVE93300!)", "PYTHON_9.3", "")
    arcpy.CalculateField_management(FC2, "R2_93300_P2", "math.pow( !SIM_93300! -
!SIMAVE93300!,2 )", "PYTHON_9.3", "")


del cur, row, cur2, row2


NSESumP1 = 0.0
PBIAS = 0.0
R2SumP1 = 0.0
R2SumP2 = 0.0
cur2 = arcpy.da.SearchCursor(FC2, FC2_Fields)
for row2 in cur2:
    NSESumP1 = NSESumP1 + row2[51]
    PBIAS = PBIAS + row2[56]
    R2SumP1 = R2SumP1 + row2[58]
    R2SumP2 = R2SumP2 + row2[59]
```

```
arcpy.CalculateField_management(FC2, "NSESUM93300_P1", NSESumP1,
"PYTHON_9.3", "")

arcpy.CalculateField_management(FC2, "NSE_93300","(!NSESUM93300_P2! -
!NSESUM93300_P1!)/!NSESUM93300_P2!", "PYTHON_9.3", "")

arcpy.CalculateField_management(FC2, "PBIAS_93300", PBIAS, "PYTHON_9.3", "")

arcpy.CalculateField_management(FC2, "R2SUM93300_P1", R2SumP1, "PYTHON_9.3",
"")

arcpy.CalculateField_management(FC2, "R2SUM93300_P2", R2SumP2, "PYTHON_9.3",
"")

arcpy.CalculateField_management(FC2, "R2_93300_P3", "math.sqrt( !NSESUM93300_P2!
* !R2SUM93300_P2! )", "PYTHON_9.3", "")

arcpy.CalculateField_management(FC2, "R2_93300", "math.pow( !R2SUM93300_P1! /
!R2_93300_P3!,2 )", "PYTHON_9.3", "")

del cur2, row2

print 'Finished process for Station 93300'


print 'Starting process for Station 80300'

Iter = 0.00

Simsum = 0.00

Simave = 0.00

cur2 = arcpy.da.UpdateCursor(FC2, FC2_Fields)

for row2 in cur2:

   cur = arcpy.da.SearchCursor(FC1, FC1_Fields, sql_clause=(None, 'ORDER BY
YYYYMMDD'))

   for row in cur:

            if row[0] == row2[0]:

              if row[1] == 3:

                 Iter = Iter + 1
```

```
    row2[4] = ((row[2]*Area3)/1000)
else:
    pass
if row[1] == 4:
    Iter = Iter + 1
    row2[4] += ((row[2]*Area4)/1000)
else:
    pass
if row[1] == 5:
    Iter = Iter + 1
    row2[4] += ((row[2]*Area5)/1000)
else:
    pass
if row[1] == 6:
    Iter = Iter + 1
    row2[4] += ((row[2]*Area6)/1000)
else:
    pass
if row[1] == 7:
    Iter = Iter + 1
    row2[4] += ((row[2]*Area7)/1000)
else:
    pass
if row[1] == 8:
    Iter = Iter + 1
```

```
    row2[4] += ((row[2]*Area8)/1000)
else:
    pass
if row[1] == 9:
    Iter = Iter + 1
    row2[4] += ((row[2]*Area9)/1000)
else:
    pass
if row[1] == 10:
    Iter = Iter + 1
    row2[4] += ((row[2]*Area10)/1000)
else:
    pass
if row[1] == 11:
    Iter = Iter + 1
    row2[4] += ((row[2]*Area11)/1000)
else:
    pass
if row[1] == 13:
    Iter = Iter + 1
    row2[4] += ((row[2]*Area13)/1000)
else:
    pass
if row[1] == 15:
    Iter = Iter + 1
```

```
    row2[4] += ((row[2]*Area15)/1000)
else:
    pass
if row[1] == 16:
    Iter = Iter + 1
    row2[4] += ((row[2]*Area16)/1000)
else:
    pass
if row[1] == 17:
    Iter = Iter + 1
    row2[4] += ((row[2]*Area17)/1000)
else:
    pass
if row[1] == 18:
    Iter = Iter + 1
    row2[4] += ((row[2]*Area18)/1000)
else:
    pass
if row[1] == 19:
    Iter = Iter + 1
    row2[4] += ((row[2]*Area19)/1000)
else:
    pass
if row[1] == 20:
    Iter = Iter + 1
```

```
    row2[4] += ((row[2]*Area20)/1000)
else:
    pass
if row[1] == 21:
    Iter = Iter + 1
    row2[4] += ((row[2]*Area21)/1000)
else:
    pass
if row[1] == 25:
    Iter = Iter + 1
    row2[4] += ((row[2]*Area25)/1000)
else:
    pass
if row[1] == 26:
    Iter = Iter + 1
    row2[4] += ((row[2]*Area26)/1000)
else:
    pass
if row[1] == 29:
    Iter = Iter + 1
    row2[4] += ((row[2]*Area29)/1000)
else:
    pass
if row[1] == 30:
    Iter = Iter + 1
```

```
            row2[4] += ((row[2]*Area30)/1000)
        else:
            pass
        if row[1] == 31:
            Iter = Iter + 1
            row2[4] += ((row[2]*Area31)/1000)
        else:
            pass
        if row[1] == 32:
            Iter = Iter + 1
            row2[4] += ((row[2]*Area32)/1000)
        else:
            pass
        if row[1] == 33:
            Iter = Iter + 1
            row2[4] += ((row[2]*Area33)/1000)
        else:
            pass
    cur2.updateRow(row2)
    Simsum = Simsum + row2[4]
    Simave = Simsum/(Iter/24)
    arcpy.CalculateField_management(FC2, "SIMSUM80300", Simsum, "PYTHON_9.3", "")
    arcpy.CalculateField_management(FC2, "SIMAVE80300", Simave, "PYTHON_9.3", "")
    arcpy.CalculateField_management(FC2, "NSE80300_P1", "math.pow( !OBS_80300! -
!SIM_80300!,2 )", "PYTHON_9.3", "")
```

```
    arcpy.CalculateField_management(FC2, "PBIAS80300_P1", "(( !OBS_80300! - !SIM_80300! ) * 100)/ !OBSSUM80300!", "PYTHON_9.3", "")

    arcpy.CalculateField_management(FC2, "R2_80300_P1", "(!OBS_80300! - !OBSAVE80300! ) * (!SIM_80300! - !SIMAVE80300!)", "PYTHON_9.3", "")

    arcpy.CalculateField_management(FC2, "R2_80300_P2", "math.pow( !SIM_80300! - !SIMAVE80300!,2 )", "PYTHON_9.3", "")


del cur, row, cur2, row2


NSESumP1 = 0.0

PBIAS = 0.0

R2SumP1 = 0.0

R2SumP2 = 0.0

cur2 = arcpy.da.SearchCursor(FC2, FC2_Fields)

for row2 in cur2:

    NSESumP1 = NSESumP1 + row2[68]

    PBIAS = PBIAS + row2[73]

    R2SumP1 = R2SumP1 + row2[75]

    R2SumP2 = R2SumP2 + row2[76]

arcpy.CalculateField_management(FC2, "NSESUM80300_P1", NSESumP1, "PYTHON_9.3", "")

arcpy.CalculateField_management(FC2, "NSE_80300","(!NSESUM80300_P2! - !NSESUM80300_P1!)/!NSESUM80300_P2!", "PYTHON_9.3", "")

arcpy.CalculateField_management(FC2, "PBIAS_80300", PBIAS, "PYTHON_9.3", "")

arcpy.CalculateField_management(FC2, "R2SUM80300_P1", R2SumP1, "PYTHON_9.3", "")

arcpy.CalculateField_management(FC2, "R2SUM80300_P2", R2SumP2, "PYTHON_9.3", "")
```

```
arcpy.CalculateField_management(FC2, "R2_80300_P3", "math.sqrt( !NSESUM80300_P2!
* !R2SUM80300_P2! )", "PYTHON_9.3", "")

arcpy.CalculateField_management(FC2, "R2_80300", "math.pow( !R2SUM80300_P1! /
!R2_80300_P3!,2 )", "PYTHON_9.3", "")

del cur2, row2

print 'Finished process for Station 80300'


print 'Starting process for Station 93390'

Iter = 0.00

Simsum = 0.00

Simave = 0.00

cur2 = arcpy.da.UpdateCursor(FC2, FC2_Fields)

for row2 in cur2:

   cur = arcpy.da.SearchCursor(FC1, FC1_Fields, sql_clause=(None, 'ORDER BY
YYYYMMDD'))

   for row in cur:

            if row[0] == row2[0]:

              if row[1] == 3:

                 Iter = Iter + 1

                 row2[5] = ((row[2]*Area3)/1000)

              else:

                 pass

              if row[1] == 4:

                 Iter = Iter + 1

                 row2[5] += ((row[2]*Area4)/1000)

              else:
```

```
    pass
if row[1] == 5:
    Iter = Iter + 1
    row2[5] += ((row[2]*Area5)/1000)
else:
    pass
if row[1] == 6:
    Iter = Iter + 1
    row2[5] += ((row[2]*Area6)/1000)
else:
    pass
if row[1] == 7:
    Iter = Iter + 1
    row2[5] += ((row[2]*Area7)/1000)
else:
    pass
if row[1] == 8:
    Iter = Iter + 1
    row2[5] += ((row[2]*Area8)/1000)
else:
    pass
if row[1] == 9:
    Iter = Iter + 1
    row2[5] += ((row[2]*Area9)/1000)
else:
```

```
    pass
if row[1] == 10:
    Iter = Iter + 1
    row2[5] += ((row[2]*Area10)/1000)
else:
    pass
if row[1] == 11:
    Iter = Iter + 1
    row2[5] += ((row[2]*Area11)/1000)
else:
    pass
if row[1] == 13:
    Iter = Iter + 1
    row2[5] += ((row[2]*Area13)/1000)
else:
    pass
if row[1] == 14:
    Iter = Iter + 1
    row2[5] += ((row[2]*Area14)/1000)
else:
    pass
if row[1] == 15:
    Iter = Iter + 1
    row2[5] += ((row[2]*Area15)/1000)
else:
```

```
    pass
if row[1] == 16:
    Iter = Iter + 1
    row2[5] += ((row[2]*Area16)/1000)
else:
    pass
if row[1] == 17:
    Iter = Iter + 1
    row2[5] += ((row[2]*Area17)/1000)
else:
    pass
if row[1] == 18:
    Iter = Iter + 1
    row2[5] += ((row[2]*Area18)/1000)
else:
    pass
if row[1] == 19:
    Iter = Iter + 1
    row2[5] += ((row[2]*Area19)/1000)
else:
    pass
if row[1] == 20:
    Iter = Iter + 1
    row2[5] += ((row[2]*Area20)/1000)
else:
```

```
    pass
if row[1] == 21:
    Iter = Iter + 1
    row2[5] += ((row[2]*Area21)/1000)
else:
    pass
if row[1] == 22:
    Iter = Iter + 1
    row2[5] += ((row[2]*Area22)/1000)
else:
    pass
if row[1] == 23:
    Iter = Iter + 1
    row2[5] += ((row[2]*Area23)/1000)
else:
    pass
if row[1] == 24:
    Iter = Iter + 1
    row2[5] += ((row[2]*Area24)/1000)
else:
    pass
if row[1] == 25:
    Iter = Iter + 1
    row2[5] += ((row[2]*Area25)/1000)
else:
```

```
    pass
if row[1] == 26:
    Iter = Iter + 1
    row2[5] += ((row[2]*Area26)/1000)
else:
    pass
if row[1] == 27:
    Iter = Iter + 1
    row2[5] += ((row[2]*Area27)/1000)
else:
    pass
if row[1] == 28:
    Iter = Iter + 1
    row2[5] += ((row[2]*Area28)/1000)
else:
    pass
if row[1] == 29:
    Iter = Iter + 1
    row2[5] += ((row[2]*Area29)/1000)
else:
    pass
if row[1] == 30:
    Iter = Iter + 1
    row2[5] += ((row[2]*Area30)/1000)
else:
```

```
    pass
if row[1] == 31:
    Iter = Iter + 1
    row2[5] += ((row[2]*Area31)/1000)
else:
    pass
if row[1] == 32:
    Iter = Iter + 1
    row2[5] += ((row[2]*Area32)/1000)
else:
    pass
if row[1] == 33:
    Iter = Iter + 1
    row2[5] += ((row[2]*Area33)/1000)
else:
    pass
if row[1] == 34:
    Iter = Iter + 1
    row2[5] += ((row[2]*Area34)/1000)
else:
    pass
if row[1] == 35:
    Iter = Iter + 1
    row2[5] += ((row[2]*Area35)/1000)
else:
```

```
                pass
    cur2.updateRow(row2)
    Simsum = Simsum + row2[5]
    Simave = Simsum/(Iter/32)
    arcpy.CalculateField_management(FC2, "SIMSUM93390", Simsum, "PYTHON_9.3", "")
    arcpy.CalculateField_management(FC2, "SIMAVE93390", Simave, "PYTHON_9.3", "")
    arcpy.CalculateField_management(FC2, "NSE93390_P1", "math.pow( !OBS_93390! -
!SIM_93390!,2 )", "PYTHON_9.3", "")
    arcpy.CalculateField_management(FC2, "PBIAS93390_P1", "(( !OBS_93390! -
!SIM_93390! ) * 100)/ !OBSSUM93390!", "PYTHON_9.3", "")
    arcpy.CalculateField_management(FC2, "R2_93390_P1", "(!OBS_93390! -
!OBSAVE93390! ) * (!SIM_93390! - !SIMAVE93390!)", "PYTHON_9.3", "")
    arcpy.CalculateField_management(FC2, "R2_93390_P2", "math.pow( !SIM_93390! -
!SIMAVE93390!,2 )", "PYTHON_9.3", "")


del cur, row, cur2, row2


NSESumP1 = 0.0
PBIAS = 0.0
R2SumP1 = 0.0
R2SumP2 = 0.0
cur2 = arcpy.da.SearchCursor(FC2, FC2_Fields)
for row2 in cur2:
    NSESumP1 = NSESumP1 + row2[85]
    PBIAS = PBIAS + row2[90]
    R2SumP1 = R2SumP1 + row2[92]
    R2SumP2 = R2SumP2 + row2[93]
```

```
arcpy.CalculateField_management(FC2, "NSESUM93390_P1", NSESumP1,
"PYTHON_9.3", "")

arcpy.CalculateField_management(FC2, "NSE_93390","(!NSESUM93390_P2! -
!NSESUM93390_P1!)/!NSESUM93390_P2!", "PYTHON_9.3", "")

arcpy.CalculateField_management(FC2, "PBIAS_93390", PBIAS, "PYTHON_9.3", "")

arcpy.CalculateField_management(FC2, "R2SUM93390_P1", R2SumP1, "PYTHON_9.3",
"")

arcpy.CalculateField_management(FC2, "R2SUM93390_P2", R2SumP2, "PYTHON_9.3",
"")

arcpy.CalculateField_management(FC2, "R2_93390_P3", "math.sqrt( !NSESUM93390_P2!
* !R2SUM93390_P2! )", "PYTHON_9.3", "")

arcpy.CalculateField_management(FC2, "R2_93390", "math.pow( !R2SUM93390_P1! /
!R2_93390_P3!,2 )", "PYTHON_9.3", "")

del cur2, row2

print 'Finished process for Station 93390'


print 'Starting process for Station 93350'

Iter = 0.00

Simsum = 0.00

Simave = 0.00

cur2 = arcpy.da.UpdateCursor(FC2, FC2_Fields)

for row2 in cur2:

   cur = arcpy.da.SearchCursor(FC1, FC1_Fields, sql_clause=(None, 'ORDER BY
YYYYMMDD'))

   for row in cur:

            if row[0] == row2[0]:

              if row[1] == 22:

                 Iter = Iter + 1
```

```
            row2[6] = ((row[2]*Area22)/1000)
        else:
            pass
        if row[1] == 24:
            Iter = Iter + 1
            row2[6] += ((row[2]*Area24)/1000)
        else:
            pass
        if row[1] == 27:
            Iter = Iter + 1
            row2[6] += ((row[2]*Area27)/1000)
        else:
            pass
        if row[1] == 28:
            Iter = Iter + 1
            row2[6] += ((row[2]*Area28)/1000)
        else:
            pass
        if row[1] == 34:
            Iter = Iter + 1
            row2[6] += ((row[2]*Area34)/1000)
        else:
            pass
cur2.updateRow(row2)
Simsum = Simsum + row2[6]
```

```
    Simave = Simsum/(Iter/5)

    arcpy.CalculateField_management(FC2, "SIMSUM93350", Simsum, "PYTHON_9.3", "")

    arcpy.CalculateField_management(FC2, "SIMAVE93350", Simave, "PYTHON_9.3", "")

    arcpy.CalculateField_management(FC2, "NSE93350_P1", "math.pow( !OBS_93350! -
!SIM_93350!,2 )", "PYTHON_9.3", "")

    arcpy.CalculateField_management(FC2, "PBIAS93350_P1", "(( !OBS_93350! -
!SIM_93350! ) * 100)/ !OBSSUM93350!", "PYTHON_9.3", "")

    arcpy.CalculateField_management(FC2, "R2_93350_P1", "(!OBS_93350! -
!OBSAVE93350! ) * (!SIM_93350! - !SIMAVE93350!)", "PYTHON_9.3", "")

    arcpy.CalculateField_management(FC2, "R2_93350_P2", "math.pow( !SIM_93350! -
!SIMAVE93350!,2 )", "PYTHON_9.3", "")


del cur, row, cur2, row2


NSESumP1 = 0.00

PBIAS = 0.00

R2SumP1 = 0.00

R2SumP2 = 0.00

cur2 = arcpy.da.SearchCursor(FC2, FC2_Fields)

for row2 in cur2:

    NSESumP1 = NSESumP1 + row2[102]

    PBIAS = PBIAS + row2[107]

    R2SumP1 = R2SumP1 + row2[109]

    R2SumP2 = R2SumP2 + row2[110]

arcpy.CalculateField_management(FC2, "NSESUM93350_P1", NSESumP1,
"PYTHON_9.3", "")
```

```
arcpy.CalculateField_management(FC2, "NSE_93350","(!NSESUM93350_P2! -
!NSESUM93350_P1!)/!NSESUM93350_P2!", "PYTHON_9.3", "")

arcpy.CalculateField_management(FC2, "PBIAS_93350", PBIAS, "PYTHON_9.3", "")

arcpy.CalculateField_management(FC2, "R2SUM93350_P1", R2SumP1, "PYTHON_9.3",
"")

arcpy.CalculateField_management(FC2, "R2SUM93350_P2", R2SumP2, "PYTHON_9.3",
"")

arcpy.CalculateField_management(FC2, "R2_93350_P3", "math.sqrt( !NSESUM93350_P2!
* !R2SUM93350_P2! )", "PYTHON_9.3", "")

arcpy.CalculateField_management(FC2, "R2_93350", "math.pow( !R2SUM93350_P1! /
!R2_93350_P3!,2 )", "PYTHON_9.3", "")

del cur2, row2

print 'Finished process for Station 93350'
```

 # final calculations of integration and accuracy

```
# Process: Calculate Field

arcpy.CalculateField_management(FC2, "NSE_AVE", "( !NSE_30700! + !NSE_20000! +
!NSE_93300! + !NSE_80300! + !NSE_93390! + !NSE_93350!)/6", "PYTHON_9.3", "")


# Process: Calculate Field (2)

arcpy.CalculateField_management(FC2, "PBIAS_AVE", "( !PBIAS_30700! +
!PBIAS_20000! + !PBIAS_93300! + !PBIAS_80300! + !PBIAS_93390! +
!PBIAS_93350!)/6", "PYTHON_9.3", "")

# Process: Calculate Field (3)

arcpy.CalculateField_management(FC2, "R2_AVE", "( !R2_30700! + !R2_20000! +
!R2_93300! + !R2_80300! + !R2_93390! + !R2_93350!)/6", "PYTHON_9.3", "")

stop = timeit.default_timer()

print str(stop - start) + ' seconds'

print 'Successfully Finished'
```

REFERENCES

Almeida, Isabel Kaufmann de, Aleska Kaufmann Almeida, Jamil Alexandre Ayach Anache, Jorge Luiz Steffen, and Teodorico Alves Sobrinho. "Estimation on Time of Concentration of Overland Flow in Watersheds: A Review." *Geociencias* 33, no. 4 (2014): 661-671.

Arnold, Jeffrey G., et al. "SWAT: Model Use, Calibration, and Validation." *Transactions of the ASABE* 55, no. 4 (2012): 1491-1508.

Arnold, Jeffrey G., J.R. Kiniry, R. Srinivasan, J.R. Williams, E.B. Haney, and S.L. Neitsch. "Soil and Water Assessment Tool: Input/Output Documentation Version 2012." *SWAT Soil & Water Assessment Tool.* Texas Water Resources Institute. 01 01, 2012. http://swat.tamu.edu/documentation/2012-io/ (accessed 03 11, 2015).

Babbar-Sebens, Meghna, Snehasis Mukhopadhyay, Vidya Bhushan Singh, and Adriana Debora Piemonti. "A Web-based Software Tool for Participatory Optimization of Conservation Practices in Watersheds." *Environmental Modelling & Software* (Elsevier) 69 (2015): 111-127.

Basnyat, Prakash, Larry D. Teeter, Graeme B. Lockaby, and Kathryn M. Flynn. "The Use of Remote Sensing and GIS in Watershed Level Analyses of Non-point Source Pollution Problems." *Forest Ecology and Management* (Elsevier) 128, no. 1 (2000): 65-73.

Beven, Keith. "TOPMODEL: A Critique." *Hydrological Processes* 11 (1997): 1069-1085.

Bhat, Salim Aijaz, Gowhar Meraj, Sayar Yaseen, and Ashok K. Pandit. "Statistical Assessment of Water Quality Parameters for Pollution Source Identification in Sukhnag Stream: An Inflow Stream of Lake Wular (Ramsar Site), Kashmir Himalaya." *Journal of Ecosystems* (Hindawi), 2014: 1-18.

Brett, Michael T., George B. Arhonditsis, Sara E. Mueller, David M. Hartley, Jonathan D. Frodge, and David E. Funke. "Non-point Source Impacts on Stream Nutrient Concentrations Along a Forest to Urban Gradient." *Environmental Management* 35, no. 3 (2005): 330-342.

Chang, Heejun. "Spatial Analysis of Water Quality Trends in the Han River Basin, South Korea." *Water Research* (Elsevier) 42, no. 13 (2008): 3285-3304.

Chinh, Le Van, Haruka Iseri, Kazuaki Hiramatsu, Masayoshi Harada, and Makito Mori. "Simulation of Rainfall Runoff and Pollutant Load for Chikugo River, Basin in Japan Using a GIS-based Distributed Parameter Model." *Paddy Water Environment* (Springer), 2011: 1-16.

Christensen, Victoria G., Xiaodong Jian, and Andrew C. Ziegler. *Regression Analysis and Real-Time Water-Quality Monitoring to Estimate Constituent Concentrations, Loads, and Yields in the Little Arkansas River, South-Central Kansas, 1995-99.* Water-resources Investigation Report, U.S. Geological Survey, Wichita: U.S. Geological Survey, 1999.

Cronshey, Roger, Richard McCuen, Norman Miller, Walter Rawls, Sam Robbins, and Don Woodward. *Urban Hydrology for Small Watersheds.* Technical Report, United States Department of Agriculture, Natural resources Conservation Service, Washington D.C.: United States Department of Agriculture, 1986, 3.1-3.4.

Cruise, James F., Charles A. Laymon, and Osama Z. Al-Hamdan. "Impact of 20 Years of Land-cover Change on the Hydrology of Streams in the Southeastern United States." *Journal of the American Water Resources Association* (Wiley) 46, no. 6 (2010): 1159-1170.

Daggupati, Prasad, et al. "Impact of Model Development, Calibration and Validation Decisions on Hydrological Simulations in West Lake Erie Basin." *Hydrological Processes* (Wiley Online Library) 29, no. 26 (2015): 5307-5320.

Davis, Allen P., Robert G. Traver, and William F. Hunt. "Improving Urban Stormwater Quality: Applying Fundamental Principles." *Journal of Contemporary Water Research & Education* 146, no. 1 (2010): 3-10.

Davis, John C. *Statistics and Data Analysis in Geology.* 3rd. New York: Wiley, 2002.

De Oliveira, Lília Maria, Nádia Antônia Pinheiro Santos, and Philippe Maillard. "Applying the Manning Equation to Determine the Critical Distance in Non-point Source Pollution Using Remotely Sensed Data and Cartographic Modelling." *Proceedings of SPIE* 8893 (2013): 1-11.

Debele, Bekele, Raghavan Srinivasan, and J-Yves Parlange. "Hourly Analyses of Hydrological and Water Quality Simulations Using the ESWAT Model." *Water Resources Management* (Springer) 23, no. 2 (2008): 303-324.

Devi, Gayathri K., Puttaswamigowda Ganasri, and Gowdagere S. Dwarakish. "A Review on Hydrological Models." *Aquatic Procedia* (Elsevier) 4 (2015): 1001-1007.

Di Luzio, Mauro, Jeffrey G. Arnold, and Raghavan Srinivasan. "Effect of GIS Data Quality on Small Watershed Stream Flow and Sediment Simulation." *Hydrological Processes* (Wiley InterScience) 19 (2005): 629-650.

Dile, Yihun T., Prasad Daggupati, Chris George, Raghavan Srinivasan, and Jeff Arnold. "Introducing a New Open Source GIS User Interface for the SWAT Model." *Environmental Modelling & Software* (Elsevier) 85 (2016): 129-138.

Donigian Jr., Anthony S., and Wayne C. Huber. *Modelling of Nonpoint Source Water Quality in Urban and Non-urban Areas.* Technical Paper, U.S. Environmental Protection Agency, Athens: U.S. Environmental Protection Agency, 1991.

Easton, Zachari M., Patrick J. Sullivan, Todd M. Walter, Daniel R. Fuka, Martin A. Petrovic, and Tammo S. Steenhuis. "A Simple Metric to Predict Stream Water Quality from Storm Runoff in a Urban Watershed." *Journal of Environmental Quality Abstract - Landscape and Watershed Processes* 39, no. 4 (2010): 1338-1348.

Eckhardt, Klaus "How to Construct Recursive Digital Filters for Baseflow Separation." *Hydrological Processes* 19, no. 2 (2005): 507-515.

Environmental Systems Research Institute (ESRI). *How Filter Works.* 11 12, 2016. http://desktop.arcgis.com/en/arcmap/10.3/tools/spatial-analyst-toolbox/how-filter-works.htm (accessed 11 12, 2016).

Erturk, Ali, et al. "Water Quality Assessment and Meta Model Development in Melen Watershed - Turkey." *Journal of Environmental Management* (Elsevier) 91, no. 7 (2010): 1526-1545.

Even, Stephanie, et al. "Modelling the Impacts of Combined Sewer Overflows on the River Seine Water Quality." *Science of the Total Environment* (Elsevier) 375 (2007): 140-151.

Fetter, Charles W. *Applied Hydrogeology.* 4th. New Jersey: Prentice Hall, 2001.

Fitzgerald, Evan P., William B. Bowden, Samuel P. Parker, and Michael L. Kline. "Urban Impacts on Streams are Scale-dependent With Nonlinear Influences on Their Physical and Biotic Recovery in Vermont, United States." *Journal of the American Water Resources Association (JAWRA)* 48, no. 4 (2012): 679-697.

Gazzaz, Nabeel M., Mohd Kamil Yusoff, Ahmad Zaharin Aris, and Hafizan Juahir. "Artificial Neural Network Modeling of the Water Quality Index for Kinta River (Malaysia) Using Water Quality Variables as Predictors." *Marine Pollution Bulletin* (Elsevier), 2012: 1-12.

Golmohammadi, Golmar, Shiv Prasher, Ali Madani, and Ramesh Rudra. "Evaluating Three Hydrological Distributed Watershed Models: MIKE-SHE, APEX, SWAT." *Hydrology* 1, no. 1 (2014): 20-39.

Gupta, Hoshin Vijai, Soroosh Sorooshian, and Patrice Ogou Yapo. "Status of Automatic Calibration for Hydrologic Models: Comparison with Multilevel Expert Calibration." *Journal of Hydrologic Engineering* 4, no. 2 (1999): 135-143.

Hall, Jim M., and Bryan J. Ellis. "Water Quality Problems of Urban Areas." *GeoJournal* (Springer) 11, no. 3 (1985): 265-275.

Hem, John D. *Study and Interpretation of the Chemical Characteristics of Natural Water.* Alexandria: U.S. Geological Survey, 1992.

Jeong, Jaehak, Narayanan Kannan, Jeff Arnold, Roger Glick, Leila Gosselink, and Raghavan Srinivasan. "Development and Integration of Sub-hourly Rainfall-Runoff Modeling Capability Within a Watershed Model." *Water Resources Management* (Springer) 24, no. 15 (2010): 4505–4527.

Khatoon, Nassema, Altaf Husain Khan, Masihur Rehman, and Vinay Pathak. "Correlation Study For the Assessment of Water Quality and its Parameters of Ganga River, Kanpur, Uttar Pradesh, India." *IOSR Journal of Applied Chemistry* 5, no. 3 (2013): 80-90.

Kim, Jeongkon, Joonwoo Noh, Kyungho Son, and Ikjae Kim. "Impacts of GIS Data Quality on Determination of Runoff and Suspended Sediments in the Imha Watershed in Korea." *Geosciences Journal* (Springer) 16, no. 2 (2012): 181-192.

Koç, Cengiz. "A Study of the Pollution and Water Quality Modeling of the River Buyuk Menderes, Turkey." *Clean - Soil, Air, Water* (Wiley) 38, no. 12 (2010): 1169-1176.

Kronis, Henry *Characterization and Treatment of Snowmelt Runoff from an Urban Catchment.* Research Publication, Wastewater Treatment Section, Pollution Control Branch, Ontario Ministry of the Environment, Ontario: Ontario Publications, 1978, 35.

Kundzewicz, Zbigniew W., and Valentina Krysanova. "Climate Change and Stream Water Quality in the Multi-factor Context: An Editorial Comment." *Climatic Change* 103 (2010): 353-362.

Lim, Kyoung Jae, et al. "Automated Web GIS Based Hydrograph Analysis Tool, WHAT." *Journal of American Water Resources Association (JAWRA)* 04133 (2005): 1407-1416.

Maharjan, Ganga Ram, et al. "Evaluation of SWAT sub-daily runoff estimation at small agricultural watershed in Korea." *Frontiers of Environmental Science & Engineering* (Springer) 7, no. 1 (2013): 109-119.

Maillard, Philippe, and Nádia Antônia Pinheiro Santos. "A Spatial-statistical Approach for Modelling the Effect of Non-point Source Pollution on Different Water Quality Parameters in the Velhas River Watershed - Brazil." *Journal of Environmental Management* (Elsevier) 86, no. 1 (2008): 158-170.

Malagó, Anna, Faycal Bouraoui, Olga Vigiak, Bruna Grizzetti, and Marco Pastori. "Modelling Water and Nutrient Fluxes in the Danube River Basin with SWAT." *Science of the Total Environment* (Elsevier) 603-604 (2017): 196-218.

Malunjkar, Vaibhav S., M.G. Shinde, S.S. Ghotekar, and A.A. Atre. "Estimation of Surface Runoff Using SWAT Model." *International Journal of Inventive Engineering and Sciences (IJIES)* (Blue Eyes Intelligence Engineering & Sciences Publication Pvt. Ltd.) 3, no. 4 (2015): 12-15.

Martinec, Jaroslav, Albert Rango, and E. Major. *The Snowmelt-Runoff Model (SRM) User's Manual.* Reference Publication, National Aeronautics and Space Administration (NASA), Maryland: NASA Publications, 1983, 118.

Miller, Jeffery E. *Basic Concepts of Kinetic-wave Models.* Professional Paper, United States Department of the Interior, U.S. Geological Survey, Alexandria: Library of Congress, 1983, 29.

Mitchell, Gordon. "Mapping Hazard for Urban Non-point Pollution: A Screening Model to Support Sustainable Urban Drainage Planning." *Journal of Environmental Management* (Elsevier) 74, no. 1 (2005): 1-9.

Mohamoud, Yusuf M., Anne C. Sigleo, and Raibir S. Parmar. *Modeling the Impacts of Hydromodification on Water Quantity and Quality.* Scientific Report, United States Environmental Protection Agency, Athens: United States Environmental Protection Agency, 2009.

Moriasi, Daniel N., Jeffrey G. Arnold, Michael W. Van Liew, Ronald L. Bingner, Daren R. Harmel, and Tamie L. Veith. "Model Evaluation Guidelines for Systematic Quantification of Accuracy in Watershed Simulations." *American Society of Agricultural and Biological Engineers* 50, no. 3 (2007): 885-900.

Mouri, Goro, Seirou Shinoda, and Taikan Oki. "Assessing Environmental Improvement Options from a Water Quality Perspective for an Urban-rural Catchment." *Environmental Modelling & Software* (Elsevier) 32 (2012): 16-26.

National Science Foundation. *Wrestore: Watershed Restoration using Spatio-temporal Optimization of Resources.* January 1, 2014. http://wrestore.iupui.edu/ (accessed April 23, 2014).

Noori, Roohollah, Mostafa S. Sabahi, Abdolreza R. Karbassi, Akbar Baghvand, and Taati H. Zadeh. "Multivariate Statistical Analysis of Surface Water Quality Based on Correlations and Variations in the Data Set." *Desalination* (Elsevier) 260 (2010): 129-136.

Peinado -Guevara, Héctor, et al. "Relationship Between Chloride Concentration and Electrical Conductivity in Groundwater and its Estimation from Vertical Electrical Soundings (VESs) in Guasave, Sinaloa, Mexico." *Ciencia e Investigacion Agraria* 39, no. 1 (2012): 229-239.

Peng, Deng, Li Zhijia, and Xie Fan. "Application of TOPMODEL in Buliu River Basin and Comparison With Xin'anjiag Model." *Water Science and Engineering* 1, no. 2 (2008): 25-32.

Peters, Norman E. "Effects of Urbanization on Stream Water Quality in the City of Atlanta." *Hydrological Processes* (Wiley InterScience) 23, no. 20 (2009): 2860-2878.

Peterson, David, Richard Smith, Iris Stewart, Noah Knowles, Chris Soulard, and Stephen Hager. *Snowmelt Discharge Characteristics, Sierra Nevada, California.* Research Publication, U.S. Department of the Interior, U.S. Geological Survey, Reston: U.S. Geological Survey Publications, 2005, 13.

Saleh, Dina K., Charles R. Kratzer, Colleen H. Green, and David G. Evans. *Using the Soil and Water Assessment Tool (SWAT) to Simulate Runoff in Mustange Creek Basin, California.* Scientific Investigation Report, U.S. Department of the Interior, U.S. Geological Survey, Reston: USGS, 2009, 28.

Sandu, Mirela-Alina, and Ana Virsta. "Applicability of MIKE SHE to Simulate Hydrology in Argesel River Catchment." *Agriculture and Agricultural Science Procedia* (Elsevier) 6 (2105): 517-524.

Sheshukov, Aleksey Y., Prasad Daggupati, Douglas-Mankin, Lee Kyle R., and Ming-Chieh. "High Spatial Resolution Soil Data for Watershed Modeling: 1. Development of a SSURGO-ArcSWAT Utility." *Journal of Natural and Environmental Science* (Academic Science Journals) 2, no. 2 (2011): 15-24.

Shrestha, Sushil, and Futaba Kazama. "Assessment of Surface Water Quality Using Multivariate Statistical Techniques: A Case Study of the Fuji River Basin, Japan, Environmental Modelling & Software." *Environmental Modelling & Software* (Elsevier) 22 (2007): 464-475.

Strager, Michael P., et al. "Watershed Analysis with GIS: The Watershed Characterization and Modeling System Software Application." *Computers & Geosciences* (Elsevier) 36 (2010): 970-976.

Texas A&M AgriLife Research. *EPIC & APEX Models.* 2016. https://epicapex.tamu.edu/apex/ (accessed 12 7, 2016).

Tian, Yong Q., Dawei Wang, Robert F. Chen, and Wei Huang. "Using Modeled Runoff to Study DOC Dynamics in Stream and River Flow: A case Study of an Urban Watershed Southeast of Boston, Massachusetts." *Ecological Engineering* (Elsevier) 42 (2012): 212-222.

United States Department of Agriculture, Natural Resources Conservation Service. *Web Soil Survey.* 10 02, 2016. https://websoilsurvey.sc.egov.usda.gov/App/HomePage.htm (accessed 10 02, 2016).

United States Environmental Protection Agency. *Clean Water Act Section 319.* February 21, 2017. https://www.epa.gov/lakes/clean-water-act-section-319#reports (accessed 11 13, 2017).

—. *Exposure Assessment Models - BASINS Framework and Features.* 2016. https://www.epa.gov/exposure-assessment-models/basins-framework-and-features#overview (accessed 03 07, 2016).

—. *Polluted Runoff: Nonpoint Source Pollution.* May 2, 2017. https://www.epa.gov/nps/what-nonpoint-source (accessed 10 5, 2017).

Wang, Yu, Jianmin Bian, Sining Wang, Jie Tang, and Fei Ding. "Evaluating SWAT Snowmelt Parameters and Simulating Spring Snowmelt Nonpoint Source Area of the Liao River." *Polish Journal of Environmental Studies* 25, no. 5 (2016): 2177-2185.

Wenner, David B., Melanie Ruhlman, and Sue Eggert. "The Importance of Specific Conductivity for Assessing Environmentally Impacted Streams." *The Importance of Specific Conductivity for Assessing Environmentally Impacted Streams.* Athens: University of Georgia, 2003. 1-3.

Wilkison, Donald H., Daniel J. Amstrong, and Sarah A. Hampton. *Character and Trends of Water Quality in the Blue River Basin, Kansas City Metropolitan Area, MO and KS, 1998 through 2007.* Scientific Investigations Report, Kansas City: U.S. Geological Survey and U.S. Department of Interior, 2009.

Winchell, Michael, Raghavan Srinivasan, Mauro Di Luzio, and Jeffrey Arnold. *ArcSWAT Interface for SWAT 2012, User's Guide.* Temple: SWAT, 2013.

Wong, Tommy S.W. "Assessment of Time of Concentration Formulas for Overland Flow." *Journal of Irrigation and Drainage Engineering* (ASCE) 131, no. 4 (2005): 383-387.

Wong, Tommy S.W., and Yunjie Li. "Assessment of Changes in Overland Time of Concentration for Two Opposing Urbanization Sequences." *Hydrological Science Journal* (Taylor & Francis) 43, no. 1 (1998): 115-130.

Xu, Huashan S., Zongxue X. Xu, W. Wu, and F.F. Tang. "Assessment and Spatiotemporal Variation Analysis of Water Quality in the Zhangweinan River Basin, China." *Procedia Environmental Sciences* (Elsevier) 13 (2012): 1641-1652.

Yang, Xiaoying, and Wei Jin. "GIS-based Spatial Regression and Prediction of Water Quality in River Networks: A Case Study in Iowa." *Journal od Environmental Management* 91 (2010): 1943-1951.

Yang, Xiaoying, Qun Liu, Yi He, Luo Xingzhang, and Xiaoxiang Zhang. "Comparison of Daily and Sub-daily SWAT Models for Daily Streamflow Simulation in the Upper Huai River Basin of China." *Stochastic Environmental Research and Risk Assessment* (Springer) 30, no. 3 (2016): 959-972.

Zhang, Xuesong, Raghavan Srinivasan, and Michael Van Liew. "Multi-site Calibration of the SWAT Model for Hydrologic Modeling." *Transactions of the ASABE* 51, no. 6 (2008): 2039-2049.

VITA

Gustavo A. Orozco Sarmiento was born in Bogotá, Colombia. He attended Francisco José de Caldas District University in Bogotá and received his Bachelor of Science degree in Surveying Engineering and Geodesy in 1997; graduating with the highest honors for his thesis. Years later, after the completion of the Bachelor, he attended Nueva Granada Military University in Bogotá and received his Graduate degree in Natural Resources and Environmental Management in 2006. During his professional path he worked with government and private owned companies such as Colombian Petroleum Company (ECOPETROL), Colombian Geologic Service (formerly INGEOMINAS), Bogotá's Cadastre Office, Environmental Studies, Meteorology and Hydrology Institute of Colombia (IDEAM), Varichem of Colombia, Petrobras of Brazil, Environmental Consultant Engineers, Johnson County Community College (JCCC), GE Oil & Gas, U.S. Environmental Protection Agency (USEPA), and Tetra Tech, Inc.

He moved to the United States of America in the summer of 2007 and started his studies in Civil Engineering Technology and Construction Management. In the fall of 2011, he started to pursue his Master of Science degree in Environmental and Urban Geosciences with emphasis in Geographic Information Science. During his Master studies he earned an Advanced Certificate in Geographic Information Systems in 2014 and through Tetra Tech and the USEPA Region VII, his GIS Team was nominated for the Mason Hewitt Award for excellence in GIS in 2016. He works for Tetra Tech, Inc., as a GIS Analyst/Python & Web Mapping Applications Developer and is a member of the Emergency Response Team of the USEPA.